Frequency and Voltage-Modulated electrochemical Aflatoxin B$_1$ immunosensor systems prepared on electroactive organic polymer platforms

OWINO JOSEPH HASAEL ODERO

A thesis Submitted in fulfilment of the requirement for the Degree of Doctor Philosophiae in the Department of Chemistry, University of the Western Cape

UNIVERSITY *of the*
WESTERN CAPE

SUPERVISORS

PROF. P. G. L. BAKER AND PROF. E. I. IWUOHA

NOVEMBER 2008

KEY WORDS

Aflatoxin B_1

Anti-aflatoxin B_1 antibody

Immunosensor

Electrochemical impedance spectroscopy

Hydrogel composite

Poly (2-hydroxyethyl methacrylate) p-(HEMA)

Gold nanoparticles

Polyaniline

Poly thionine

ABSTRACT

In the presented work, immunosensors for detection of Aflatoxin B_1 based on different immobilization platforms were studied. Synthesis of an electroactive hydrogel was also carried out. Aflatoxins are a group of mycotoxins that have deleterious effects on humans and are produced during fungal infection of plants or plant products. Electrochemical immunosensor for the determination of Aflatoxin B_1 (AFB_1) was developed with anti-aflatoxin B_1 antibody immobilized on Pt electrodes modified with polyaniline (PANi) and polystyrene sulphonic acid (PSSA). Impedimetric analysis shows that the electron transfer resistances of Pt/PANi-PSSA electrode, Pt/PANi-PSSA/AFB_1-Ab immunosensor and Pt/PANi-PSSA/AFB_1-Ab incubated in BSA were 0.458, 720 and 1066 kΩ, respectively. These results indicate that electrochemical impedance spectroscopy (EIS) is a suitable method for monitoring the change in electron-transfer resistance associated with the immobilization of the antibody. Modelling of EIS data gave equivalent circuits which showed that the electron transfer resistance increased from 0.458 kΩ for Pt/PANi-PSSA electrode to 1066 kΩ for Pt/PANi-PSSA/AFB_1-Ab immunosensor, indicating that immobilization of the antibody and incubation in BSA introduced an electron transfer barrier. The AFB_1 immunosensor had a detection limit of 0.1 mg/L and a sensitivity of 869.6 k ΩL/mg.

In the second platform an immunosensor based on gold nanoparticles (AuNP) and polythionine-modified glassy carbon electrode (GCE) for the determination of aflatoxin B_1 (AFB_1) was developed. Aflatoxin B_1-BSA conjugate was immobilised on the modified GCE. Horseradish peroxidase (HRP) or Bovine serum albumin (BSA) were used to block sites against non-specific binding of the AFB_1-conjugate with other compounds such as the salts used in preparing the buffer when the antibody interacts with the AFB_1 conjugate and free AFB_1. Competition reaction was allowed to take place between the free AFB_1 and AFB_1-conjugate for the binding sites of the anti-aflatoxin B_1 antibody. Cyclic voltammetry (CV) was employed to characterize the electrochemical properties of the modified process.

The peak separation of the immunosensor (Δ_{Ep}) was 62 mV indicating a quasi reversible process. Differential pulse voltammetry (DPV) was used to monitor the analytical signal. The response decreased with an increase in AFB_1 concentration in the range of 0.6-2.4 ng/mL with a limit of detection of 0.07 and 0.16 ng/mL for HRP and BSA blocked immunosensors respectively. Significantly the low detection limit of 0.07 ng/mL is within the limits set by worl health organization (WHO) for AFB_1 and its derivatives which is 2 ng/mL The proposed method eliminates the use of secondary antibody enzymatic labels.

Synthesis and characterization of (p-(HEMA)-polyaniline hydrogels were investigated. The hydrogels were synthesized using: 2-Hydroxyeththyl methacrylate (HEMA), N-Tris (hydroxymethyl) methyl] acrylamide, 3-Sulfopropyl methacrylate potassium salt, Tetraethylene glycol diacrylate, Poly-(2-hydroxyethyl methacrylate), 2, 2-Dimethoxy-2-phenylacetophenone and aniline by UV irradiation. Two sets of the hydrogels were prepared using water / 1, 3, 3, 3-(tetramethyl butyl phenyl polyethylene glycol [Triton X-100] and water / ethylene glycol as the solvent. Scanning electron microscopy (SEM) revealed a more uniform pore size when Triton X 100 (TX-100 HG) was used as compared to ethylene glycol (EG-HG). Thermogravimetric analysis (TGA) showed that both hydrogels were stable up to 270 ^{o}C. Fourier transform-Infra red (FTIR) spectrum confirmed the incorporation of polyaniline (PANi) and HEMA in the composite. Electrochemical properties of the hydrogels evaluated using Cyclic Voltammetry and Electrochemical Impedance Spectroscopy (EIS) demonstrated the electroactivity and conductivity.

DECLARATION

I declare that **Frequency and Voltage-Modulated Electrochemical Aflatoxin B1 Immunosensor Systems Prepared on Electroactive Organic Polymer Platforms** is my own work, that it has not been submitted before for any degree or examination in any other university, and that all sources I have used or quoted have been indicated and acknowledged as complete references.

Owino Joseph Hasael Odero   November 2008

Signed...............................

ACKNOWLEDGEMENTS

DEDICATION

To my parents

George Edwin Owino Okeyo

and

Mary Atieno Owino

LIST OF PUBLICATIONS

Joseph, H. O. Owino, Ignaszak, A., Al-Ahmed, A., Baker, P.G. L., Alemu, H., Ngila, J. C. and Iwuoha, E. I. Modelling of the impedimetric responses of an aflatoxin B_1 immunosensor prepared on an electrosynthetic polyaniline platform. *Analytical and Bioanalytical Chemistry*. 2007. 388, 1069-1074.

Joseph, H. O. Owino, Omotayo, A. Arotiba, Priscilla, G. L. Baker, Anthony, Guiseppi – Elie. and Emmanuel, I. Iwuoha. Synthesis and characterization of poly (2-hydroxyethyl methacrylate)-polyaniline based hydrogel composites. *Reactive and Functional Polymers*. 2008, 68, 1239-1244.

Joseph, H.O. Owino, Omotayo A. Arotiba, Nicolette Hendricks, Everlyne A. Songa, Nazeem Jahed, Tesfaye T. Waryo, Rachel, F. Ngece, Priscilla G .L. Baker and Emmanuel I. Iwuoha. Electrochemical Immunosensor Based on Polythionine/Gold Nanoparticles for the Determination of Aflatoxin B_1. *Sensors* 2008, 8, 8262-8274.

TABLE OF CONTENTS

List of Figures

List of Tables

Chapter One

1.1 BACKGROUND

1.2 Introduction

Mycotoxins are naturally occurring toxic substances produced by fungi or moulds on agricultural crops. Among the 300-400 mycotoxins known to exist in nature, important groups include: aflatoxins, Ochratoxin A, fumonisins and deoxynivalenol.

Aflatoxins are a group of chemically related mycotoxins produced by common fungi (*Aspergillus flavus*, *A.parasiticus* and *A.nomius*) found in corn, cotton seed, peanuts and other nuts, grains and spice (Stroka and Anklam, 2002). Fungal infection and aflatoxin production can occur at any stage of plant growth, harvesting drying, processing and storage. Both the infection process and aflatoxin accumulation are strongly affected by environmental conditions such as insect damage i.e physical damage caused by ingestion of crop/seed, temperature, and humidity. The four most commonly occurring aflatoxins are B_1, B_2, G_1 and G_2 along with two common metabolic by products, M_1 and M_2, which are secreted in the milk of lactating animals that have consumed feed contaminated with aflatoxin. Exposure by ingestion or inhalation of aflatoxins may lead to serious medical conditions that vary considerably depending on the animal species, dose, diet, age and gender (Eaton and Groopman, 1994). Acute effects are primarily observed in structural and functional damage of the liver cell necrosis, haemorrhage, lesions, fibrosis and cirrhosis. Additionally, hepatic encephalopathy, immunosupression, lower respiratory infections, gastrointestinal haemorrhage, anorexia, malaise and fever have been observed (Jarvis and Miller

1

2005). Chronic exposure to aflatoxins often leads to liver cancer, as well as carcinomas of other organs (kidney, lung, colon and the nervous system) (IARC 1993). An international report by the Food and Agricultural Organization of the UN (Van Egmond and Jonker, 2003) into mycotoxin regulations revealed that as of December 2003, at least 99 countries worldwide had regulations in place for permitted mycotoxin levels in food/or feed, limits having being set for AFB_1 alone or for the sum of aflatoxins B_1, B_2, G_1 and G_2.The maximum tolerated level for AFB_1 in food is set at 2 µg/kg (2 ppb).

UNIVERSITY *of the*
WESTERN CAPE
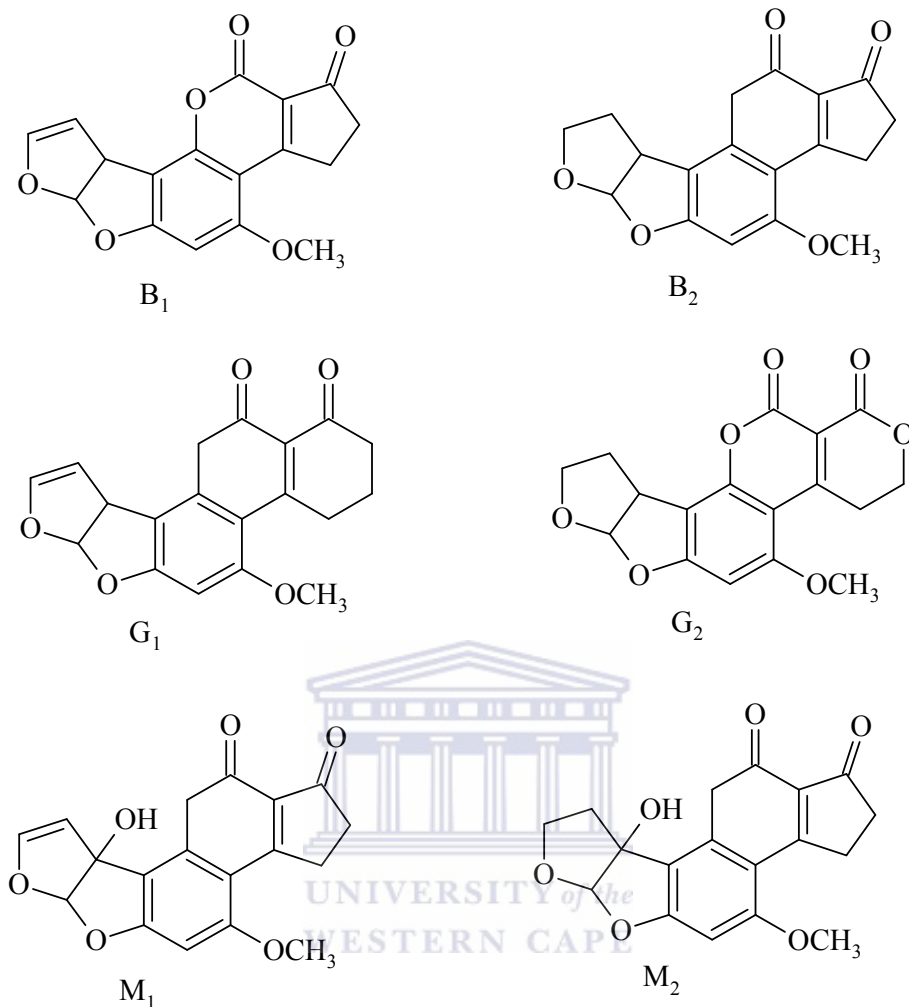
Figure 1.1 Chemical structures of the most occurring forms of aflatoxin

Ochratoxin A is a toxic metabolite produced by several moulds of the Aspergillus flavus and Penicillium genera, including Aspergillus ochraceus. The fungal species has the potential to produce ochratoxin A, a known nephrotoxin and carcinogen. It has been frequently detected in human foods and animal feed, mainly in cereal products, although a range of commodities has been reported to contain the toxin. In humans, exposure to ochratoxin A has been linked with Balken endemic nephropathy (BEN), a chronic kidney disease associated with tumours of the renal system. In animals, impairment of renal function has been

reported in swine. In turkeys and chickens symptoms included retarded growth, decreased feed conversion, nephropathy and mortality. Other harmful effects observed in poultry which can be attributed to the ingestion of toxic levels of aflatoxin include: refusal to feed and a decreases in egg production. (Mantle, 2002; Holzhäuser et al., 2003).
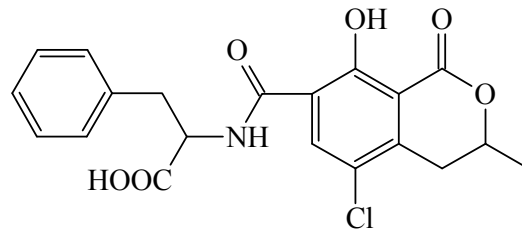
Figure 1.2 Chemical structure of Ochratoxin A

Fumonisins are a group of mycotoxins produced by several *Fusarium* moulds. Fumonisin B_1 (FB_1) has been found at significant levels in corn (Sydenham et al., 1991; Doko et al., 1996). Human consumption of fumonisin has been linked to the esophageal cancer in Transkei (South Africa) and China (Marasas et al., 1981; Li et al., 1980). Bath et al., 1997 carried out an epidemiological survey on African population and found that FB_1 contaminated maize was responsible for toxicity at the gastrointestinal level, causing abdominal pain and diarrhoea. Fumonisin are also known as the causative agent for leukoencephalomalacia (ELEM) in horses (Kellerman et al., 1990) pulmonary edema (PPE) in pigs (Harrison et al., 1990) hepatocarcinoma in rats (Voss et al., 1990) and brain haemorrhage in rabbits (Bucci et al., 1996).

4
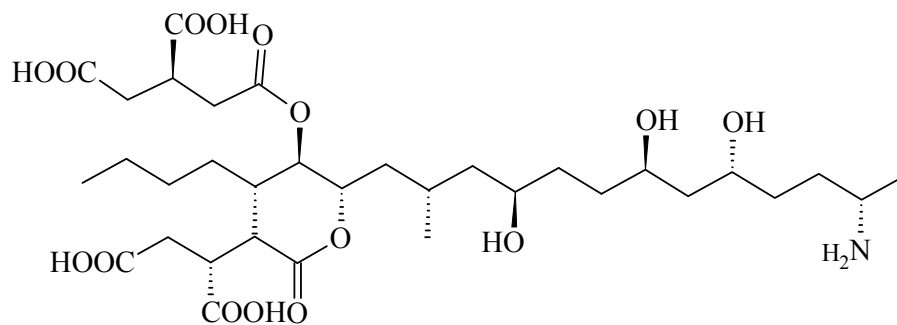
Figure 1.3 Chemical structure of fumonisin B

Deoxynivalenol (DON) is a mycotoxin produced by fungi of the Fusarium genus, i.e. *Fusarium clulmorum* and *Fusarium graminearium*, which are abundant in various cereal crops (wheat, maize, barley, oats and rye) and processed grains (malt, beer and bread). In contaminated cereals, 3-and 15-acetyl DON can occur concomitantly in significant amounts (10-20%) with DON. The fungi producing trichothecenes are soil fungi and are important plant pathogens which grow on the crop in the field (Eriksen and Alexander, 1998). The substance is a very stable compound, both during storage /milling and the processing/cooking of food and it does not degrade at high temperatures (Creppy, 2002; Wolf-Hall et al., 1999). DON inhibits the synthesis of DNA and RNA and protein synthesis at the ribosomal level. The toxin has a haemolytic effect on erythrocytes. An acute dose of DON can induce vomiting in pigs. According to the GEMS (Global Environment Monitoring system)/Food regional diets (WHO, 2002), the total human intake of DON was estimated to range from 0.77µg/kg body weight per day in the African diet to 2.4µg/kg body weight per day in the Middle Eastern diet. Despite the estimated low average intake, outbreaks of acute disease involving nausea, vomiting, gastrointestinal upset, dizziness, diarrhoea and

headache have been reported in Asia which has been attributed to consumption of grains contaminated with Fusarium species and especially with DON at concentrations of 3-93 mg/kg in grains for human consumption (WHO, 2002).
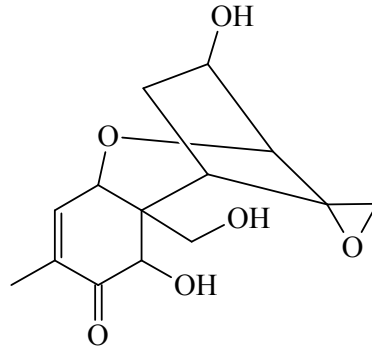
Figure 1.4 Chemical structure of deoxynivalenol

From the preceding information, it is evident that the various mycotoxins represent a significant public health concern. Although contamination from ubiquitous causative agents cannot be eliminated, exposure to the toxins can be minimized. The US government agencies monitor and tightly regulate aflatoxin levels in animal and various food products. The permissible levels are typically 2

ppb (Maria and Toby, 2003).The safe limit of detection for ochratoxin A is 2.0 ppb (Mantle, 2002) and 1 ppm for DON (Trucksess et al., 1998). Accurate monitoring of mycotoxins is therefore necessary to ensure safe exposure.

1.3 Rationale and Motivation

Conventional methods for detection and quantification of mycotoxins are high performance liquid chromatography (HPLC) with UV and/or fluorescence chromatography (FLD) detection, thin layer chromatography (TLC), and gas chromatography (GC) (Angelo and Michelangelo, 1998; Gonzalez et al., 2004; Kim et al., 2004). These methods provide a highly sensitive response and have been have been widely used as routine monitoring tool. The instrumental methods provide sensitive and specific assays but have the following problems

(i) They are laborious, and not really suitable for screening large number of samples for field work

(ii) The extraction and clean-up processes involve numerous time-consuming steps

iii) Different derivatization reagents have been used for converting the toxins into the corresponding fluorescent derivatives, which is a complex analysis procedure and needs highly skilled personnel.

The aim of more recent studies has been to simplify and expedite the method of detection while attempting to maintain or improve the sensitivity. Sensors and biosensors have rapidly developed in the past decades because of they are rapid convenient and practical. The prospect of miniaturization for direct on-site monitoring of samples has made biosensors an attractive approach.

1.4 The Aims of the Research

The following aims and objectives are identified:

To electropolymerize polystyrene sulphonic acid (PSSA)-doped aniline on platinum electrode

To immobilize AFB$_1$ antibody on the electrode

To evaluate the immunosensor performance by DC voltammetry and electrochemical impedance spectroscopy

To develop an amperometric Immunosensor for AFB$_1$ based on polythionine/gold nanoparticles

To synthesize and characterize poly (2-hydroxyethyl methacrylate)-polyaniline based hydrogel composites for the application as an immobilization platform of the AFB$_1$ antibody

1.5 Thesis layout

The thesis is divided into seven chapters. Chapter one gives a general introduction to mycotoxins and the motivations of undertaking the study, the objectives are also highlighted.

Chapter two gives a general review of the different types of immunosensors; the role of antibodies in immunosensors is also discussed. A review of conducting polymers, hydrogel composites, gold nanoparticles and electrochemical impedance spectroscopy and the role they play in immunosensors is also presented.

Chapter three describes the various analytical techniques used and the general experimental procedures are presented.

Chapter four discusses the experimental results of the Impedimetric immunosensor for aflatoxin B_1 prepared on electrosynthetic polyaniline platform

Chapter five discusses the experimental results of electrochemical immunosensor based on polythionine/gold nanoparticles for the determination of AFB_1.

Chapter six presents the experimental results of the synthesis and characterization of poly (hydroxyl methyl methacrylate)-polyaniline based hydrogel composites.

Chapter seven gives the conclusions and recommendations for future research.

Chapter Two

2.1 The Literature Review

2.2 Biosensors

A biosensor is described as a compact analytical device, incorporating a biological or biomometic sensing element, either closely connected to, or integrated within a transducer system. The principle of detection is the specific binding of the analyte of interest to the complimentary bio recognition element immobilised on a suitable support medium. The specific interaction results in a change in one or more physico-chemical properties (pH change, electron transfer, mass change, heat transfer, uptake or release of gases or specific ions) which are detected and may be measured by the transducer. The usual aim is to produce an electronic signal which is proportional in magnitude or frequency to the concentration of a specific analyte or group of analytes to which the bio sensing element binds (Powner and Yalcinkaya, 1997; Karube and Nomura, 2000).

There are two types of biosensors: biocatalytic and bioaffinity-based biosensors. The bio catalytic biosensor uses mainly enzymes as the biological compound, catalyzing and signalling biochemical reaction. The bio affinity- based biosensor, designed to monitor the binding event itself, uses specific binding proteins, lectins, receptors, nucleic acids, membranes, whole cells, antibodies or antibody-related substances for bio molecular recognition. In the latter two cases, these biosensors are referred to as immunosensors (Turner et al., 1999).
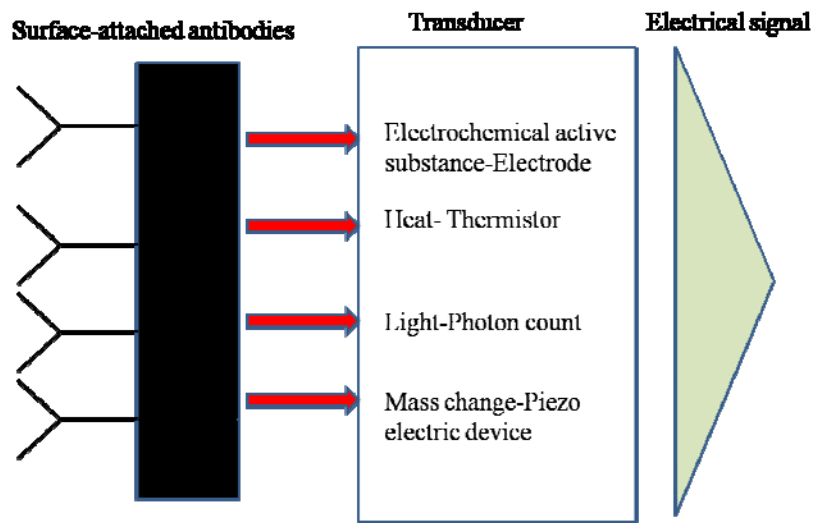
Figure 2.1 Scheme of the general immunosensor design depicting the intimate intergration of immunological recognition at the solid-state surface and the signal transduction
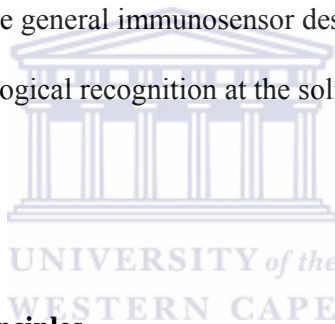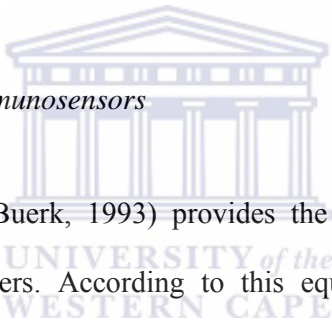
2.3 Immunosensor Principles

The main types of immunosensor detection devices: electrochemical (potentiometric, amperometric or conductometric/capacitive), optical and microgravimetric. All types can either be described as direct (nonlabelled) or as indirect (labelled) immunosensors. The direct sensors are able to detect the physical changes during the immunocomplex formation, whereas the latter sensors use signal-generating labels which allow more sensitive and versatile detection modes when incorporated into the complex.

There is a great variety of different labels which have been applied in indirect immunosensors. The most common enzyme labels include enzymes such as peroxidase (EC 1.11.1.7), glucose oxidase (EC 1.1.3.4). alkaline phosphatase (aP), catalase (EC1.11.1.6) or lucifarase (EC 1.13.12.7) due to their excellent stability and high turnover number. Electroactive compounds such as ferrocene or In^{2+} salts, and a series of fluorescent labels (rhodamine, fluorescein, Cy5, ruthenium diamine complexes and phosphorescent porpyhrin dyes) have also been used (Oswald et al., 2000 ; Wolfbeis, 2000).

2.4 Electrochemical immunosensors

2.4.1 Potentiometric immunosensors

The Nernst equation (Buerk, 1993) provides the fundamental principle of all potentiometric transducers. According to this equation, potential changes are logarithmically proportional to the specific ion activity. Potentiometric transducer electrodes, capable of measuring surface potential alterations at near zero current flow, are being constructed by applying the following methodologies:

2.4.1.1 Transmembrane transducer

This transducer principle is based on the accumulation of a potential across a sensing membrane. Ion selective electrodes (ISE) use ion-selective membranes which generate a charge separation between the sample and the sensor surface. Analogously, antigen or antibody immobilized on the membrane binds the

corresponding compound from the solution at the solid-state surface and change the transmembrane potential.

2.4.1.2 Electrode as a transducer

This transducer involves the electrode which provides a single surface for creation of immunocomplex, changing the electrode potential in relation to the concentration of the analyte.

2.4.1.3 Field effect transistor (FET)

The FET is a semi conductor device used for monitoring of changes at the surface of an electrode, which have been built up on its metal gate between the so-called source and drain electrodes. The surface potential varies with the analyte concentration. The intergration of an ISE with FET is realized in the ion-selective field effect transistor (ISFET). This technique can also be applied to immunosensors. An advantage of potentiometric sensors is the simplicity of operation, which can be used for automation, and the small size of the solid state FET sensors. The major disadvantages of all potentiometric methods are: poor sensitivity; non specific binding; susceptibility to signal interference (from other other ions present in the sample) The signal to noise ratio causes analytical problems, which are difficult to circumvent (Morgan et al., 1996; Pearson et al., 2000). A potentiometric immunosensor for the determination of human α-fetoprotein has been reported. Immobilization of anti-AFP on the surface of platinum disk electrode was achieved by employing Gelatin-silver film as the carrier. Glutaraldehyde was employed to improve the character of complex film

by enhancing its stability. The resulting AFP sensor exhibited a short time response time, high sensitivity, low interference from other antigens and the results were in satisfactory agreement with those by ELISA (Qiang et al., 2006). A potentiometric immunosensor for detection of Japanese B encephalitis vaccine was developed by immobilizing antiserum of Japanese B encephalitis on nano-Au/polymerized o-phenylenediamine (o-PDA) film on platinum electrode (Zhang et al., 2004). A potentiometric immunosensor for the detection of hepatitis B surface antigen was developed by means of self-assembly to immobilize hepatitis B surface antibody on platinum disk electrode based on gold nanoparticles, nafion and gelatine as matrices. The detection was based on the change in the electrical potential before and after antibody-antigen reaction (Tang et al., 2004). The method allowed immobilization of a higher loading amount of antibodies and greater retention of immunoreactivity as compared to the commonly applied methods such as glutaraldehyde cross linking. This was deduced from the potentiometric measurements. Analytical results obtained using the developed technique compared well with ELISA. (Tang et al., 2004).

A quantitative polypyrrole based potentiometric immunosensor that provides broad-spectrum assay capability was designed by Purvis et al., 2003. The biosensor detected enzyme labelled immuno-complexes formed at the surface of a polypyrrole coated, screen printed gold electrode. Detection was mediated by a secondary reaction that produces charged products. A shift in potential was measured at the sensor surface, caused by local changes in redox state, pH and ionic strength. The magnitude of the difference in potential was related to the

concentration of the formed receptor-target complex. The sensor was applied for detection of hepatitis B surface antigen, Troponin I, Digoxin and tumour necrosis factor. This technology was found to be rapid, ultrasensitive, and reproducible and had a wide dynamic range. Feng et al., 2000 reported a potentiometric immunosensor for the detection of immunoglobin G (IgG).The immunosensor was based on covalent immobilization of anti-immunoglobin G on silver (Ag) electrode. Detection was based on the change in the electric potential before and after the antigen-antibody reaction. Sergeyeva et al., 1996 fabricated an immunosensor for α-2 interferon detection based on pH sensitive field effect transistor (pH FET). The sensing element was fabricated by immobilizing α-2 interferon on the gate of pH FET. The interaction of anti-interferon antibodies labelled with β-lactamase with interferon- pH-FET (in the presence of specific enzyme substrate) leads to a local pH-change at the surface of transducer and produced an electrochemical signal which was proportional to the conjugate concentration. Analytical data obtained were in accordance with conventional ELISA assays.

2.4.2 Amperometric immunosensors

Amperometric immunosensors are designed to measure a current flow generated by an electrochemical reaction at constant voltage. There are only a few applications available for direct sensing, since most (protein) analytes are not intrinsically able to act as redox couples in an electrochemical reaction. Therefore, electrochemically active labels (directly or as products of an enzyme reaction) are needed for the electrochemical reaction of the analyte at the sensing electrode.

There are a series of enzymes with high catalytic reaction rates (>103/s) in use for substrate transformation in amperometric systems (Ghindilis et al., 1998). In general, oxidizing rather than reducing potentials are applied. Besides oxygen, generated by catalase from H_2O_2, there are other amperometrically detectable compounds, such as ferrocene derivatives or In^{2+} salts (Aizawa, 1994). Another approach is the use of the redox polymer [PVP-Os (bipyridyl) $_2$ Cl], which is coimmobilized with specific antibodies (Lopez et al., 1998). Additionally, there are examples of enzymes with electrochemically active products. Alkaline phosphatase (aP) catalyzes the hydrolysis of phenyl phosphate or *p*-aminophenyl phosphate (4-APP) compounds, which result in electrochemically active phenol or p-aminophenol (Aizawa, 1994). Enzymes, such as horseradish peroxidase (HRP), glucose oxidase, glucose-6-phosphate dehydrogenase (EC 1.1.1.1.49; with subsequent amperometrical oxidation of NADH) have been successfully applied as labels (McNeil et al., 1997). The main disadvantage for amperometric immunosensors of having an indirect sensing system is compensated for by an excellent sensitivity. This is due to a linear analyte concentration range compared to a logarithmic relationship in potentiometric systems. Special attention must be directed to the system-inherent transport rate limitations for redox couples on the electrode surface (Ghindilis et al., 1998). Amperometric immunosensors have found numerous applications in measurements of different analytes. They have been the subject of different studies. A highly sensitive amperometric enzyme immunosensor was developed by Zhuo et al., 2006 for the detection of carcinoembryonic antigen (CEA). The concept was based - on redox-biocompatible composite protein membrane fabrication, double enzyme

membrane fabrication and antibody immobilization. The immunosensor developed had good stability and long life term. Ferreira et al., 2006 carried out an investigation of the interaction between Tc85-11 protein and antibody anti-*T.cruzi* by AFM and amperometric measurements. An atomically flat gold surface on a silicon substrate and gold screen-printed electrodes were functionalized with cysteamine and later activated with glutaraldeyhde (GA), which was used to form covalent bonds with the purified recombinant antigen (Tc85-11). The immunosensor was applied to sera of chagasic patients and patients having different systematic diseases. An amperometric immunosensor for nonylphenol (NP) has been developed by immobilization of specific antibodies together with horseradish peroxidase on the surface of carbon screen printed electrode. The signal of the immunosensor is generated by the involvement of NP accumulated in the peroxidase oxidation of mediator (Methylene blue, hydroquinone or iodide). The sensitivity of the detection depends on the nature of mediator (Evtugyn et al., 2006). A highly sensitive amperometric immunosensor for microcystin detection in algae has been developed based on the affinity between this cyanotoxin and the corresponding monoclonal and polyclonal antibodies. The immunosensor was applied to the analysis of cyanobacterial samples from a river. The limits of detection attained from the calibration curves and the results obatained from the real samples demonstrated the potential use of the imunosensors as screening tools for routine use in assessment of water quality and the control of toxins in algae (Campàs and Marty, 2007a).

An amperometric immunosensor for the rapid determination of 17β estradiol was fabricated by Butler and Guilbault, 2006a. The immunosensor was based on disposable screen printed carbon electrodes. Both monoclonal and polyclonal antibodies were assessed and the use of monoclonal antibodies resulted in a more sensitive assay. Detection was facilitated by labelling the antibody with alkaline phosphatase and carrying out amperometric measurements using p aminophenyl phosphate as substrate .An amperometric immunosensor for the specific detection of 3, 4 methylenedioxyamphetamine (MDA) and its analogues, 3, 4-methylene dioxymethamphetamine (MDMA) and 3, 4 methylenedioxyethylamphetamine (MDEA) in saliva and urine was developed, by Butler et al., 2006b A direct competitive assay in which free analyte and HRP labelled species were simultaneously added to an immobilised polyclonal antibody was employed. Amperometric detection was performed after addition of tetramethylbenzidine (TMB)/hydrogen peroxide as substrate. Ferreira et al., 2005 constructed an amperometric immunosensor for serological diagnosis of Chagas disease. The gold electrode was treated with cysteamineand glutaraldehyde prior to antigen immobilization. Antibodies present in the serum of patients with Chagas' disease were captured by the immobilized antigens and the affinity interaction was monitored by chronoamperometry using peroxidase-labelled IgG conjugate and hydrogen peroxide, iodide substrate. Aluoch et al., 2005 described an amperometric biosensor for monitoring the level of protein amylase in human saliva. The biosensor sensing elements comprise of a layer of salivary antibody (or antigen) self-assembled onto Au-electrode via covalent attachment. Molecular recognition between the immobilized antibody and the salivary amylase proteins

was monitored via an electroactive indicator. The electroactive indicator was oxidized or reduced and the resulting current change provides the analytical information about the concentration of the salivary proteins. A copolymer modified amperometric immunosensor for the detection of cholera antitoxin (anti-CT) by the electropolymerization of pyrrole-biotin and pyrrrole-lactitobionamide monomers on platinum or glassy carbon electrodes has been reported. Different enzymatic markers were utilized for the detection of cholera antitoxin. HRP based amperometric immunosensor was found to be more sensitive as it offered a lower detection limits (Ionescu et al., 2005). Studies have been carried out on a disposable amperometric immunosensor for the rapid detection of carp (*Carassius auratus*) Vitellogenin (Vtg). The sensor was fabricated based on screen-printed carbon arrays (SPCAs) containing eight carbon working and an integrated carbon counter electrodes. Poly-terthiophene carboxylic acid was electropolymerized on the surface of working electrodes. HRP and monoclonal antibody (anti-Vgt) specific to carp Vtg were covalently attached onto the polymer-coated SPCAs. The performance of the immunosensor for the determination of Vtg was evaluated by a standard addition method performed in fish serum samples (Darain et al., 2005). Rao et al., 2005 developed an amperometric immunosensor for detection of *Salmonella typhi* antibodies. The sensor was fabricated using SPEs and recombinant flagellin fusion protein. The sensor considerably reduced the time for detection as compared to the conventional Widal test. Yu et al., 2003 fabricated a disposable amperometric immunosensor for rapid detection of AFP in human serum. The immunosensor was prepared by entrapping HRP labelled AFP antibody in chitosan membrane to modify the SCPCE. The immunosensor had a

19

better accuracy compared to results obtained from immunoradiometric assays. An amperometric immunosensor for rapid separation-free determination of CEA in was prepared by co-immobilizing thionine and HRP labelled antibody on a GCE through covalently binding them to GCE with a glutaraldehyde linkage (Dai et al., 2004). A separation-free bienzyme immunoassay system was developed for the electrochemical determination of the herbicide chlorsulfuron. SPE with HRP was used as the detector. A membrane with immobilised anti-chlorsulfuron antibodies was attached to the electrode. Free chlorsulfuron in the sample under test and chlorsulfuron-glucose oxidase conjugate competed for the available binding sites of the membrane-immobilised antibodies. Addition of glucose induced the generation of hydrogen peroxide by the glucose oxidase conjugate, which was in turn reduced by the peroxidase. This resulted in change of electrical current which was measured to determine the chlorsulfuron content in the sample (Dzantiev et al., 2004). A renewable amperometric immunosensor for determination of β-indole acetic acid (IAA) in plant samples was fabricated based on enzyme-linked competitive immunoreactions between free IAA and IAA labelled with HRP to bind on the anti-IAA IgG immobilized on the SACE surface. (Li et al., 2003). A disposable and meditorless immunosensor based on a conducting polymer (5, 2':5'2''-trthiophene-3-3'-carboxylic acid) coated SPCE was developed using a separation-free homogenous technique for the detection of rabbit IgG as a model analyte. HRP and streptavidin were covalently bonded with the polymer on the electrode biotinylated antibody immobilized on the electrode surface using avidin-biotin coupling. The sensor was based on the competitive assay between free and labelled antigen for the available binding sites of the antibody. Glucose oxidase

was used as a label and in presence of glucose, hydrogen peroxide formed by the analyte-enzyme conjugate was reduced by the enzyme channelling via HRP bonded on the electrode. The catalytic current was then monitored amperometrically (Darain et al., 2003). An amperometric immunosensor based on the adsorption of anti III antibody onto an electrochemically pre-treated carbon-paraffin electrode was proposed for the detection of complement III (C_3).The competitive immunoassay format was adopted with HRP-C_3 as a tracer, 3, 3'5, 5'-tetramethylbenzidine (TMB) and hydrogen peroxide as the enzyme substrates. Measurement of the amount of HRP-C_3 binding onto the electrode surface was achieved by detecting the product of the enzyme catalytic reaction amperometrically (Zhou et al., 2003). Fähnrich et al., 2003 fabricated an amperometric immunosensor for polycyclic aromatic hydrocarbons (PAHs).The sensor was based on disposable screen-printed carbon electrodes. The coating antigen used was phenanthrene-9-carboxaldehyde coupled to BSA via adipic acid dihydrazide. Antibodies were monoclonal mouse anti-phenathrene. Alkaline phosphatase was used in combination with the substrate *p*-aminophenyl phosphate (*p*APP) for the amperometric detection. An amperometric immunosensor for haemoglobin-A1c (HbA1c) determination has been developed utilizing membrane-immobilized haptoglobin as affinity matrix fixed in front of a Pt-working electrode. The HbA1c assay was carried out in a two step procedure including the selective haemoglobin enrichment on the sensor surface and the specific HbA1c detection by glucose oxidase (GOx) labelled anti HbA1c antibody. (Stöllner et al., 2002). An amperometric immunosensor based on highly dispersed immunoelectrodes has been developed for rapid and sensitive assay for

Hantavirus infection in mouse blood serum. Napthol formed as a result of enzymatic reduction of napthyl phosphate in the presence of alkaline phosphatase label was detected amperometrically. The performance of the sensor was comparable to the strip immunoblot assay (SIA).The overall time of analysis was also considerably reduced (Vetcha et al., 2002). Kreuzer et al., 2002 optimised a SPE system for the measurement of a variety of seafood toxins. A disposable SPCE coupled with amperometric detection of *p*-aminophenol produced by alkaline phosphatase label was used for signal measurement. ELISA was primarily used to develop all toxin system prior to transferring to SPE. A simple and cost effective technique for identification and monitoring of prostate cancer using an amperometric biosensor was developed by Sarkar et al., 2002. Monoclonal capture antibody (Mab) to Prostate specific antigen (PSA) was immobilised on the working electrode and the other Mab labelled by the enzyme marker, HRP was used as the tracer antibody. The electrochemical response was directly observed due to the enzymatic reaction via a sandwich immunoassay on the working electrode. Pemberton et al., 2001 fabricated electrochemical immunosensors for cow's milk progesterone. The sensors were fabricated by depositing anti-progesterone monoclonal antibody onto SCPCEs. After competitive binding of the sample/conjugate (alkaline-phosphate-labelled progesterone) mixture, measurement of the signal was done amperometrically in the presence of enzyme substrate which was 1-naphthyl phosphate. An amperometric enzyme immunosensor for the determination of antigen (Ag) of pathogenic fungi Trichophyton rubrum (TR) was prepared by Medyantseva et al., 2000. The immunosensor was based on a specific immunoreaction of Ag with

antibodies of Ag with antibodies which were immobilized together with cholinesterase into a nitrocellulose membrane which was the biosensitive part of the immunosensor. The sensor was applied for the determination of Ag TR in human blood serum. Abdel-Hamid et al., 1999 developed a flow-injection amperometric immunofiltration assay system for the rapid detection of bacteria. The system was based on the use of disposable porous nylon membranes which acted as a support for the immobilization of the anti bacteria antibodies. The assay system consisted of a flow-injection system, a disposable filter membrane and an amperometric sensor. Parameters affecting the performance of the sensor were evaluated and optimized. An amperometric immunosensor based on a rigid immunocomposite was designed to measure human gonadotropin β-subunit (β-HCG).The immunosensor was formed by conducting graphite-methacrylate containing the anti-β-HCG antibody. β-HCG was determined with a sandwich assay using anti- β-HCG conjugate labelled with HRP. The extent of the immunological interaction is quantified by the activity of the labelling enzyme (Santandreu et al., 1999). Crowley et al., 1999 developed an amperometric immunosensor for the cytokine granulocyte-macrophage colony-stimulating factor (GM-CSF). A competitive assay was employed, using free and alkaline phosphatase labelled GM-CSF. *p*-aminophenyl phosphate is converted to *p*-aminophenol in the presence of alkaline phosphatase and the current generated by its subsequent oxidation is detected amperometrically. An amperometric, enzyme-channelling immunosensor has been used to study the qualitative and quantitative aspects of molecular biorecognition. The immunosensor consisted of a polyethylenimine-modified carbon electrode on which glucose was

coimmobilized with a specific antibody. The immunological reactions were monitored electrochemically. The approach was applied for estimating the kinetic constants of the reaction between IgG and its specific anti-IgG antibodies (Ivnitski et al., 1998). A disposable amperometric immunomigration sensor for the detection of triazine pesticides in real samples using monoclonal antibodies against atrazine and tertbutylazine as biorecognition element was fabricated by Bäumner and Schmid, 1998. Generation and amplification of the signal was achieved by using hapten-tagged liposomes entrapping ascorbic acid as marker molecule. An amperometric immunosensor for the detection of red blood cells based on a non-competitive sandwich assay and flow injection analysis (FIA) was developed by Lu et al., 1997. Specific IgM and non specific IgM were chemically immobilised on two electrodes to form the sensing electrodes and blank electrodes, respectively. This was employed to determine the binding of specific blood cells and non-specific adsorption. In one determination, HRP-labelled anti-blood group A IgM was utilized in the assay. An immunosensor that allows for the rapid estimation of fatty acid-binding protein (FABP) in neat plasma samples based -on screen-printed graphite working electrode was designed by Schreiber et al., 1996. The capture antibodies were bound to the electrode surface by adsorption and trapped FABP from the plasma sample. The sandwich was then completed by a second monoclonal antibody conjugated with alkaline phosphatase. The enzyme converts p-aminophenyl phosphate to p-aminophenol which was then detected amperometrically. Ivnitski and Rishpon, 1996 developed a one-step, separation free enzyme immunosensor. The sensor consisted of an antibody electrode. The immunosensor combines enzyme channelling

24

immunoassay, accumulation of redox mediators, cyclic regeneration of an enzyme (peroxidase) substrate at the polymer (polyethylenenimine)/electrode interface and control of the hydrodynamic conditions at the interface of the antibody electrode. The immunological reactions were monitored electrochemically.

2.4.3 Conductimetric and capacitive immunosensors

Condutimetric transducers measure the alteration of the electrical conductivity in a solution at constant voltage, caused by biochemical (enzymatic) reactions which specifically generate or consume ions. The capacitance changes are measured using an electrochemical system, in which the bioactive element is immobilized onto a pair of noble metal electrodes (Au or Pt). Another approach is the measurement of changes of the surface conductivity Yagiuda et al., 1996 developed a conductimetric immunosensor for the determination of methamphetamine (MA) in urine. Anti MA antibodies were immobilized onto the surface of a pair of platinum electrodes. The immune-complex formation caused a decrease in the conductivity between the electrodes. The measurement of the reciprocal capacitance, performed at alternating voltage is advantageous compared to conductometric devices, and serves two purposes. The first is to test the insulating monolayer on the sensor noble metal surface. Self assembled monolayers have insulating properties and also provide the additional advantage of immunosensor protection against non specific binding. Minor desorption of the monolayer results in an essential increase in capacitance, thus the actual quality of the device can verified. The second application is the measurement of changes in the effective dielectric thickness of the insulating layer during antigen binding,

when antibodies are linked to the alkylthiol layer. A marked decrease of the electrical capacitance is observed and is used to quantitate the analyte Yagiuda et al., 1996).

2.4.4 Optical sensors

Optical immunosensor are popular for bioanalyis. Light often provides the advantage of an immediate visible signal as compared to other transducer techniques. Additional benefits are the non-destructive operation mode and the rapid signal generation and data acquisition. In particular the introduction of fibre bundle optics as optical waveguides and sophisticated optoelectronics offers increased versatility of these analytical devices (Gizeli, and Lowe, 1996; Morgan, et al., 1996; Pearson, et al., 2000) Changes in adsorption, fluorescence, luminescence, scatter or refractive index (RI) occur when light is reflected at sensing surfaces. This forms the basis for optical sensor techniques.There are applications of either direct label free-detection of the immunological reaction, of labelled immunospecies, or of the products of enzymatic reactions. Most labels are fluorescent, but bio and chemiluminescense species are also possible. Optical sensors can further be divided into:

2.4.4.1 Total internal reflection spectroscopy (TIRS)

These involve two materials with two materials with different refractive indices (RI), total internal reflection occurs at a certain angle of the light beam being directed through the layer with the higher RI towards the sensing interface. By

this, an evanescence wave is generated in the material with the lower RI. This wave, being an electrical vector of the wavelength of the incident light beam, penetrates further into the medium with exponentially attenuated amplitude. Biomolecules attached in that portion of the medium will interact inevitably with the evanescent wave and therefore, lead to a distinctive diminution of the reflected light. The resolution is directly proportional to the length of interaction. (Domenici et al., 1995).

Another phenomenon, the optical diffraction, is used by the optical biosensor assays (OBA) system (Tsay et al., 1999): biomolecules are attached to the surface of a silanized wafer. The protein-coated surface is illuminated through a photomask to create distinct periodic areas of active and inactive protein. Upon illuminating with laser light, the diffraction grating caused by the ligand-binding process diffracts the incident light. An analyte-free (negative) sample does not result in diffraction because no antigen-antibody binding occurred creating the diffraction grating. The presence or absence of a diffraction signal differentiates between positive and negative samples. The intensity of the signal provides a quantitative measure of the analyte concentration.

2.4.4.2 Ellipsometry

Linearly polarized light of known orientation is reflected at oblique incidence is elliptically polarized. The shape and orientation of the ellipse depend on the angle of incidence, the direction of the polarization of the incident light, and the

27

reflection properties of the surface. On adsorption of biomolecules onto a planar solid surface, phase and amplitude of the reflected light are altered and can be recorded by ellipsometric techniques. The changes in the polarization of the light are due to the alterations of the RI and the coating thickness (Stenberg and Nygren, 1982).

2.4.4.3 Optical dielectric wave guides

Optical wave guides are glass, quartz or polymer films or fibres made of high RI material embedded between or in lower index dielectric materials. If a linearly polarized helium-neon laser light wave, introduced into the high index film or fibre, arrives at the boundary at an angle which is greater than the critical angle of total reflection, it is confined inside the waveguide. An evanescent field develops at the sensors surface. Most of the laser light is transmitted into the device and multiple reflections occur as it travels through the medium if a bioactive substance is placed over the surface. Some of the light, however, however, penetrates the bio layer. This light is reflected back into the waveguide with a shift in phase interfering with the transmitted light. Thus, changes in properties of the bio layer can be followed by detecting the changes in interference. (Delisa et al., 2000).

2.4.4.4 Surface plasmon resonance (SPR)

Polarized light is directed is directed from a layer of high RI towards a layer with low RI to result in total internal reflection. The sample is attached to the layer of low RI. At the interface of the two different media, a thin (approximately 50nm) gold film is interposed. Although light does not propagate into the low RI medium, the interfacial intensity is not equal to zero. The physical requirement of continuity across the interface is the reason for exciting the surface electrons (plasmons) in the metal film by the light energy. As a result, the electrons start oscillating. This produces an exponentially decaying evanescent wave penetrating a defined distance into the low RI medium, which is accountable for a characteristic decrease in the intensity of the reflected light. Hence, direct insight changes of the RI at the surface interface is made possible by monitoring the intensity and the resonance angle of the reflected angle of the reflected light, caused by the bio specific interactions which took place there (Liedberg et al., 1995).

2.4.5 Microgravimetric imunosensors

A direct measurement of mass changes induced by the forming of antigen/antibody complexes is also enabled by acoustic sensors. The principle of operation is based on the propagation of acoustic shear waves in the substrate of the sensor. Phase and velocity of the acoustic wave are influenced by the specific adsorption of antibody molecules onto the antigen-coated sensor surface. Piezo

electric materials such as quartz (SiO_2), zinc oxide (ZnO) resonate mechanically at a specific ultrasonic frequency (in the order of tens of megahertz) when excited in an oscillating electrical field. The resonant frequency is determined by the distance between the electrodes on both sides of the quartz plate, which is equal to the thickness of the plate and the velocity of the acoustic wave within the quartz material (Aberl et al., 1997).The microgravimetric sensor devices are divided into quartz crystal microbalance (QCM) devices applying thickness-shear mode (TSM), and devices applying a surface acoustic wave (SAW) detection principle (Cavic et al., 1999)

2.5 Conducting Electroactive polymers (CEPs)

CEPs and in particular polyaniline, polypyrrole, polythiophene and their derivatives have unique electrical, electrochemical and optical properties. These materials are finding growing applications in a number of industrial sectors, including electrical conductors, non linear optical devices, polymer light emitting diodes (LEDs), electro chromic or smart windows, photoresist, antistatic coatings, sensors, batteries, electromagnetic shielding materials, artificial noses and muscles, solar cells, electrodes, microwave absorbing materials, new types of memory devices, nanoswitches, optical modulators, and valves, imaging materials, polymer electronic interconnects, nanoelectronic and optical devices and transistors (Skotheim et al., 1998;Kumar and Sharma,1998;Jia et al., 2003;Ogurtsov et al., 2004). CEPs also referred to as conjugated polymers because they are macromolecules containing a spatially extended π-bonding
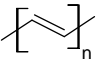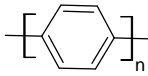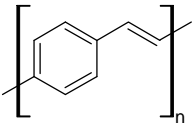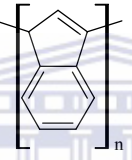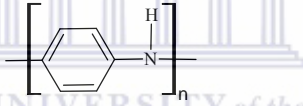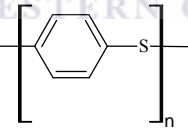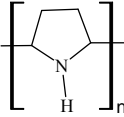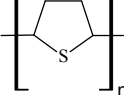
system, which is the reason of their semi conducting nature. Generally, conjugated polymers become electrically conductive by means of doping reactions (Dispenza et al., 2006).The chemical nature of CEPs and the facile methods of assembly available makes them compatible with many of the chemistries found in nature. Polypyrrole are formed under mildly oxidative conditions from aqueous media. The mild conditions used for polymerization are ideal for incorporation of enzymes, antibodies or even whole living cells. Polyaniline can be formed under similar conditions, although formation of the highly conducting form requires the presence of acid. Simple polythiophenes require a more extreme oxidation potential and these monomers are not water soluble. However attachment of simple functional groups e.g. alkyl sulphonate, to the monomer overcomes this problem. The unusual surface chemistry of these conductors, being organic in nature as opposed to metallic, appears to facilitate interactions with biological molecules. The electronic properties of CEPs enables information about biomolecular events occurring on/in the active polymer to be relayed back to the electronic interface to produce analytical signals. The electronic information relayed back may be due to direct oxidation/reduction of the analyte or a product from an enzymatic reaction involving the analyte. In cases where no electroactive species are present, the biomolecular interaction of interest may give rise to a change in electronic properties (conductivity, capacitance) of the polymer and the electrochemical switching properties of the polymer (Wallace et al, 1999).

Polythionine belongs to phenothiazine group of organic compounds. Thionine is a promising material since it contains two amino groups in the α positions and can be electrochemically polymerized by potentiodynamic methods from acidic (Saez

31

et al., 1993; Bruckenstein et al., 1990; Lee et al., 1990) to neutral (Gao et al., 2003; Yang et al., 1999) and slightly alkaline media (Karyakin et al., 1999; Xiao et al., 1999) and onto different substrates as gold (Schlereth and Karyakin, 1995), platinum (Hammet and Hillman, 1987) and carbon (Gao et al., 2003). An electropolymerization similar to polyaniline has been proposed due to the presence of primary amine electron-donating groups and at least one non-substituted *ortho* or *para* position in the aromatic ring. In this case, it occurs it occurs after the formation of a stable single charged cation-radical, upon monomer irreversible oxidation at fairly positive potential, just before oxygen evolution (Schlereth et al., 1995).

UNIVERSITY *of the*
WESTERN CAPE

Table 2.1: Names, structures, and conductivities of some common conducting polymers.

Conducting polymer	Structure	Conductivity (S/cm)
Polyacetylene		1000
Polyparaphenylene		100-500
Polyparaphenylene vinylene		3
Polyazulene		0.1
Polyaniline		1-100
Polyparaphenylene sulfide		1-100
Polypyrrole		40-100
Polythiophene		10-100

2.5.1 CEPs based electrochemical sensors

Ivaska et al. 2001 reported a Ca^{2+}-selective polyaniline based membrane consisting of polyaniline, bis [4-(1, 1, 3, 3-tetramethylbutyl) phenyl] phosphoric acid, and dioctyl phenylphosphonate. A polypyrrole based potassium micro sensor in plasticized polyvinyl chloride membranes was also been reported by Zachara et al., 2004. A ternary hybrid system glass/polypyrrole/Pt was been reported by Kaden et al., 2004. They used it as a solid inner contact for an all solid state pH glass electrode. Polypyrrole with chloride or nitrate doping was coated chemically onto pH sensitive silicate glasses with high lithium content. The sensor showed favorable for pH sensor applications. Potentiometric Ag^+ sensors have been prepared by galvanostatic electropolymerization of 3, 4-ethylenedioxythiophene on glassy carbon electrodes (Mousavi et al., 2006). A thiophene derivative, (4-benzeno-15-crown-5 ether)-thiophene-3-methylene-amine monomers on Au(III) surfaces have been reported to promote ordered polymerization to form polymer nanoparticles or clusters by which the size of the polymer nanoparticles could be controlled electrochemically. The resulting sensor exhibited the selective response towards potassium ion with a detection limit of 4 x 10^{-5} M (Si et al., 2007). Electropolymerization of polypyrrole in the presence of Eriochrome Blue-Black B as the counter anion has been reported to generate selective recognition for silver ions in the range of 1x 10^{-8} to $1x10^{-1}$ M Ag^+, with a detection limit of 6 $x10^{-9}$ M (Zanganeh and Amini, 2007). Electrochemical properties of poly (3, 4-ethylenedioxythiophene) doped with hexacyanoferrate (II, III) ions have been studied in the presence of Cu^{2+} ions. Binding of Cu^{2+} ions in the conducting

polymer layer results in analyte ions flux into the transducer phase and a lower detection limit of 10^{-7} M Cu $^{2+}$ was achieved (Ocypa et al., 2006). Zejli et al., 2006 developed a mercury ion sensor by electropolymerization of 3-methylthiophene on the surface of a bare sonogel-carbon electrode. This electrode showed a detection limit of 1.4×10^{-3} mg L^{-1} Hg (II). An all solid-solid-state calcium selective electrode has been constructed with polypyrrole solid-contact doped with calcium complexing ligand Tiron (Konopka et al., 2004). The good potentiometric response of this sensor was linear in the concentration range between 10^{-4} to 10^{-9} M with a slope close to Nernstian and detection limit equal to $10^{-9.6}$ M. Polypyrrole derivatized at the 3-position with dimethoxybenzyl and dihydroxybenzyl functionalities has been used to develop a pH sensor (Aquino-Binag et al., 1996). Anodic coupling of 5, 5'-bis (3, 4-(ethylenedioxy) thien-2-yl)-2, 2'-bipyridine has been reported to produce a polymer film that are able to coordinate protons and divalent transition metal ions (Fe^{2+}, Co^{2+}, Ni^{2+} and Cu^{2+} with corresponding spectral and redox changes (Zotti et al., 1999). Wu et al., 2000 reported a sensor array for Fe^{3+}, Cu^{2+}, Co^{2+} and Ni^{2+} consisting of 15 phenolic homopolymers and copolymers generated from phenolic monomers by peroxidase-catalyzed oxidative polymerization. The different metal ions had different binding capabilities with heteropolymers. This property can be utilized to prepare a wide variety of sensors with commercially available phenols. Potentiometric Ag^{+} sensors were prepared by galvanostatic electropolymerization of 3, 4 ethylenedioxythiophene and pyrrole on glassy carbon electrodes by using sulphonated calixarenes as doping ions (Jovanovi et al., 1995). Gonzalez-Bellavista et al., 2007 reported a nitrate ion selective electrode

using sulphonated poly (etherketone), an ion conducting polymer, as a polymer matrix. Electrochemically coated films of over oxidized polypyrrole directed single walled carbon nanotubes onto glassy carbon electrode were reported, which exhibited excellent electroactive properties for nitrite, ascorbic acid, dopamine and uric acid (Li et al., 2007). A perchlorate ion (ClO_4^{-}) sensor based on doped poly (3, 4-ethylenedioxythiophene) film was reported by Bendikov and Harmon, 2005. This conducting polymer was extremely stable in oxidized state and the prepared sensor exhibited a longer life time for more than 8 months, which is higher than the analogous sensors. Platinum electrodes modified with a cellulose acetate membrane or with poly (1, 8-diaminonapthalene) film were used for the rapid amperometric detection of nitrite and nitrate ions in water (Badea et al., 2001). This is a reagentless method. Although it has a short lifetime of less than 12 weeks, it is almost free from interferences. A potentiometric sensor for sulfide ion based on electrochemically deposited film of poly (3-methylthiophene) and poly (dibenzo-18-crown-6) onto an alloy substrate has been reported by Atta et al., 1998. An NO sensor based on a carbon fiber microelectrode modified by a poly (N-methylpyrrole) incorporating $[(H_2O) Fe^{III}PW_{11}O_{39}]^{4-}$ sub layer and coated by a Nafion external layer was reported by Fabre et al., 1997. An ammonia sensor has been developed by using an amino-silane ((CH_3O) $_3$-Si-(CH_2)$_3$NH (CH_2)$_2$-NH_2) self- assembled monolayer, employed as artificial seeds for chemical polymerization of polyaniline (Sutar et al., 2007). The sensor exhibited a detection limit of 2.99 x 10-5 M but at low concentrations of ammonia, response time was very slow. Polyaniline-(acrylonitrile-butadiene-styrene) composite film has also been reported for aqueous ammonia (Koul et al., 2001).

Polythionine modified electrodes have been used for the development of catalytic biosensors with enzyme immobilization by cross linking (Gao et al., 2003) or using a nafion membrane (Yang et al., 2004).

2.5.2 CEPs-based electrochemical immunosensors

Electrochemical immunosensors combine the analytical power of electrochemical techniques with the specificity of biological recognition process. Electropolymerization of electrically conducting polymers is an alternative method for controlling the thickness and dielectric properties of the immunosensor surface. The incorporation of antibodies into conducting polymer films was first reported in 1991 (John et al., 1991). Anti-human serum albumin (anti-HSA) was corporated into a polypyrrole film, which was galvanostatically polymerized onto a platinum wire substrate. When the pyrrole anti-HSA was exposed to HSA, a reduction peak was observed suggestibg that it could be due to an antibody/antigen interaction with the polymer. Further work by the same group gave rise to reports of a reversible real-time immunosensor (John et al., 1991). Other early work utilized a pulsed amperometric detection technique for other analytes, including p-cresol (Barnett et al., 1994), thaumatin (Sadik et al., 1994) and polychlorinated biphenyls (Bender and Sadik, 1994). As the use of conductive electroactive polymers in the development of electrochemical immunosensors continues to grow, there is need to understand the electrochemistry of antibody-modified conducting polymer electrodes. Studies on the charge transfer mechanism of an antibody (i.e. antihuman serum albumin) immobilized on a

polypyrrole electrode was carried out. The results revealed that the antibody-antigen reaction was responsible for varying the capacitative behaviour of the polymer. It was suggested that the interactions between the negatively charged antibody and the positively charged polypyrrole chain gave rise to the variations in capacitance. Investigations of several antibody immobilization methods (entrapment in a polypyrrole layer and covalent attachment with a silane molecule) were done and a form of impedance spectroscopy (differential impedance spectroscopy) developed to characterize the surface density and antibody-antigen reaction (Sargent et al., 1999; Sargent and Sadik, 1999; Sadik et al., 2002). Ouerghi et al electrodeposited polypyrrole onto a gold surface and immobilized an anti-human IgG via an avidin-biotin coupling reaction. EIS detected impedance changes in the low frequency region as a function of antigen concentration, suggesting that the surface layer of the immunosensor becomes modified.
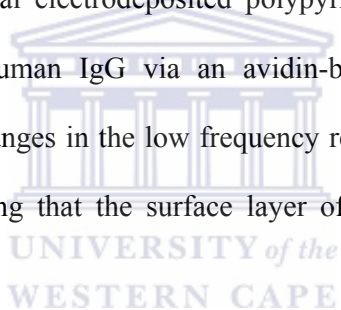
Miao and Guan, 2004 developed an impedance-based immunosensor for a-fetoprotein by immobilizing an anti-human monoclonal a fetoprotein immunoglobin G onto a polyaniline modified carbon electrode. EIS confirmed that the electron-transfer resistance increases with elevated a fetoprotein levels in the range 200-800 ng/ml, and both the number of polymerisation cycles and the applied potential influenced the sensitivity of the immunosensor towards a fetoprotein. Impedimetric transduction platform was used to detect chagas disease in blood sera. Impedance spectra were collected at a range of potentials, surface treatments and in the presence and absence of a redox system (Diniz et al., 2003).

A label free and reagentless immunosensor based on direct incorporation of antibodies into conducting polymer films at the surface of the screen-printed electrode (SPE) using an AC impedimetric response electrochemical interrogation was reported by Grant et al., 2005. They indicated that the real component of the impedimetric response acts as a dominant component of AC impedimetric response of anti BSA loaded conducting polypyrrole (PPy) film on its exposure to the different concentration of BSA. BSA could be detected with a linear response from 0 to 1.136 x 10^{-6} M. The nature of the observed Faradaic current arose due to antibody-antigen interaction. The use of SPE may be advantageous for miniaturization of the immunosensor. Gooding et al., 2004 fabricated a glassy carbon electrode modified with anti-rabbit IgG antibody entrapped in an electrodeposited polypyrrole membrane for label free amperometric detection of IgG antigen in flow injection system. Tahir et al., 2005 described the characteristics of polyaniline compounds in different protonic acid for application to diarrhea virus detection based on polyclonal and monoclonal BVDV antibodies. The proved that polyaniline with perchloric acid shows the highest conductivity in pH 6.6 and the sensitivity of the immunosensor ranged from 103 to 104 cell culture infective dose (CCDI)/mL . Lillie et al., 2001 fabricated a simple immunosensor format by polymerizing pyrrole loaded with avidin or antibody to luteinizing hormone (LH) on a gold inter-digitated electrode and demonstrated that impedance spectroscopy can be used to detect LH between 1 and 800 IU/L⁻ Farace et al., 2002 developed a reagentless immunosensor for the detection of luteinizing hormone based on antibody entrapped in a conducting polypyrrole matrix using impedance spectroscopy. Grennan et al., 2003 developed

39

an amperometric immunosensor for the analysis of atrazine using recombinant single chain antibody (scAb) fragments. The sensors were based on carbon paste SPE incorporating PANi/PVSA, which enabled direct mediator less coupling to take place between the redox centres of antigen-labelled HRP and the electrode surface. No separation of bound and unbound species was necessary as is the case with conventional immuno assays. An immunosensor based on multilayer-coated GCE was designed to determine to determine isopentenyl adenosine (iPA) in plants. The multilayer consisted of polypyrrole and poly (m-phenylenediamine) with $K_4Fe (CN)_6$ and HRP entrapped during electroploymerization. The ferrocyanide doped in polypyrrole functioned as the mediator. The glucose

oxidase bound on the immunosensor by the competitive immunoreaction involving iPA catalyzed the oxidation of the added glucose with the formation of hydrogen peroxide, which is in turn reduced in the presence of HRP entrapped in poly (m-phenylenediamine). The current of the oxidized production of ferrocyanide is inversely proportional to the concentration of iPA (Li et al., 2003). A strategy for fabrication of amperometric immunosensor for human IgG assay based on ZnO/chitosan composite as sensing platform was described by Wang et al., 2006. The immunosensor which combined the advantage of inorganic species ZnO and organic polymer, chitosan, can maintain the biological activity. A sequential sandwich immunoassay format was performed on the ZnO/Chitosan composite supported by glassy carbon electrode using goat-anti-human IgG antibody and human IgG as a model system. An impedimetric immunosensor for the antibiotic ciprofloxacin was fabricated by Garifallou et al., 2007. Polyaniline was electrodeposited onto the sensors and then utilized to immobilize a

biotinylated antibody for ciprofloxacin using classical avidin-biotin interactions.Electrodes containing the antibodies were exposed to solutions of the antigen and interrogated using AC impedance protocol. The faradaic component of the impedance of the electrodes was found to increase with increasing concentration of antigen.

2.6 Role of Gold Nanoparticles in Immunosensors

Gold nanoparticles have attracted considerable interest due to their specific electronic, optical, magnetic, and chemical properties. Immobilization of redox proteins on colloidal gold is thought either to help the protein to assume a favoured orientation or to make possible conducting channels between the prosthetic groups and the electrode surface, and they will both reduce the effective electron transfer distance, thereby facilitating charge transfer between electrode and the redox proteins. (Liu et al., 2003). In immunosensors gold nanoparticles play an important role both in the enhancement of the electrochemical signal transducing the binding reaction of antigens at antibody-immobilized surfaces and in stabilizing the immunoreagents.

A potentiometric immunosensor for direct and rapid detection was developed by self assembling of monoclonal diphtheria antibody onto a platinum electrode based on the use of gold nanoparticles-silica nanoparticles mixture and polyvinyl butyric as matrices. Anti-Dip was adsorbed onto the surface of the nanoparticles mixture, and then they were entrapped into the polyvinyl butyric sol-gel network. The immobilized Daphna exhibited direct potentiometric response towards Dip hag. The immunosensor using the nanoparticles mixture exhibited much higher sensitivity, better reproducibility and long term stability than those constructed with gold nanoparticles or silica nanoparticles alone (Tang and Ran. 2005). A highly sensitive electrochemical impedance immunosensor was developed using an amplification procedure with a colloidal gold-labelled antibody as the primary amplifying probe, and a multistep amplification sequence. Rabbit anti-human IgG antibody was immobilized through a self assembled colloidal gold layer on a gold electrode. The analyte, human IgG, was detected through the impedance measurements with the sensing interface modified by rabbit anti-human IgG antibody. In the primary amplification, the colloidal gold-labelled goat anti-human IgG antibody was used to amplify the electron transfer resistance resulting from the antigen binding to the immunosensor surface. A further amplification was performed through sequential binding of the colloidal gold labelled goat anti-human IgG antibodies (Chen et al., 2006). A separation-free electrochemical immunosensor for carcinoma antigen-125 (CA 125) was developed based on the immobilization of CA 125 antigen on colloidal gold nanoparticles that was stabilized with cellulose acetate membrane on a glassy carbon electrode. A competitive immunoassay format was employed to detect

CA125 antigen with HRP labelled CA125 antibody as tracer, o-phenylenediamine and hydrogen peroxide as enzyme substrates. Amperometric response decreased with an increasing CA125 concentration in the sample solution (Wu et al., 2006). Carbohydrate antigen 19-9 (CA-19-9) is one of the most important carbohydrate tumour markers, expressed in many malignancies as pancreatic, colorectal gastric and hepatic carcinomas. Dan et al., 2007 developed a reagentless immunosensor for rapid determination of carbohydrate antigen 19-9 (CA19-9).The strategy was based on the immobilization of antibody in colloidal gold nanoparticles modified carbon paste electrode and the direct electrochemistry of horseradish peroxidase (HRP) that was labelled to a CA19-9 antibody. The nanoparticles were efficient in for preserving the activity of immobilized biomolecules. The method avoids the addition of electron transfer mediator, thus simplifies the immunoassay procedure and decreases the analytical time. A strategy to construct amperometric immunosensor for Schistosoma japonicum antigen (SjAg) assay based on nano-size particulate gold (nano-Au) monolayer as sensing platform was designed by Lei et al., 2003. The nano-Au monolayer was obtained through chitosan-entrapped carbon paste electrode (CCPE). The high affinity of chitosan entrapped in CCPE for nano-Au associated with its amino groups facilitated the formation of nano-Au monolayer on the surface of CCPE. A sequential competitive immunoassay format was performed on the nano-Au monolayer supported by CCPE using S. japonicum (SjAb) SjAg as a model system. The assay comprised of loading SjAb on nano-Au monolayer, then blocking in BSA solution, followed by a competitive incubation in buffer containing the SjAg and SjAg labelled with HRP and amperometric detection with hydroquinone as enzymatic substrate.

Carcinoembryonic antigen (CEA) is a well known marker associated with progression of colorectal tumours. A current amplified immunosensor for its determination was fabricated by coating negatively charged polysulfanilic acid modified GCEs with positively charged toluidine blue. This approach provided an interface containing amine groups to assemble gold nanoparticles for immobilisation of the carcinoembryonic antibody and HRP (Xuelian et al., 2006). Wang et al., 2004 has showed that it is possible to improve the sensitivity of an immunosensor by using a combined self assembled monolayer of 4-aminothiophenol and Au colloidal particles to increase the efficacy of antibody immobilization. The assembly of various surface layers along with the effect of incubation time and antigen were evaluated by EIS. These studies revealed that the electron transfer resistance increases with elevated antigen concentrations.
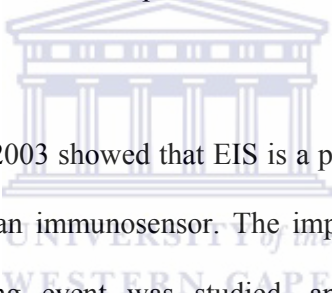
Li et al., 2006 fabricated an amperometric immunosensor based on toluidine blue/nano-Au through electrostatic interaction for determination of CEA. The electrode was fabricated by positively charged toluidine blue (TB) coated on negatively charged polysulfanilic acid (PSSA) modified glassy carbon electrode (GCE) surface through electrostatic interactions to form TB/PSAA film, which provided an interface containing amine groups to assemble gold nanoparticles for immobilization of CEA and HRP. The proposed method is economical, efficient and potentially attractive for clinical immunoassays. Amperometry was used to determine the amount of HRP fixed on the sensor surface, which was related to the content of the desired human IgG. An amperometric immunosensor for the detection of AFP based on the integration of microelectronics technology; mixed with self-assembled monolayers (SAM), gold nanoparticles and enzyme

amplification was developed by Xu et al., 2006. The immunosensor was fabricated using Au, Pt and Pt three microelectrode system and two microwells constructed by SU-8 photoresist on silicon wafer. Using mixed SAMs and nanogold, a mixed monolayer comprising cysteamine and 1, 6 hexanedithiol was formed on the working electrode surface to assemble nanogold and further to immobilize AFP antibody for detecting AFP in human serum samples. The resulting immunosensor has advantages, such as miniaturization, compatibility, high specificity, good reproducibility and long-term stability, which make it potentially attractive for clinical immunoassays. Zhuo et al., 2005 fabricated an amperometric immunosensor for rapid determination of AFP in human serum. The immunosensor was prepared by entrapping thionine (Thi) into nafion (Nf) to form a composite Thi/Nf membrane, which yields an interface containing amine groups to assemble gold nanoparticles layer for immobilization of anti-AFP. Yuan et al., 2005 developed a label free amperometric immunosensor for fast and sensitive assay of Japanese B encephalitis vaccine. Antiserum of Japanese B encephatilis were immobilized on bilayer nano-Au/o-phenylenediamine polymer film deposited Prussian blue as an electronic mediator on the Pt electrode. The variation of amperometric response to the concentration of Japanese B encephalitis vaccine, the target antigen was evaluated with cyclic voltammetry.

2.7 Electrochemical impedance spectroscopy (EIS) based immunosensors

The development of hand held devices for point of care measurements is a promising alternative to existing laboratory based immunochemical assays. In most immunosensors, the antibody is immobilized onto a conductive support, and

the electrical properties of the interface are modified when the antibody reacts with the antigen of interest. The surface organization and assembly of antibodies is a critical step in the fabrication of an immunosensor device. Characterizing the immobilization of the antibody along with its stability/activity and interaction with the antigen are important steps in optimising the analytical performance (i.e. selectivity, stability, sensitivity, response time etc) of the immunosensor. The formation of an antigen-antibody complex on a conductive support alters the impedance features of the interface, and impedance spectroscopy has been used to study the antigen-antibody molecular recognition event by measuring the resistive and/or capacitive change that accompanies this reaction.

Studies by Corry et al. 2003 showed that EIS is a powerful method for predicting the surface activity of an immunosensor. The impact of immobilization on the antibody-antigen binding event was studied, and it revealed that covalent attachment of an antibody to the electrode surface is needed for a successful impedance-based immunosensor. An immunosensor was developed for human mammary tumour and EIS used to collect mechanistic information (charge transfer resistance and double layer capacitance) on antibody adsorption onto gold and interaction with the specific antigen (Jie et al., 1999). Cui et al. 2003 used EIS to characterize the growth of a multilayer film that comprised avidin and biotin labelled antibody (goat anti hIgG antibody) formed on a mercaptopropionic acid modified gold electrode. It was observed that the electron transfer resistance increases proportionally with the number of avidin/biotin antibody layers. EIS is extremely useful in monitoring the immunosensor surface properties

46

before and after antibody immobilization in a phosphate buffer solution (Zhou and Muthuswamy, 2004). The generation of a precipitate onto the electrode surface via bio catalysis can lead to a substantial increase in the interfacial impedance. An antibody modified indium tin oxide electrode has been used in conjunction with EIS in detection of *Esherichia coli*. Signal amplification was accompanied by using combined redox probe and antibody labelled enzyme (alkaline phosphatase), and it was demonstrated that the interfacial electron transfer resistance increases at elevated levels of *E. coli*. Similar impedance trends were observed without enzymatic amplification (Ruan et al., 2002; Yang et al., 2004). Zayats et al., 2002 fabricated an ISFET device to monitor antigen-antibody binding processes, and used EIS to follow the thickness of various films formed on the ISFET surface. Betty et al 2004 fabricated a capacitative immunosensor based on electrolyte insulator porous silicon structures, and employed EIS to characterize the interfacial region after different surface treatments

In most EIS studies, measurements are made over a wide frequency range in order to obtain the various interfacial parameters (charge transfer resistance or double layer capacitance). However, Dijksma et al 2001 developed an electrochemical immunosensor for the detection of the protein interferon-γ by monitoring the biorecognition event at a single frequency. The immunosensor comprised a self-assembled monolayer of cysteine attached to polycrystalline Au surface, and the antibody was covalently bonded using carbodoiimide/succinimide chemistry.

2.8 Immunosensors for Mycotoxins detection

Conventional methods for mycotoxins analysis are usually performed by thin layer chromatography (TLC), gas chromatography (GC) coupled to ultraviolet/visible, fluorescence or mass spectrometry (MS) and high performance liquid chromatography (HPLC). (Pittet et al., 2005). These methods involve expensive and time-consuming steps: extraction with organic solvents from complex matrices, sample clean-up to remove interferents, pre concentration and sometimes analyte derivatization. The goal of more recent studies has been to simplify and expedite the method of detection while attempting to maintain or improve the sensitivity. Biosensors have rapidly developed in the past decades for the rapid sensitive and specific assays for analysis/monitoring of food, water and air samples for contamination by mycotoxins. Various biosensors for the detection of mycotoxins have been developed some of which are mentioned in the following paragraphs below.

Vangelis and Dimitrios, 1997 and Siontorou et al., 1998 explored the transduction of interactions of aflatoxin M_1 with bilayer lipid membranes (BLMs). This was used for the direct electrochemical sensing of aflatoxin M_1 and for the construction of single-use devices. Christina et al., 1998, explored the interaction of AFM_1 with self assembled metal-supported bilayer lipid membrane (s-BLMs) and its effects on the DNA hybridization. The interactions of AFM_1 with s-BLMs composed of egg phosphatidylcholine produced reproducible ion current increases within 8-10 seconds after exposure to the toxin. The magnitudes of the current

48

signals were related to the toxin concentration, which could be determined within the range of 1.9-20.9 Nm (Christina et al., 1998). An impedimetric immunosensor based on colloidal gold and silver electrodeposition for the detection of AFM_1 was reported by Attila et al., 2009. An indirect ELISA procedure was performed on SPEs in presence of anti-AFM_1 gold-labelled antibodies. Silver was chronoamperometrically electrodeposited at afixed applied potential and for a determined period of time to amplify the signal.The calculated charge transfer resisitance (R_{ct}) correlated well with the concentration of AFM_1.The linear working range was 15-1000 ng/L with alimit of detection of 15 ng/L (Attila et al.,2009). An electrochemical immunosensor fabricated by immobilising antibodies directly on the screen printed electrodes (SPEs) was evaluated for the determination of AFM_1 in milk. Detection was achieved by allowing competition to occur between free AFM_1 and that conjugated with peroxidase enzyme. Corresponding results showed screen printed electrodes for detection of AFM_1 provided a detection limit of 25 ppt.Comparison of spectrophotometric and electrochemical results suggest that a better detection limit and shorter analysis time could be achieved using electrochemical detection (Micheli et al., 2005).

Campàs et al., 2007b developed an enzyme sensor for the electrochemical detection of the marine toxin okadaic acid (OA). The strategy was based on the inhibition of the immobilized protein phosphatase by this toxin and the electrochemical measurement of the enzyme activity by the use of appropriate enzyme substrates, electrochemically activated after dephosphorylation by the enzyme. Colorimetric inhibition assays demonstrated that the phosphatase from human red blood cells was more sensitive and provides a wider linear range than

49

the one produced by genetic engineering. Two different enzyme substrates have been tested. The previous sensors rely on the inherent character of mycotoxins, such as blocking of ion channels and inhibition of the enzyme active site. The optical wave guide lightmode spectroscopy (OWLS) technique was applied for the detection of aflatoxin and ochratoxin in both competitive and in direct immunoassays by Adanyi et al., 2007. After immobilizing the antibody or antigen conjugate for the direct or indirect measurement, respectively, the sensor chip was used in a flow injection analyzer (FIA) system. Alarcón et al., 2006 developed a monoclonal antibody based electrochemical immunosensor for the determination of ochratoxin A (OTA) in wheat. The assays were carried out using monoclonal antibodies in the direct and indirect format, thereby resulting in the development of disposable screen-printed electrodes for quantitative determination of OTA. Oliveira et al., 2007 studied the redox properties of OTA using electrochemical techniques which provided insights into the biological redox reactions of this molecule. The in situ evaluation of the OTA interaction with DNA using a DNA-electrochemical biosensor is also reported. Prieto et al., 2008 investigated two indirect competitive ELISA strategies with different OTA immobilization procedures for the development of OTA electrochemical immunosensors. Khan et al., 2008 developed a sensitive CS/TiO_2 bioactive electrode to determine OTA. The limit of detection was 10 ng/mL. Yu et al., 2005 synthesized a molecularly imprinted polypyrrole film on a SPR sensor surface for detection of OTA. The molecularly imprinted polypyrrole film was electrochemically polymerized on the sensor surface from a solution of pyrrole and OTA in ethanol/water (1:9 v/v). The film growth was monitored in situ by determination of the increasing SPR angle.

Binding properties of the molecularly imprinted polypyrrole film were investigated by loading OTA standard solutions in an integrated 20-µL flow cell.

A biosensor array was used for the detection of ochratoxin A (OTA), fumonisin B (FB), aflatoxin B_1 (AFB$_1$) and deoxynivalenol (DON). The limit of detection (LOD) was 0.3 ng/mL for AFB$_1$ (Sapsford et al., 2006a). An indirect competitive immunoassay array biosensor was applied for detection of AFB$_1$ in corn and nut products. LODs obtained ranged from 1.5-5.1 ng/g and 0.6-1.4 ng/g for corn and nut products respectively (Sapsford et al., 2006b). A disposable electrochemical immunosensor for simple and fast measurement of AFB$_1$ in barley has been reported. The immunosensor strip was assembled by immobilising the biological component with the monoclonal antibody anti-AFB$_1$ (MAb). Results showed a detection limit of 30 pg/mL (Nagwa et al., 2004). Piemarini et al., 2009 developed an enzyme-linked-immuno-magnetic-electrochemical-array (ELIME-array) for rapid detection of AFB$_1$ in corn samples. The system was based on an indirect competitive ELISA format using magnetic beads as immbolisation support and magnetised SPEs as electrochemical transducers. After optimisation sudies, the detection limit and sensitivity of the assay were calculated to be 0.6 and 1.5 ng/mL respectively. A biosensor assay format for AFB1 based on acetylcholinesterase (AChE) inhibition by AFB$_1$ was fabricated by Ben Rejeb et al., 2009. To develop the biosensor, choline oxidase was immobilized by crosslinking onto SPEs modified with Prussian blue. After optimization the linear working range was assesed to be 10-60 ppb with adetection limit of 2 ppb.

Gaag et al., 2003 developed an immunochemical biosensor for the detection of AFB$_1$, Zearalenone, OTA, FB$_1$ and DON in a single measurement. The different mycotoxins could be detected simultaneously in relevant concentrations within a time frame of 25 minutes, including the time needed for sensor regeneration. The application of the developed sensor on the miniature SPR device allowed for the development of low cost instruments, which can be used in field measurements. An immuno affinity fluorimetric biosensor was developed for detecting and quantifying aflatoxins. The aflatoxin biosensor provided rapid sampling and measurement capability with minimal sample handling and consumables. It provided very high sensitivity from 0.1 to 50 ppb in less than 2 minutes with 1mL/ sample and made over hundred measurements before refurbishment was required (Carlson et al., 2000). A plasmon surface resonance immunosensor was developed to determine fumonisins B$_1$ (FB$_1$) in spiked samples Polyclonal antibodies produced against FB$_1$ were adsorbed onto a thin gold film substrate, which were coupled to a glass prism in the Kretshmann configuration. When a sample containing FB$_1$ was added to a cell on the outside of the gold film, the angular profile of reflected light intensity shifted. This changed the resonance angle and the reflected beam intensity at a selected angle both of which were proportional to the FB$_1$. After optimization of the antibody over a layer, a detection limit of 50 ng/mL was obtained (Mullet et al., 1998).

2.9 Biological Recognition-Bio receptors

The sensing element in a biosensor is a highly receptive bio receptor. Compared to the most chemical sensing elements, these bio receptors show remarkable specificity towards one particular analyte or a group of analytes. Over the years, a number of different biological elements have been used in biosensors. The most important biomolecules for biosensors are enzymes with their specificity towards certain substrates. Also important is the biorecognition between antibody and antigen, used for immunological sensors. Other biomolecules frequently used are DNA strands with affinity towards complimentary strands or other molecules. Lectin was used due to its affinity to sugars. Other systems include whole cells, bacteria, yeasts, sub cellular fractions, membrane receptors and tissue slices (Blum, 1997).Depending on their biological element, biosensors can be catalytic sensors or affinity sensors (Tothill, 2001). In catalytic sensors, an enzyme reaction often involving the analyte causes the concentration change of a detectable compound. In affinity sensors, the binding between the analyte and receptor is monitored e.g. with antibodies or DNA.
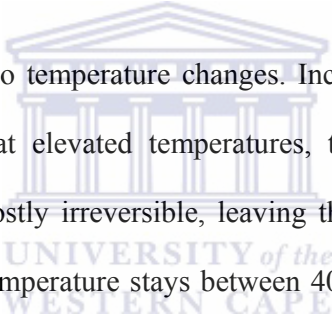
2.9.1 Enzymes

Enzymes are biological catalysts responsible for most chemical reactions in living organisms. Their main task is to initiate or accelerate reactions that would

otherwise not take place, or only very slowly, at the moderate temperatures predominant in organisms. They also slow down reactions if necessary, or split them up into separate steps, to control the heat evolution of exothermic reactions, otherwise the heat evolution could lead to cell death. Enzymes are the most commonly used biocatalysts in biosensors. Some enzymes such as urease are highly specific for one compound (Coulet et al., 1991). Other enzymes on the other hand, are specific for a whole group of substrates. The structure of enzymes is mainly made up of a single polypeptide chain, but the active site can be a separate molecule, embedded in the polypeptide backbone. Only certain molecules are allowed access through the protein shell and the binding site, and not the active site itself. When the substrate (S) binds to the binding site of the enzyme (E), a reactive intermediate, the enzyme substrate complex (ES) is formed. The complex ES is converted to E and a product (P) by the active site. During enzymatic reactions, substrates are consumed and products formed. These compounds can be monitored with suitable transducers. In the case of glucose oxidase, these compounds are O_2 and H_2O_2, which are easily detected. Some enzymes have additional active areas referred to as co-factors, e.g. NADH. Such co-factors can be used for measuring enzyme activity (Coulet et al., 1991). Many enzymes also require metal ions for their catalytic activity.

There are two main applications for enzyme in biosensors. They can either be used as catalytic biosensors or as markers in affinity biosensors, such as immunosensors and DNA sensors. In catalytic enzyme sensors, the concentration of enzyme (E) is constant and the substrate concentration is much smaller. When

the enzyme is used as a label for antibodies or DNA strands, the substrate must be used in excess and the enzyme concentration (E) is the only limiting factor. Since enzymes can convert hundreds of substrate molecules per second, they are highly efficient chemical amplifiers for the detection of other molecules (Aizawa et al., 1991). Various enzymes are used as labels; including horseradish peroxidise (HRP), glucose oxidase and alkaline phosphatase (AP). Products of these enzymes can be detected spectrophotometrically and electrochemically. Other enzymes such as peroxidise or luciferase deliver products for luminal or luciferin luminescence, allowing optical detection.

Enzymes are sensitive to temperature changes. Increasing temperatures increase the reaction rate, but at elevated temperatures, the protein structure (tertiary structure) denatures, mostly irreversible, leaving the enzyme inactive. For most enzymes, this critical temperature stays between 40 $^{\circ}$C and 50 $^{\circ}$C, however, few enzymes possess high thermal stability above 100 $^{\circ}$C. Enzymes consist of amino acids and are therefore sensitive to pH. Enzyme reactions can be inhibited by various species. Inhibition may be reversible, allowing the enzyme to regain full activity after dissociation from the inhibitor. These inhibitors can competitively block the active sites or alter the enzyme activity by other mechanisms. Other inhibitors inhibit the enzyme and deactivate it irreversibly. These irreversible inhibitors can work in different ways, for example blocking the binding site, reacting with the central metal ion or denaturing the enzyme. Enzyme inhibition sensors have been reported for the detection of toxic compounds and heavy metal ions and are based on the selective inhibition of enzymes (Tothill, 2001).

2.9.2 Antibodies

The use of highly specific antibodies is very popular. The most important analytical applications of antibodies are immunoassay, immunosensor and immunoaffinity columns. Immunochemical techniques are highly sensitive, selective, simple and inexpensive (Hock et al., 1995). They are based on the ability of antibodies to form complexes with corresponding antigens. This interaction is highly specific and leads to very selective immunoassays. The extremely high affinity of the antibody antigen interaction leads to great sensitivity. New antibody technologies such as the production of antibody fragments or recombinant antibodies allow tailoring of the biomolecules for analyte and matrix requirements, within certain limits.

2.9.3 Antibodies-Production and Properties
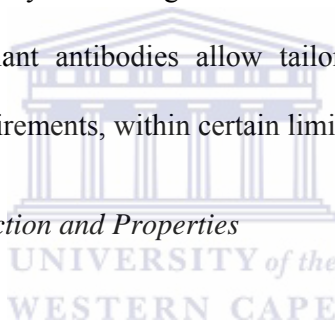
2.9.3.1 The immune system

Anti bodies are produced by mammals as part of an immune response of the host to foreign intruders such as micro-organisms, viruses, bacteria and parasites (Harlow and Lane, 1988; Crowther, 1995; Tijssen, 1985). The immune system specifically recognises and eliminates pathogens. The first line of defence is innate immunity, a non-specific defence reaction. More important for analytical science is the second line of defence, adaptive immunity. Adaptive immunity is directed specifically against the intruder and is mediated by cells called lymphocytes. The lymphocytes have specific cell surface receptors and secrete

proteins which are antibodies that specifically binds to the foreign species (antigen). At least 10^9 lymphocytes guarantee a quick adaptive immune response .These cells are omnipresent in the body, but accumulate in organs such as the spleen and lymph nodes. There are many different types of lymphocytes, but only three main classes all of which have surface receptors specific for the antigen. B cells (lymphocyte B) secrete antibodies and are therefore the most important lymphocytes for the analytical chemist. Cytotoxic T cells bind to the antigen via surface receptors and lyse the antigen. Helper T cells control and configure B cells and T cells. A single cell has only one type of receptor. Mutation and recombination can generate 10^8 different surface receptors and therefore 10^8 antibodies with different receptors (binding sites). Lymphocytes that produce antibodies against molecules of the host system are eliminated by a process called tolerance. A failure of the tolerance system leads to autoimmune disease. On the first exposure to a foreign molecule, the immune response is relatively slow. On the second exposure, lymphocytes produced during the first exposure recognise the antigen early and can react in a fast and strong immune reaction (antibody production). This mechanism is known as immunological memory. During the immune response, lymphocytes are produced and after removal of the antigen a few remain in the host system (memory). The process of introducing a foreign species (immunogen) into the organism of the host animal is termed immunisation.

2.9.3.2 Antibody Structure

Antibodies are a large family of glycoproteins. They can be classified in five classes, IgG, IgM, IgA, IgE and IgD. Immunoglobin G (IgG) is the most abundant immunoglobin species in serum and also the most commonly used antibody in sensor applications. Structural features are easiest explained using the IgG molecule that consists of one Y shaped unit (Figure 2.2). The other immunoglobin classes are also based on these Y shaped units. An IgG molecule can be described as consisting of four polypeptide chains, two identical heavy (H) chains and two identical light (L) chains (Figure 2.2) (Killard et al., 1996). The length of the two chains is 450 amino acids for the H-chain (~55,000 Dalton) and 212 amino acids for the L-chain (~25,000 Dalton). The two identical H-chains are connected via disulphide bridges. The connection between the L-chain and the H-chain consists also of disulphide bonds. Since all these bonds connect two chains they are named interchain disulphide bridges. Both chains L and H also have interchain disulphide bridges. The globular structure of the protein, that is responsible for the name immunoglobulin, is a result of these interchain bonds. The H-chain is divided into four sub domains and the L-chain into two sub domains. These sub domains are classified according to the variability of their amino acid sequence, into constant (C) and variable (V) regions. The sub domains of the H-chain are three C regions, C_H1, C_H2, C_H3 and one V region, V_H. The two sub domains of the L-chain are one C region and one C region C_L and one V region V_L. The base of the Y shape is called the Fc fragment (fragment that crystallises) and is formed by the association of the two C_H2 and the two C_H3 domains. Each arm of the Y shape is

called a Fab (fragment containing antigen binding site) and is formed by association of C_H1 with C_L and V_H with V_L. The small domain between C_H1 and C_H2 is called the hinge region and allows lateral and rotational movement of the Fab fragments. Furthermore, the terminal amino group of the amino acid sequence is allocated at the end of the Fab fragment, whereas the Fc fragment contains the terminal carboxyl group. For the antibody antigen interaction however, most of the IgG fragments are of minor importance. The binding site (paratrope) is located within the V_H and V_L domains and each arm contains one binding site. In the variable regions, amino acid sequences can vary from antibody to antibody and allow the specific adaptation to certain antigens. The exact regions within these variable regions that have very high amino acid variability are called hypervariable regions, also known as complimentary determining regions (CDRs). Three CDRs are integrated into the L-chain and three into the H-chain, resulting in six CDRs for each arm. The variability created by the CDRs of each Fab fragment allows the creation of 10^8 different binding sites.

The other sub domains are also of functional importance. C_H1 binds complementary C4b fragment, C_H2 contains carbohydrate binding sites and C_H3 domains are responsible for the interaction with the rest of the immune system. The H-chain is different for different immunoglobulin. IgG has a γ-chain, IgM a μ-chain, IgE a ε-chain and IgD a δ-chain. Differences in the chains result in subclasses such as IgG_1, IgG_{2a}, IgG_{2b} and IgG_3. All these different IgG subclasses mainly differ in the Fc fragment, and they appear and function in different stages

of the immune response. The analytical important IgG molecule, for example is dominant in the secondary response.
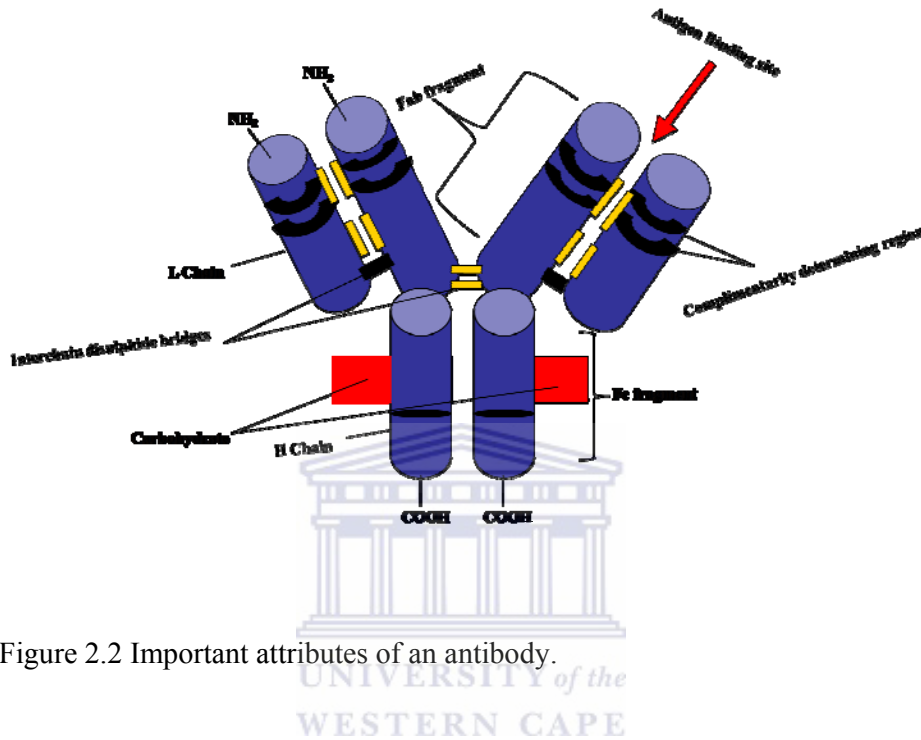
Figure 2.2 Important attributes of an antibody.

2.9.3.3 Antibody Antigen Interaction-Affinity

The region of an antigen that interacts with the antibody binding site (paratrope) is called the epitope. This means that epitopes are not intrinsic parts of the molecule. The actual part of the antigen molecule that acts as an epitope can vary from one antibody to another for exactly the same molecule. Antibody antigen interactions are reversible and non covalent and involve hydrogen bonds, van der waals forces, ionic coulombic interactions and hydrophobic bonds. Both, antibody and antigen can undergo substantial conformational changes upon interaction, but they may also stay unchanged depending on the specific antibody antigen pair. The measure

of the strength of the binding of an epitope to an antibody is their affinity. The equilibrium of their interaction can (Eq 2.1) can be described with the affinity constant K_A (Eq 2.2) Ab represents antibody and Ag antigen.

$$Ab+Ab \leftrightarrow Ab\text{-}Ag$$ Eq 2.1

$$K_A=[Ab\text{-}Ag] / [Ab].[Ag]$$ Eq 2.2

Even when, in theory the time to reach the actual equilibrium is independent from the affinity, in practice high affinity interactions can be considered almost complete in a substantially shorter time than low affinity interactions. High affinity complexes are also much more stable. Affinity constants range from 10^5 to 10^{12} M^{-1}. These high affinities are achieved by the tailored binding sites of the epitopes. The loss of one hydrogen bond in an interaction can result in 1,000 fold decreased affinity. Whereas the affinity constant for a monoclonal antibody can be determined, K_A for polyclonal serum is more difficult to determine. Polyclonal antibodies represent a mixture of antibodies, specific for the antigen, whereas monoclonal antibodies consist of identical immunoglobulin molecules. The specifications of immunosensors are determined to a large extent by the affinity of their components. High affinity results in sensitive sensors, but too high affinities might result in virtually irreversible sensors.

2.9.3.4 Avidity

Avidity is the measure of the overall stability of the antibody antigen complex (Harlow and Lane, 1988). For immunochemical reactions avidity is of more

practical importance than affinity, because it refers to intrinsic affinity of the paratrope for the epitope, the valency of the antibody and the geometric arrangement of the interacting compounds. High avidity is reached when all the paratropes can bind epitopes. In the case of IgM this can be up to ten epitopes. Avidity is also increased by multivalent systems, which many antibodies bind to different epitopes of the same antigen and also crosslink the antigens. This is easily achieved using polyclonal antibodies and large antigens with multiple epitopes. Further cross-linking (higher avidity) can be achieved by adding anti-IgG immunoglobulin, protein A or protein G beads. For surface bound antigens, avidity is increased by relatively dense antigen layers which allow bivalent binding and therefore increase the overall stability of the antibody antigen complex.
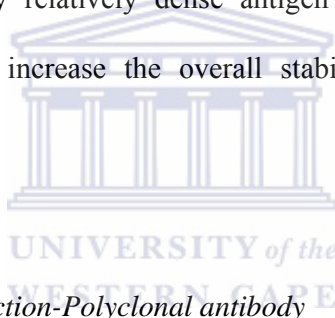
2.9.3.5 Antibody Production-Polyclonal antibody

For the production of polyclonal antibodies, an immunogen (analyte or analyte conjugate) is injected into a host animal. After immunisation, the host species, e.g. mouse, goat rabbit or sheep reacts with a primary immune response and mainly IgM is produced. In the following days and weeks, the host animal is injected again (boost injections), provoking a secondary response that produces IgG. The serum is tested throughout by ELISA for specific antibodies. After multiple boost injections, a high serum titre (high specific antibody concentration) is achieved. Polyclonal antibodies are used as serum or in purified form. Purification includes immunoprecipitation, protein A or protein G affinity purification and

immunoaffinity purification. As part of the immune response, B lymphocytes produce antibodies. Each lymphocyte produces only one type with exactly the same amino acid sequence, but many different lymphocytes produce many different antibodies. Many of these antibodies can be specific for one analyte, but for different regions with different affinities. These different antibodies specific for one analyte are called polyclonal antibodies. Phagocytosis refers to the first antigen processing steps. Antigens are non-specifically engulfed in antigen presenting cells (APCs), processed (lysed) and presented in fragments for further steps. Phagocytosis is difficult, or not possible for small soluble molecules. They are not immunogenic, i.e. trigger no immune response. For immunogenicity other factors such as degradability, binding to virgin B cells and cell to cell communication promotion are also important. In order to provoke an immune reaction of these low molecular weight analytes, they are coupled to carrier proteins, such as bovine serum albumin (BSA) or keyhole limplet haemocyanine (KLH). Antibodies are then raised against the analyte, the carrier and the analyte carrier complex including the spacer bridge. For immunoassay conjugates, special precautions have to be taken, such as different type conjugates for immunisation and immunoassay. The problem of polyclonal antibodies is that different animals or individuals or even exact same animal at a different time, will produce a polyclonal antibody serum of different composition, sensitivity and specificity. A limitless supply of a single antibody of defined specificity is guaranteed by using monoclonal antibodies.

2.9.3.6 Antibody Production- Monoclonal Antibodies

Production of monoclonal antibodies is based on the proliferation of a single antibody producing cell, yielding a uniform population of antibodies of the same type with identical affinities and specificities (Hock et al., 1995). A method called hybridoma technology guarantees unlimited production of monoclonal antibodies of the same isotype with constant properties. B lymphocytes only grow and divide for a short period of time (Killard et al., 1996). Myeloma cells are immortalised, to tumourigenic B lymphocytes, which grow and divide in vitro, but do not produce the antibody molecule required. A fusion of myeloma cells with cells that have antibody growing abilities is required for antibody production. Mice are immunised with the antigen and polyclonal antibodies are produced. The spleen of the mouse is removed (spleen cells contain a very high concentration of B lymphocytes) and spleen cells are fused with non-antibody producing myeloma cells using polyethylene glycol. The membranes of both cells fuse and merge. The cell nucleus also merges, the chromosomes are mixed and immortalised antibody producing hybridoma cells are obtained. Unfused spleen cells die and unfused myeloma cells are terminated on a selective HAT medium. The resulting mixture of polyclonal hybridoma is grown in culture wells, divided and diluted. If the supernatant of the wells contain specific antibodies, the well is further diluted and divided until the hybridomas in the well are clones from only a single parent cell, producing only one type of antibody. A monoclonal antibody producing hybridoma is derived. Normally, this procedure yields many hybridomas, which

produce specific antibodies. These monoclonal antibodies are tested for affinity and specificity and a few hybridoma cells are chosen for further development. Monoclonal antibodies can be grown in vitro, in culture flasks or bioreactors. Monoclonal antibodies can also be grown in vivo. Hybridoma cell are injected into the peritoneum of mice and the tumour-like growth rate produces large amounts of antibodies in ascetic fluid. In vitro methods deliver pure antibody in low yields and the in vivo method results in high yields of antibody, which are contaminated with proteins and other antibodies, and purification is necessary.

2.9.3.7 Antibody fragments and Recombinant Antibodies

A genetic technique called combinatorial phage display allows the production of the Fab fragment of antibodies, by combining the genes for these regions with phage particles and consequently producing them in bacteria cells (Killard et al., 1996). The two Fab fragments of an antibody are identical, containing two identical binding sites; however it is possible to create antibodies with two different binding sites. These bifunctional antibodies can be created chemically by cleaving the disulphide bonds and cross linking them with another antibody fragment. Biological production is achieved by fusing two hybridoma cells and the resulting antibody is called a quadroma. Genetically, it is possible to connect only the variable regions of two different antibodies. The resulting antibodies contain two different V_H regions and two different V_L regions. These bifunctional biomolecules are able to recognise two different molecules. It is possible to attach them to one molecule, while the second binding site is analyte specific. Examples

65

for the usefulness of bifunctional antibodies are immune-immobilisation and drug delivery to tumours (Killard et al., 1996).

Instead of using whole antibodies, it is also possible to use only the binding sites, parts of the binding sites containing fragments which can be obtained either enzymatically or genetically. Enzyme scan cleave the important Fab fragments from the Fc fragment which is less important for most sensor applications. The enzyme papain produces two Fab fragments per antibody, cutting the antibody between the hinge region and the Fab fragment. The enzyme pepsin cuts the antibody between the hinge region and the Fc segment, resulting in F (ab) $_2$ fragments. Genetic methods are more versatile and numerous antibody fragments have been produced and used in sensors. It is also possible to produce Fab fragments genetically. Fv and scFv fragments have been produced genetically. Fv is the smallest possible fragment that still guarantees complete antigen binding and scFv is cross-linked Fv for increased stability. Furthermore, the Fab fragment has been cleaved into H-chain segment (Fd) and the L-chain and both fragments have been used in biosensor applications.

It is also possible to produce single CDRs and to use them in affinity sensors. These CDRs are useful, since they consist only of a short amino acid chain and can be synthesised easily and cheaply. It is also possible to replace human CDRs in human antibodies with analyte specific mouse CDRs. The resulting antibody is specific for a certain analyte and can be used even in vivo in humans, since the rest of the antibody is not recognised as an intruder in the human system. Due to

the potential of recombinant antibodies, antibodies can be produced faster, with new binding properties and animal experiments can be reduced (Hock et al., 1995).

2.10 Immobilization of the Biomolecules

The immobilization of the biological element onto the transducer is very important for the biosensor performance (Blum, 1997; Barker, 1987; Karube and Nomura, 2000, Taylor, 1991). The optimal immobilization method would yield a biomolecule immobilized on the surface of a transducer, retaining its full activity with long-term stability regarding its function and immobilization. Furthermore, the biomolecule should be fully accessible for substrate, analyte, co-reactant, antigen, antibody or oligonucleotide. The transducer should be unaffected by the immobilization step. Many immobilization methods can fulfil a number of these requirements, but they also have disadvantages. Therefore, the immobilization method has to be chosen and adapted for the particular bio element, transducer, matrix and other assay requirements. The most common immobilization methods used for biosensors can be divided into physical and chemical methods. Physical methods include adsorption entrapment, encapsulation and confining. Chemical methods are cross linking and covalent immobilization. Cross linking is mostly carried out to improve the stability of physical methods.

2.10.1 Physical Adsorption

Physical adsorption of biomolecules to solid surfaces is a simple technique (Blum, 1997; Barker 1987). Many different surfaces are used for adsorbing biomolecules. These materials include cellulose, collagen, PVC, gold and carbon. Proteins are attached to these surfaces by low energy bonds such as charge-charge interactions, hydrogen bonds, van der waals forces and hydrophobic interactions. The advantage of adsorption as an immobilisation method is its simplicity. Frequently, the surface is only incubated in the protein solution for a certain time and then washed to remove excess protein. However, the stability of the protein layer is generally poor and can be affected by many factors, such as pH, ionic strength or temperature. To improve the stability of the adsorbed molecules, they are sometimes cross-linked with bifunctional reagents such as glutaraldehyde. This results in an adsorbed network rather than adsorbed molecules. Unfortunately, the process of cross-linking can deactivate the biomolecules to some extent.

Other techniques passively adsorb proteins, such as protein A or protein G, on the transducer surface resulting in oriented immobilization of antibodies. These proteins are specific for the specific for the Fc region of certain antibodies and allow the Fab fragments to freely interact with the antigen. Passive adsorption is often used in disposable sensors and ELISAs, where the protein layer is not reused and extended stability is not required to the same extent as in permanent or reusable sensors.

2.10.2 Entrapment

The biological element can be entrapped in a three dimensional polymeric lattice. This is normally achieved by forming a networked polymer gel around the biomolecule. Starch gels, nafion, silicate and polyacrylamide gels are frequently used. The network can be formed by polymerizing a three dimensional structure or by cross-linking two-dimensional polymer strands. Polymerization is also carried out electrochemically. Whereas conducting polymers allow polymer films of ant thickness, the formation of non-conducting polymers (e.g. poly-phenol) is restricted to thin compact films in which growth is self limited. The gel can also be formed with a technique called co-reticulation. A mixture of excess of inactive protein, such as BSA, and the active biomolecule are cross-linked. The resulting network is a gel, formed by the cross-linked inactive protein with the active biomolecule trapped and cross-linked inactive protein with the active biomolecule trapped and cross-linked in the gel. The biological element is homogenously entrapped in the gel but is often only accessible for small molecules. On the other hand, the irregular (heterogeneous) structure of the gel might cause leakage of the biomolecules from less densely polymerized regions. Cross-linking of the molecules might overcome the problem and retain more biomolecules in the gel, but the bifunctional cross-linkers might also deactivate the biological elements. Damage or deactivation might also occur during polymerization, depending on the mechanism and the conditions used.

Gel entrapment is a popular immobilization method for whole cells, but not for antibodies or antigens. Whole cells are retained very well in the gel due to their size and their analytes and substrates are mostly small molecules. In immunogenic reactions, however, mainly large molecules are involved and such as such cannot move freely through the gel. Another form of entrapment is the incorporation of the biological element in the electrode matrix. Enzymes can also be incorporated in composite elements. A mixture of graphite particles, enzymes and plasticiser (water insoluble liquid or solid) forms the electrode. Direct incorporation of biomolecules is also possible when electrodes are screen printed. Carbon ink, for example, is mixed with an enzyme and printed onto a solid support. After drying, the enzyme is permanently entrapped in the electrode.
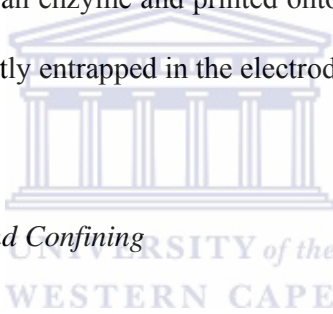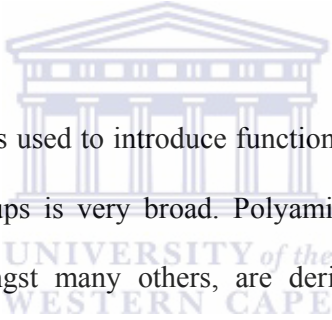
2.10.3 Encapsulation and Confining

Encapsulation and confining as an immobilization method is mainly used for enzymes. A simple system that was employed in early biosensors is the retention of enzymes on transducers, such as electrodes, by semi-permeable membranes, such as dialysis membranes. Substrates and products can cross this barrier, but the enzyme cannot. Biomolecules can also be confined in microcapsules of either semi-permeable materials or liposomes. However, even when the enzymes are immobilized in the microcapsules, association with the transducer is often difficult.

2.10.4 Covalent Binding

The immobilization of biomolecules on solid supports by covalent coupling usually leads to stable linkages. Proteins can be bound to an activated surface via their amino acid residues or terminal groups. These groups include amino, thiol, carboxyl, phenolic, imidazole, disulphide, hydroxyl and thioether groups. An important factor for covalent immobilization is the support material and especially the presence of functional groups. These functional groups can be present either directly at the solid support or be introduced via another matrix, such as membranes.

If an additional matrix is used to introduce functional groups to the solid support, the range of these groups is very broad. Polyamide, polysaccharide, polyvinyl type membranes, amongst many others, are derivatized to contain hydroxyl, aldehyde, amine, carboxyl, thiol or other residues. The reaction between membrane and protein sometimes involves chemical activation and mild chemistry, but often it is only required to dip the pre-activated membrane into a protein solution or apply a drop of this solution onto the membrane. The variety and availability of these immobilisation process immobilization procedures allow the comparison of different membranes for proteins. Every protein is different and has different amino acid residues exposed. Membranes exhibiting excellent results with one protein may be unsuitable for another. In other cases of covalent immobilization, the solid support can be directly modified, resulting in a covalent bond between the support material and biomolecule. This can be achieved by

71

silanization of glass or gold, oxidation of carbon or the formation of self-assembled monolayers (SAMs) on gold. Carbon surfaces, such as screen printed electrodes can be functionalised by chemical oxidation or by heat treatment. The resulting functional groups include hydroxyl, carboxyl and phenolic groups, which can further be activated, e.g. with carbodiimide chemistry, and used for protein immobilisation. The knowledge of the exact reaction and which groups are reacting during covalent binding gives the researcher more control over the immobilization process than with most physical methods. Oriented immobilization is possible by targeting certain groups in the biomolecule, such as the terminal amino or carboxyl groups. The resulting bond is very strong and leakage normally does not occur for covalent immobilization. However, the biomolecule might be deactivated by the chemical reaction or by steric hindrance.
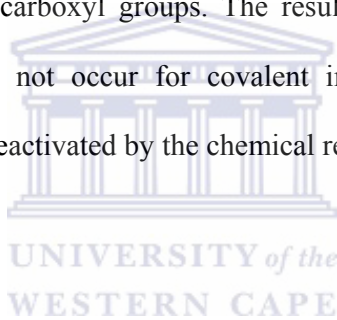
2.11 Hydrogels

Hydrogels are polymers in three dimensional network arrangements, which are able to retain large amount of water. In order to keep the spatial structure, the polymer chains are usually physically or chemically cross linked. The importance of hydrogels in the biomaterial field is justified by some unique characteristics: the elastomeric and soft nature of the hydrogels minimizes mechanical and frictional irritation to the tissues and the very low interfacial tension contributes in reducing the protein adsorption and the cell adhesion. Due to their swelling capacity, hydrogels can easily be rinsed to remove reagents residues. In addition, they are permeable to low molecular metabolites (Li et al., 2004). These

characteristics have allowed hydrogels to be used in biomedical applications as biosensors, drug delivery systems, contact lenses, catheters and wound dressings. They have found use as matrices for enzyme immobilization (Jiménez et al., 1997; Arica et al., 2004; Dorreti et al., 1994; Schulz et al., 1999). Hydrogels have been employed as the sensing layer in, potentiometric conductometric and fiber-optic sensors (Crosfet et al., 1995; Sheppard et al., 1995; Li and Walt 1995).

Different methacrylate monomers have been used to prepare hydrogels for enzymatic immobilization as described in this section. Schulz et al., 1999 investigated the immobilization of glucose oxidase (GOx) using p (HEMA). Mixtures of HEMA containing AIBN and buffer solutions of GOx were polymerized by UV radiation. The entrapment of GOx in pHEMA provides long enzyme stability, which can then be used to fabricate stable biosensors for application *in vivo*. Traitel et al. 2000 studied a glucose-responsive insulin controlled release system based on the hydrogel p (HEMA-co-DMAEMA) with entrapped GOx, catalase (EC 1.11.1.6) and insulin. The hydrogel matrices were prepared by mixing monomers, tetraethyleneglycol dimemethacrylate (TEGDMA) as cross linker, distilled water and ethylene glycol to obtain a homogenous solution where the initiators were added and the polymerization was carried out at room temperature. When exposed to physiological fluids, glucose diffuses into the hydrogel; glucose oxidase catalyzes the glucose conversion to glucorinic acid causing the swelling of the pH- sensitive hydrogel and the subsequent release of insulin. The higher the glucose concentration in the medium, the higher and faster the swelling and release rate. The study described

the swelling and release kinetics of the hydrogel and its dependence on oxygen availability and polymer morphology demonstrating that cross-linked hydrogels are effective in reducing blood glucose levels when used as insulin release systems.

The epoxide groups of grafted p (GMA) brushes were utilized by Xu et al., 2005, for direct coupling of GOx. Well defined p (GMA) brushes covalently tethered on silicon surfaces [Si-g-p (GMA) hybrids] were prepared via surface-initiated atom-transfer radical polymerization (ATRP), on the 4-vinylbenzyl chloride (VGC)-coupled silicon surface. The activity of the immobilized GOx was measured on a biochemistry analyzer and it was found that the brushes improved the stability of the enzyme during storage as compared to the free enzyme. Podual et al., 2000a developed glucose hydrogels prepared by copolymerization of diethyl aminoethyl methacrylate (DEAEM), polyethylene monomethacrylate (PEGMMA), GOx and catalase in solution and they investigated their dynamic response. The copolymerization was carried out by mixing the two monomers, the cross-linker (TEGDMA) and the enzyme solution under nitrogen atmosphere at room temperature. The aqueous monomer mixture was then photo polymerized to obtain films. The same authors also studied the equilibrium and dynamic swelling of the hydrogels as a function of pH (Podual et al., 2000b). They found that hydrogels have complex non-linear swelling and deswelling and in some cases show pulsated swelling. The latter properties are of great interest for applications in stimulus-sensitive release of insulin. Tzoris et al., 2003 illustrated a polymixin B (PMB) modified copolymer of ethyl acrylate and pHEMA. The copolymer was

designed for biosensor interfaces to provide protection against microbial contamination. The copolymer prepared by solution polymerization was deposited on an ion-sensitive field effect transistor (ISFET). The ion-step ISFET technique was adopted as a method to study the PMB immobilization and leaching.

Di Nino et al., 2004 reported the anchoring of lactoperoxidase (LPO; 1.11.1.7) onto the macroporous hydroxylic resin formed by copolymerization of HEMA and GMA and the stabilization of the enzyme and maintaining its catalytic activity. The mixture of GMA, HEMA and water was polymerized upon γ-ray exposure. LPO was linked to the resin using the reactivity of the epoxy groups of GMA monomers and the accessible nucleophilic groups of the enzyme. The determination of LPO was carried out with the atom-transfer radical polymerization (ABTS-assay) following the absorbance of the oxidized ABTS. The γ-ray synthesized functional resin p (HEMA-GMA) appears to be an effective resin able to anchor LPO and to preserve its catalytic activity. Dispersing LPO onto amphiphilic resin can regulate the molar fraction of water put in contact with LPO in each individual resin particle. The immobilization of trypsin (EC 3.4.21.4) in porous cross-linked-p-glycidyl methacrylate-glycodyl methacrylate-co-1, 3-dimethacrylate (pGMA-GDMA) beads was investigated by Malmsten and Larsson, 2000. In particular, they reported the effects of the surface modification of the beads (through hydrophilic polymers) on the amount of protein immobilized and on the extent of retained enzymatic activity. Furthermore, the immobilization within unmodified and hydrophilised beads prepared from aqueous solutions was compared with beads synthesized from water-in oil

micro emulsion. It was found that the amount of trypsin immobilized within the unmodified GMA-GDMA beads was higher in the hydrophilised GMA-GDMA beads. However, the specific-enzymatic loss after immobilization was larger for the unmodified beads than for the hydrophilised ones. Hussain et al., 2005 reported a decrease in the intrinsic fluorescence of yeast hexokinase (EC 2.7.1.1) entrapped in a silica sol-gel matrix when glucose is added. The sol-gel films containing entrapped hexokinase were covered with a biocompatible pHEMA for in vivo application, and glucose was monitored by the decrease of the intrinsic fluorescence of hexokinase. This system could be considered as a first stage in the development of in vivo glucose sensor.

2.12 CEPs Hydrogel Composites

Studies on composites formed from CEP and hydrogels have been carried out. . An electrically conductive composite material, consisting of polyaniline nanoparticles dispersed in a polyvinyl pyrrolidone (PVP) hydrogel was prepared by water dispersion polymerization of aniline using PVP as steric stabilizer, followed by γ-irradiation which induced cross linking of the PVP component (Dispenza et al., 2006). Moscou et al., 2006 developed an artificial muscle material based on a hydrogel that is composed of acrylamide and acrylic acid which is doped with a polypyrrole/carbon black composite. Lira et al 2005 synthesised polyaniline-polyacrylamide composites by electroploymerization of the conducting polymer inside an insulating hydrogel matrix of different pore sizes. The obtained new material was electroactive due to the presence of polyaniline inside the pores. The composites were applied to electrochemically

controlled drug delivery devices. The synthesis of a hydrogel composite in which polyaniline (linear) is entrapped within cross linked polyelectrolyte gel poly (2-acrylamido-2-methyl propane sulphonic acid) (PAMPS) was reported by Samir and Rupali, 2005. Nikpour et al 1999 synthesized conducting polymer composites PPy with poly (methylmethacrylate), demonstrating that these materials as controlled delivery devices. The membranes were prepared using porogen leaching techniques. The liquid porogen used was polypropylene glycol while sodium chloride powder was used as the solid porogen. Koul et al 2001 reported on the synthesis of a polyaniline (acrylonitrile-butadiene-styrene) composite membrane as a sensor material for aqueous ammonia. The resistance change of the composite film on exposure to different concentrations of aqueous ammonia showed its utility as a sensor material. Park and Park 2002 investigated the electrical properties of the conducting composite poly (methylmethacrylate-co-pyrrolmethylstyrene)-g-polypyrrole (PMMAPMS-g-PPy).The PMMAPMS-g-PPy was synthesized by the electrochemical reaction of PMMAPMS and pyrrole in the electrolyte solution containing lithium perchlorate and a mixture solvent of acetonitrile and dicloromethane. Enzymes entrapped within polypyrrole (PPy) films prepared by electropolymerization from aqueous solution have been commonly used to prepare electrodes. Brahim et al., 2002a developed a glucose biosensor based on GOx entrapment within a composite p HEMA/PPy membrane. A mixture of HEMA, tetraethylene glycol (TEGDA) as cross linker and enzyme was deposited on the platinum electrode surface and the polymerization of HEMA was performed by irradiating with UV under argon atmosphere. Subsequently, the pyrrole monomer entrapped within the hydrogel network was electrochemically

polymerized. The same authors Brahim et al., 2001 reported the development of an amperometric biosensor for cholesterol analysis prepared by entrapping cholesterol oxidase (ChlOx; E.C 1.1.3.6) onto the pHEMA/PPy matrix. Brahim et al. 2002b synthesized bioactive composites of polypyrrole containing pHEMA hydrogels. These materials were incorporated into an amperometric biosensor for clinically important analytes (galactose, glucose and cholesterol). They demonstrated that replacing pyrrole (Py) by dimethylaminoethyl methacrylate (DMA) and propylmethacrylate (PMA) the biosensing capability of the films were enhanced. The proposed biosensor showed excellent screening of physiological interferents such as ascorbic acid, uric acid and acetoaminophen. The resulting polymer proved its potential to control the delivery of insulin and to function as a chemically synthesized artificial pancreas.
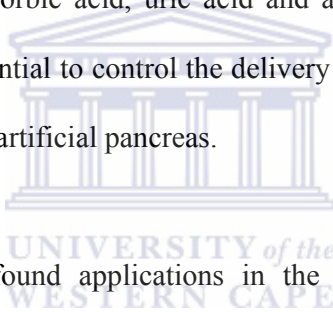
Hydrogels have also found applications in the field of immunosensors. An immunosensor for ferritin based on agarose hydrogel has been developed (Zhang et al., 2006).The immunosensor was prepared by immobilizing ferritin antibody on a glassy carbon electrode based on agarose hydrogel. Parellada et al., 2004 developed an affinity electrochemical biosensor incorporating graphite electrodes with tyrosinase immobilized in a hydrogel for the determination of phenol index in environmental samples. An immunosensor for the determination of okadaic acid using quartz crystal microbalance (QCM) was developed. Significant improvement of the performance of the device was obtained by incorporating an antibody-BSA hydrogel (Tang et al., 2002).

Chapter three

3.1 Experimental

3.2 Analytical techniques

The analytical techniques employed in this study were electrochemical impedance spectroscopy (EIS), cyclic voltammetry (CV), differential pulse voltammetry (DPV); spectroscopic techniques used were Ultra Violet-Visible spectroscopy (UV-Vis), Fourier transform –infra red spectroscopy (FT-IR). Morphological studies were carried out using transmission electron microscopy (TEM) and scanning electron microscopy (SEM)
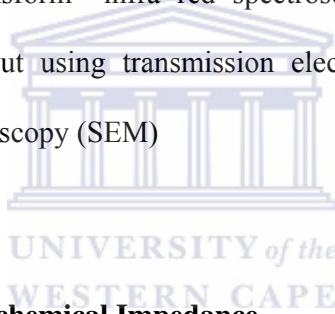
3.3 Measuring Electrochemical Impedance

3.3.1 Apply a Voltage, Measure a Current

Electrical impedance is defined as a ratio of an incremental change in voltage to the resulting change in current. Either and AC test voltage or AC test current is imposed while the other variable is measured. Mathematically, if the applied voltage is $V_{test}=V_{DC} + V_{AC} \sin(\omega t)$ and the resulting current test is

$I_{test} = I_{DC} + I_{AC}\sin(\omega t-\psi)$, then the complex-valued impedance $Z(\omega)$ has magnitude V_{AC}/I_{AC} and phase ψ. The electrode- solution impedance depends on both the bias conditions (V_{DC}) and the measurement frequency (ω). By exciting with a single

frequency, a lock in amplifier can be used to accurately measure the output signal at the same frequency. Voltage excitation is usually employed in EIS because the most troublesome parasitic impedances are in parallel with the measured electrode-solution impedance. In most cases, the measurement process is repeated at different frequencies yielding $Z(\omega)$. In impedance biosensors, the applied voltage should be quite small, usually $\geq$ 10 mV or less for 2 main reasons: (i) the current-voltage relationship is often linear for only small pertubations (Barbero et al., 2005). (ii) To avoid disturbing the probe layer.Therefore, impedance is frequently defined in the context of the linear current voltage relationship. Furthermore, since typical covalent bond energies are in the order of 1-3 eV, it is very important to prevent disturbance of the probe layer especially since applied voltages can exert a disruptive force on the charged molecules. This second consideration also applies to DC bias voltages across the electrode-solution interface. However, accurate EIS measurements do not damage the biomolecular probe layer, an important advantage over conventional voltammetry or amperometry where more extreme voltages are applied.

Variations of standard impedance spectroscopy include using multiple excitation frequencies simultaneously (Garland et al., 2004; Hazi et al., 1997), exciting with noise (Macdonald, 1987) (Bard and Faulkner 2001) (Barbero, et al., 2005) Macdonald, 1987), and exciting with a voltage step (which contains frequency components) (Berggren et al., 1999). Such approaches could decrease the time required per measurement and avoid complications due to the fact that impedance is poorly defined especially when the experimental system is likely to undergo

localised changes in the course of the electrochemical measurement and data acquisition.

3.3.2 Electrodes

At minimum two electrodes are needed to measure electrolyte-solution impedance, and usually three are used. The current is measured at the working electrode and is biofunctionalized with the probe. In order to establish a desired voltage between the working electrode and solution, electrical contact must be made with the solution using a reference electrode and/or counter electrode. A reference electrode maintains a fixed, reproducible electrical potential between the metal contact and the solution allowing a known voltage to be applied. A simple piece of wire-a pseudo reference or quasi reference electrode (Kahlert, 2002)-can sometimes suffice. A counter electrode supplies current to the solution to maintain the desired electrode-solution voltage, usually in electronic feedback with the reference electrode monitoring the solution voltage.

3.3.3 Instrumentation in Electrochemical Impedance spectroscopy

A potentiostat imposes a desired command voltage between the solution and working electrode while simultaneously measuring the current flowing between them. EIS analyzers are potentiostats designed especially for measuring AC impedance and have typical frequency ranges of 10 MHz-100 kHz. Computer control is ubiquitous for both potentiostats and EIS analyzers. Digital post

processing is commonly employed to amplify the signal and to eliminate background noise.

3.3.4 Faradaic vs. Non-Faradaic

Faradaic EIS requires the addition of a redox-active species and DC bias condition such that it is not depleted. In contrast, no additional reagent is required for non-Faradaic impedance spectroscopy, rendering non-Faradaic schemes somewhat more amenable to point of care applications. The term capacitive biosensor usually designates a sensor based on a non-Faradaic scheme, usually measured at a single frequency.

3.3.5 Data Fitting

The measured impedance data can be used to extract equivalent values of resistances and capacitances if a circuit model is assumed a priori, though there is not a unique model or even necessarily a one-to-one correspondence between circuit elements and the underlying physical processes (Macdonald, 2006). Figure 3.1 shows typical circuit models, and Figures 3.2 and 3.3 shows examples of impedance data. It is not always necessary to fit data to a model, and even the best models of the electrode-solution interface do not always perfectly fit experimental data without relevant fitting parameters. Sometimes the raw impedance is fit to a model and changes in model elements are reported as the sensor output. Alternatively the impedance at a particular frequency is used. Depending on the values of the respective model circuit parameters, data at a particular frequency

can contain information about various circuit elements or be influenced by a single element

Complex nonlinear least (CNLS) fitting (Macdonald et al., 1982) is needed to incorporate both magnitude and phase and is available in several software packages such as LEVM, Zview and ZSimpWin. The Kramers-Kronig transform can act as an independent check against invalid experimental data (Macdonald, 1987; Macdonald, 2006).

3.3.6 Circuit Models

Figure shows the two most common models used to fit impedance biosensor data, depending on whether a Faradaic or non-Faradaic measurement is made. The solution resistance R_{sol} arises from the finite conductance of the ions in bulk solution, and thus generally not affected by binding. The capacitance between the metal electrode and ions in solution C_{surf} can be modelled as a series combination of the surface modification capacitance and the double layer capacitance. The component due to surface modification depends on the thickness and dielectric constant of the probe layer. It can be thought as a parallel plate capacitor, whose capacitance is given by $C = \varepsilon_r\, \varepsilon_o\, \dfrac{A}{t}$ where $\varepsilon_r\varepsilon_o$ is the relative dielectric constant, A is the electrode area and t is the insulator thickness. The capacitance C_{surf} is often modelled by a constant phase element instead of a pure capacitance

In parallel with this capacitance there is a resistive path modelled by R_{leak} for non Faradaic sensors or the series combination of Z_w and R_{ct} for Faradaic sensors. For an ideal insulator or when no redox species is present, R_{leak} is theoretically

infinite. The Warburg impedance (Z_w), is only of physical significance in Faradaic EIS, represents the delay arising from diffusion of the electroactive species to the electrode (Bard and Faulkner, 2001; Macdonald, 2006). It is only appreciable at low frequencies, is affected by convection (and thus may be invalid for experimental time scales), and has a phase shift of 45°. The charge transfer resistance (R_{ct}) is a manifestation of two effects (1) the energy potential associated with the oxidation or reduction event at the electrode (i.e. the overpotential) and (2) the energy barrier of the redox species reaching the electrode due to electrostatic repulsion or steric hindrance. The two circuit elements most commonly used as indication of affinity binding are C_{surf} for non-Faradaic biosensors and R_{ct} for Faradaic ones (Bard and Faulkner, 2001).

3.3.7 Constant Phase Element

The impedance of solid electrodes usually deviates from purely capacitative behaviour, this is empirically modelled as a constant phase element (CPE). The complex impedance of a CPE is given by $1/J\omega A)^m$ where A is analogous to a capacitance, ω is the frequency expressed in rad/s and $0.5 < m < 1$ (m = 1 corresponds to a capacitor and m = 0.5 corresponds to a Warburg element; m for C_{surf} modelling is typically 0.85 and 0.98). This introduces a sub 90° phase shift, or equivalently a frequency-dependent resistor in addition to a pure capacitor.

CPE behaviour can be explained mathematically by dispersion in local capacitance values. Microscopic chemical inhomogenities, Ion adsorption and inhomogeneous current distribution contribute to CPE behaviour (Pajkossy, 1994; Kerner and Pajkossy, 2000; Jorcin et al., 2006). Since solid electrodes can be

expected to have a certain amount of intrinsic CPE behaviour, modelling the electrode-solution interface as purely capaciitative is often an over simplification which can therefore reduce the quality of the data fit.

3.3.8 Double Layer Capacitance

When an electrode is polarized relative to the solution, it attracts ions of opposite charge. This tendency is countered by the randomizing thermal motion of the ions, but results in a local build-up of excess ions of opposite charge. Thus, any electric field arising at the electrode or within ionic solution decays exponentially because the excess ions screen the field. The characteristic length of this decay or Debye length is proportional to the square root of ion concentration (Bard and Faulkner, 2001) (about 1 nm for biological ionic strengths). This effect creates a capacitance called double layer capacitance or diffuse layer capacitance. This arrangement of a bare electrode and nearby layer of ions is conceptually similar to a double-plate capacitor, with thickness of the Debye length (Stokes and Evans, 1997), corresponding to ca. 70 $\mu F/cm^2$ for bare metal next to solutions of biological ionic strength. Ions adsorbed at bare electrodes also increase the capacitance in accordance with the Gouy-Chapman-Stern model (Bard and Faulkner, 2001). The double layer capacitance is voltage-dependent because increasing the electrode voltage attracts the diffuse ion layer, increasing capacitance (Bard and Faulkner, 2001). If an insulator (e.g. an insulating probe layer) covers the electrode, forming a capacitance, the double layer capacitance appears in series with it. In impedimetric biosensors, the ionic double layer usually plays a minor in the overall measured impedance since it is so large relative to series capacitance of

the probe layer for non Faradaic sensors and because the parallel path through Z_w

and R_{ct} dominates at relevant frequencies for Faradaic sensors.

(a) Rsol Csurf
Rleak

(b) Rsol Csurf
Rct W1
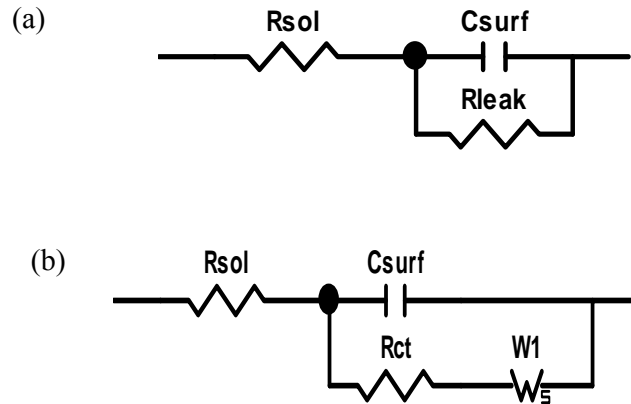
Figure 3.1: Common circuit models for (a) non-Faradaic and (b) Faradaic

interfaces.
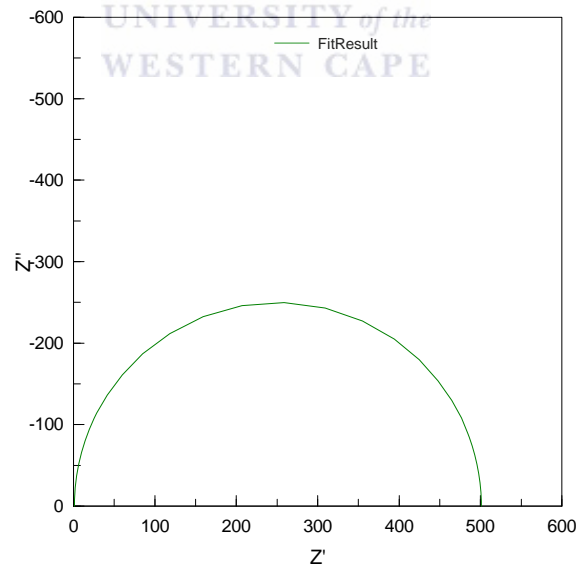
Figure 3.2 Example of non-Faradaic impedance data in Nyquist representation
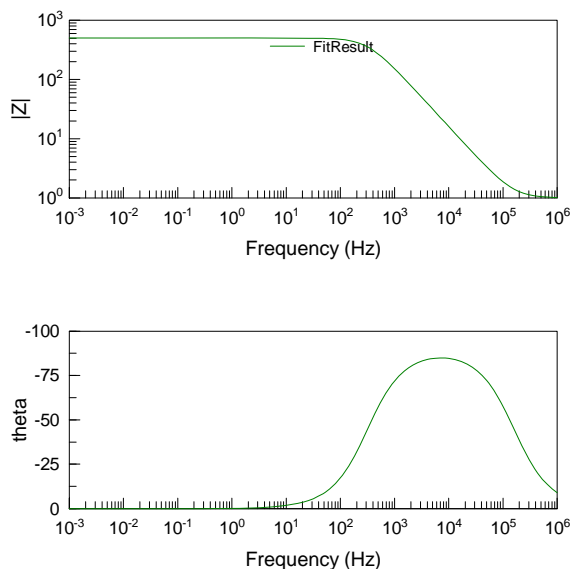
Figure 3.3 Example of a Faradaic impedance data in magnitude/phase (bode plot) representation.

3.4 Cyclic Voltammetry

Cyclic voltammetry is the most widely used electrochemical technique for studying the nature of electrochemical reactions in detail (Kaifer and Kaifer, 1999; Brett and Brett, 1993). During the cyclic voltammetry experiment the potential is scanned from the starting potential (E_i) to the final potential (E_f) and back to E_i and the resulting current is measured. During the electrochemical measurement the solution is kept stationary. The data obtained is represented as a current-potential plot known as a cyclic voltammogram shown in Figure 3.4.

87

In Figure 3.4 the forward scan represents the oxidation of reductant (Red) to it oxidized (Ox) species, which on the backward scan is reduced. The electrochemical change in species from the reductant (Red) to the oxidized species (Ox) results in the loss of electrons and this process is observed in cyclic voltammogram as a peak, referred to as an anodic peak. The reverse scan, the oxidized species (Ox) undergo reduction to its reduced (Red) species resulting in the gain of electrons and a peak is observed in the cyclic voltammogram, referred to as cathodic peak. The information obtained from the cyclic voltammogram includes the anodic (E_{pa}) and cathodic (E_{pc}) peak potentials and the anodic (I_{pa}) and cathodic (I_{pc}) peak currents. Cyclic voltammetric processes may be reversible, irreversible or quasi-reversible (Brett and Brett, 1993).
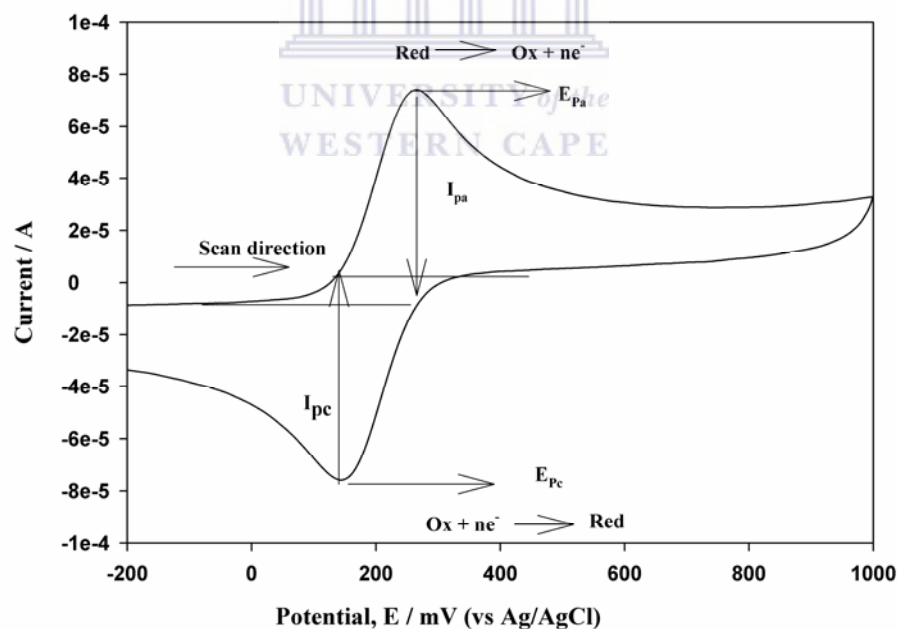
Figure 3.4 A typical cyclic voltammogram for a reversible process.

(i) *Reversible process*: occurs when an electroactive species in solution is oxidized (or reduced) in a forward scan and reduced (or oxidized) in the backward scan. This type of system is in equilibrium throughout the potential scan.

(ii) *Irreversible process* is the process where the reaction goes one-way, the most common is when only a single oxidation or reduction peak with a weak or no reverse peak (Brett and Brett, 1993) is observed. Irreversible processes are a result of slow electron transfer or chemical reactions at the surface of the working electrode. A large peak potential separation (>200 mV) also indicates an irreversible reaction, if there is a return peak.

(iii) *Quasi-reversible process* exhibits behaviour which lies between the reversible and irreversible processes. Differences between the three cylic voltammetric processes are summarised in table 3.1
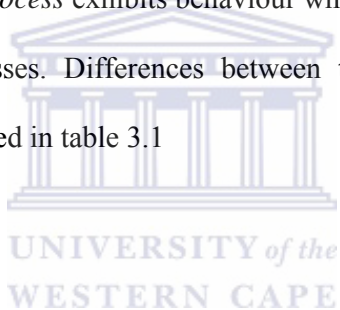
Table 3.1: Summary of parameters for diagnosis of reversible, irreversible and quasi reversible cyclic voltammetric processes.

Parameter	Reversible	Quasi-reversible	Irreversible
E_p	Independent of υ	Shift with υ	Sift cathodically by $0.03/\alpha n$ V for a 10-fold increase in υ
$E_{pa} - E_{pc}$	~ 0.059/n V at 25 ^{o} C	May approach 60/n at low υ but increases as υ increases.	No return peak or >200 mV
I_{pa}/I_{pc}	Equals 1 and independent of υ	Equals 1 only if $\alpha = 0.5$	Usually no current on the reverse scan
$I_p/\upsilon^{1/2}$	Constant	Constant	Constant

α = transfer coefficient, υ= scan rate (V/s), V = volts.

3.5 Differential Pulse Voltammetry

Differential pulse voltammetry (DPV) is one of the most popular electroanalysis tools. In DPV, a linear potential ramp of dE/dt is applied to the working electrode. The current is is monitored twice per drop: the first sample is taken just before the rise in potential when the pulse starts, while the second is taken at the end of the current pulse just just before it decreases back to the baseline. The difference between these two currents is ΔI_{pulse}. The differential pulse voltammogram is a

plot of current difference against potential. ΔI_{pulse} is only significant when redox activity occurs. The height of the current peak ΔI_p is proportional to analyte concentration (Monk, 2001).

The advantages of DPV over normal pulse voltammetry are two fold: (i) many analytes can be sampled with a single voltammogram since the analytical peaks for each analyte are well resolved, and (ii) by working with a differential current, and hence obtaining a voltammetric peak, the analytical sensitivity can be improved to about 5×10^{-8} to 10^{-8} mol/L.

3.6 Materials and Reagents

2-Hydroxyeththyl methacrylate (HEMA), N-Tris (hydroxymethyl) methyl] acrylamide (HMMA), 3-Sulfopropyl methacrylate potassium salt, Tetraethylene glycol diacrylate (TEGDA), Poly-(2-hydroxyethyl methacrylate), 2, 2-Dimethoxy-2-phenylacetophenone (DMPA), aniline. 1, 3, 3, 3-(tetramethyl butyl phenyl polyethylene glycol [Triton X-100] Ammonium persulfate (APS), aniline, thionine, hydrochloric acid, AFB_1, AFB_1 antibody, AFB_1-BSA conjugate, bovine serum albumin (BSA), Horseradish peroxidase (HRP EC.1.11.1.7) with an activity of 169 U/mL, hydrogen peroxide (30% solution), methanol, auric salt, sodium citrate were purchased from Sigma-Aldrich.

The antibody reagent was an immunoglobin (Ig) fraction of rabbit antiserum AFB_1 antibody that contained 6.8 mg of total protein per mL and was quoted as having reactivity with aflatoxins B_1, G_1 and B_2, but no cross reactivity with B_{2a},

91

G_2, G_{2a} or M_1. This solution containing 0.15 M NaN_3 as preservative was aliquoted and stored at -20 ^{o}C until use. Aflatoxin B_1−BSA Conjugate from *Aspergillus flavus* contained 8-12 moles Aflatoxin B_1 per mol BSA

Buffers used in this study were:

Phosphate buffer saline (PBS) contained: KCl (2.7 mM), NaCl (0.137 mM). KH_2PO_4 (0.1 M), Na_2HPO_4 (0.1 M).The adjusted pH value was 7.2.

Acetate buffer contained: 0.1 M HAcO and 0.1 M NaOAc. The adjusted pH value was 6.5.

Aflatoxin B_1 solutions were prepared by dissolving AFB_1 in methanol at 1mg/mL followed by dilution in PBS/10% methanol to give a series of standards over the concentration range 0-6 mg/L and 0-3 ng/mL.
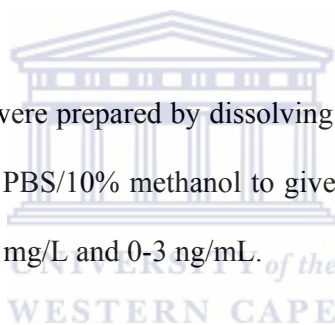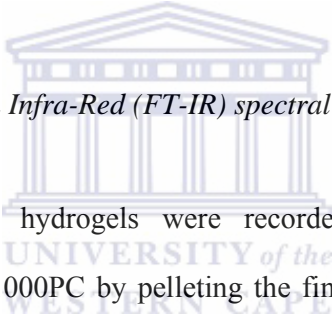
All solutions were prepared using analytical grade reagents and purified water from a Milli-pore Milli Q system. Analytical grade argon (Afrox, SA) was used to degas the system. All experiments were performed at room temperature (25±1 ^{o}C).

3.7 Instrumentation

3.7.1 Electrochemical measurements

All electrochemical experiments were carried out and recorded with a computer interface to a BAS/50W integrated automated electrochemical workstation

(Bioanalytical Systems Lafayette, IN, USA). Cyclic voltammetry was carried out in a 10 ml electrochemical cell, with Ag/AgCl (3 M NaCl type) and platinum wire as reference and auxiliary electrodes respectively. A platinum disc and glassy carbon electrode obtained from BAS were used as the working electrode. The AC impedance of the modified electrode membranes were measured with Voltalab model (Radiometer Analytical S.A, France). Impedance measurements were performed at the frequency range from 10^5 to 10^{-1} Hz at 0 V. The AC amplitude was 5 mV. Alumina micropolish and polishing pads (Buehler, IL, USA) were used for electrode polishing.

3.7.2 Fourier Transform Infra-Red (FT-IR) spectral analysis

FT-IR spectra of the hydrogels were recorded on Perkin Elmer FT-IR spectrometer, Paragon 1000PC by pelleting the finely grounded compound with KBr salt. The spectra were recorded in the wavenumber region of 400-4000 cm^{-1}. The characteristic set of absorption bands in the spectrum were used to identify various functional groups.

3.7.3 Ultra Violet-Visible techniques (UV-Vis)

UV-Vis absorption spectrum of the colloidal gold nanoparticles was recorded at room temperature on a GBC UV/Vis 920 spectrophotometer (GBC Scientific Instruments, Australia) between 200 and 700 nm using a 1 cm path length quartz cuvette. Distilled water was used as the reference

3.7.4 Thermogravimetric analysis

Thermogravimetric analysis was carried out using a TGA-Perkin Elmer TGA7 thermogravimetric analyzer. About 9 mg of the sample was placed in a ceramic crucible and analyzed over the temperature range of 45-600 ^{o}C at 10 ^{o}C/min and 600 ^{o}C-950 ^{o}C at 20 ^{o}C/min. This was done under the dry flow of nitrogen at the rate of 30 ml/min
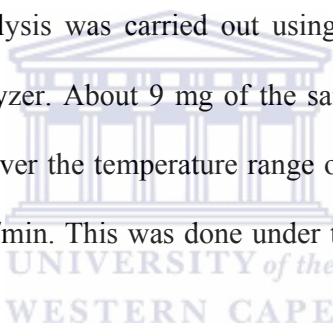
3.7.5 Morphological studies

Morphology of the hydrogels was studied using a Hitachi model X-650 Scanning electron microanalyser. The air dried samples were gold sputtered prior to SEM analysis, in order to enhance contrast. The analysis was carried out at 25 keV. Transmission electron microscopy (TEM) was carried out using JEOL JEM-1200 EX II electron microscope. A sample of the colloidal gold was dropped on a carbon coated copper grid and let to dry for 24 hrs after which the TEM images were recorded.

3.8 Procedures for Chapter four

3.8.1 Polymerisation of Aniline

A mixture of 7.8 ml 1 M HCl, 186 µl aniline and 36.4 µl Polystyrene sulphonic acid was degassed under argon for 10 minutes. Aniline was polymerised using cyclic voltammetry. A platinum wire auxillary and Ag/AgCl reference electrode were used. 10 voltammetric cycles were required between -200 and 1200 mV versus Ag/AgCl electrode at 20 mV/s and sensitivity at 1×10^{-3} A/V in order to reach the required PANi layer thickness.

3.8.2 Anti-AFB$_1$ antibody immobilisation

Following polymerisation of aniline, the electrode was transferred to a 2 ml cell. The surface of the polymer was reduced in 2 ml of PBS (degassed for 10 min under nitrogen) at -500 mV versus Ag/AgCl for 1500 s at sensitivity of 1×10^{-4} A/V. The antibody was prepared in PBS by dilution in 1:200 v/v. After reduction was complete, PBS buffer was removed from the cell very quickly and replaced with the antibody solution, not under stirring or degassing. Oxidation was performed at 700 mV versus Ag/AgCl for 1500s. During the oxidation, the antibody becomes electrostatically attached to the polymer surface. The antibody solution was carefully recovered from the cell and re-stored for further use. The Pt/PANi-PSSA/AFB$_1$-Ab was then incubated in 3% BSA solution for 1 hour.

3.8.3 Anti-AFB₁ and AFB₁ binding in PBS solution

The resulting Pt/PANi-PSSA/AFB1-Ab/BSA was then placed in PBS for measurement of AFB1 in the concentration range of 0-6 mg/L. The equivalent circuit parameters were measured during the immunological binding reaction. The various steps are given in Figure 3.5
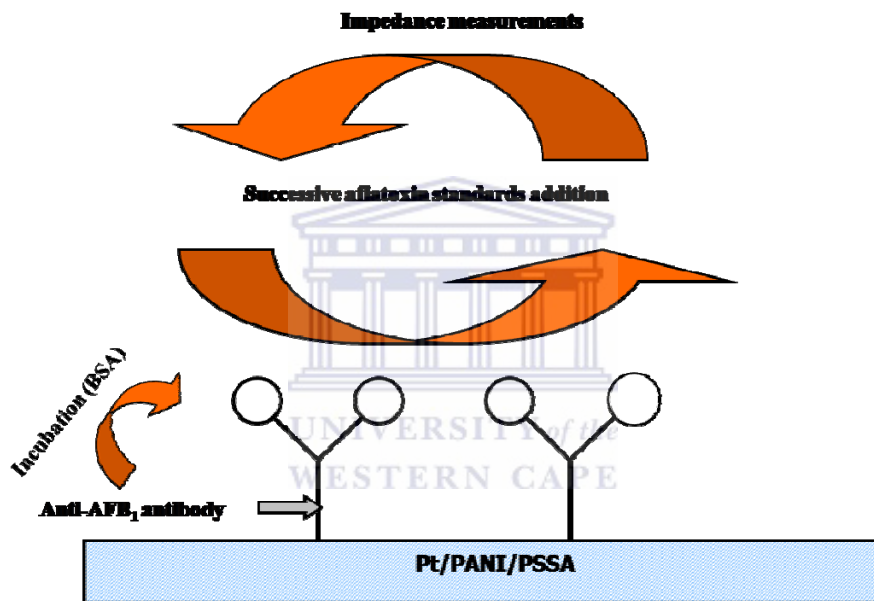

Figure 3.5 Schematic presentation of the assembly of the impedimetric immunosensor.

3.9 Procedures for Chapter five

3.9.1 Fabrication of the amperometric immunosensor

A GCE was polished repeatedly with aqueous slurry of alumina micropolish (Buehler, IL, USA) 1.0, 0.3 and 0.05 µM alumina slurry followed by successive sonication in double distilled-distilled water and ethanol for 5 min and dried in air. Thionine (1 x 10^{-4} M in acetate buffer pH 6.5) was polymerised using cyclic voltammetry. A platinum wire auxillary and Ag/AgCl reference electrode were used. 20 voltammetric cycles were required between -400and 1200 mV versus Ag/AgCl electrode at 50 mV/s and sensitivity at 1×10^{-3} A/V in order to reach the required PTH layer thickness. The nano Au was drop coated on the PTH modified electrode and let to dry for 24 hours. Subsequently the electrode was coated with 5µL of AFB$_1$-BSA conjugate (1µg/mL) and incubated for 1 hour at 37 ^{o}C. The modified immunosensor was incubated in 1 mg/mL HRP solution for 60 min at 4 ^{o}C in order to block possible remaining active sites of the nano Au layer and avoid non-specific adsorptions. The same procedure was followed for the BSA blocked immunosensor using 3% BSA in PBS solution. The immunosensor was stored at 4 ^{o}C when not in use. To perform the competition step, the following procedures were adopted

i) Procedure for 0 ng/mL

5 µL of the antibody solution (dilution of1:2000 v/v in PBS) was dropped on the AFB$_1$-BSA conjugate/nano-Au/PTH modified GCE blocked with HRP and

allowed to react for 15 minutes. The DPV was then run on acetate buffer pH 6.5 containing 3.2 μM of H_2O_2.

Ii) Procedure for 0.6 ng/mL

10 μL of the antibody solution was mixed with 10 μL of the 0.6 ng/mL AFB_1 solution. 5μL of this mixture was dropped on the AFB_1-BSA conjugate/nano-Au/PTH modified GCE blocked with HRP and allowed to react for 15 mins. The DPV was then run on acetate buffer pH 6.5 containing 3.2 μM of H_2O_2. Procedure (ii) was repeated for the subsequent concentrations

iii) Procedures i and ii were repeated for the BSA blocked immunosensor. The DPV was run in acetate buffer pH 6.5 in the presence of 3.2 μM of H_2O_2. The schematic illustration of the stepwise assembly procedure is shown in Figure 3.6
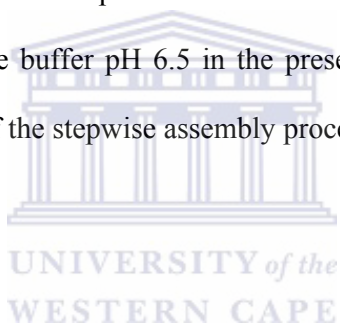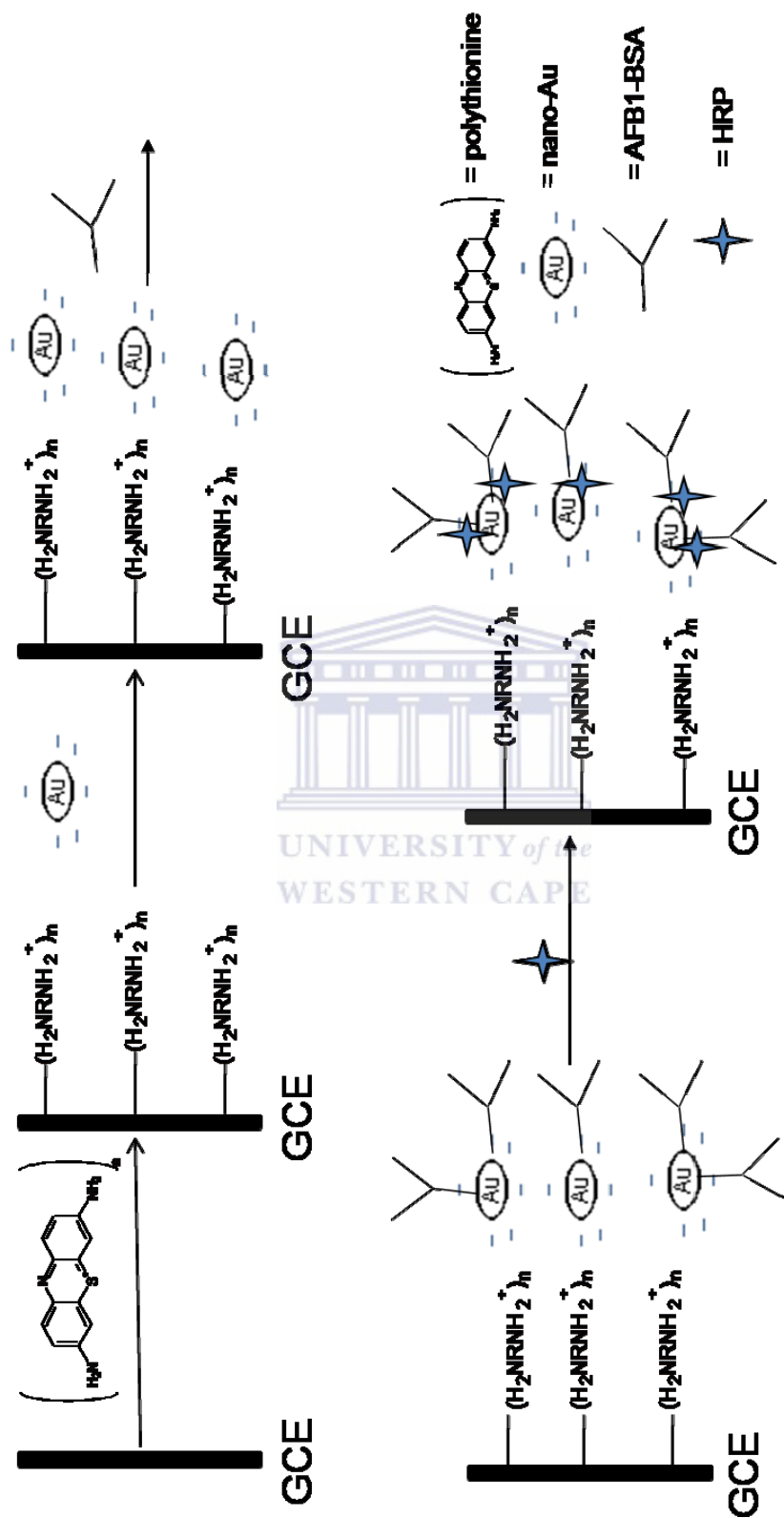
Figure 3.6 Schematic illustration of the stepwise immunosensor fabrication process: (a) polymerization of thionine; (b) formation of nano-Au layer; (c) AFB₁-BSA conjugate loading; (d) blocking with HRP/BSA.

99

3.10 Procedures for Chapter six

3.10.1 Formulation of the hydrogels

A 5 g batch was prepared consisting of ratios given in Table 3.2. The acrylate monomers HEMA and TEGDA together with aniline monomer were first mixed together with the other components and used as the receiving mixture to dissolve the photo initiator. To each batch of the formulation, 20% by weight of deionised water (DI) and ethylene glycol or Triton X 100 was added as mixed solvent. The aqueous solution of the composites was taken within a glass cell. The cell was degassed with argon and placed within a photo chamber full of nitrogen and subjected to UV radiation (λ = 365 nm). After 3 hours the gel formation was complete and the gel was taken out of the cell for the second step of polymerization. At this state the gel contains aniline monomer dispersed within the composite gel; the gel was cut into strips of different sizes and were immersed in the solution of 0.1M APS in 1M HCl (at room temperature) for aniline polymerization to take place. The gels were seen to swell slightly, and nucleation of polymerization was indicated by blue colouration within the transparent gel. Gradually the gel became green after 1 h. The unpolymerized monomer was removed by sequential washing for 1h in each of 100% ethanol, 75%, 50%, 25% ethanol –water mixture and eventually in DI water. For electrochemical studies the gels were prepared in an identical way, except that 3µL of the gel –monomer mixture was applied on the Pt electrode, followed by UV radiation for 45 mins. Polymerization of aniline within the hydrogel was effected by dropping about 5 µL of 0.1 M APS in 0.1M HCl on the electrode surface for 1 h.

Table 3.2: Formulation of electro conductive hydrogels based on PANi

Compounds	Mole %	g %
2-Hydroxyeththyl methacrylate	59.34	52.87
N-Tris (hydroxymethyl) methyl] acrylamide	8.9	11.74
3-Sulfopropyl methacrylate potassium salt	2.97	8.26
Tetraethylene glycol diacrylate,	2.97	6.08
Poly-(2-hydroxyethyl methacrylate)	8.9	8.26
2,2-Dimethoxy-2-phenylacetophenone	2.08	3.43
Aniline	14.84	9.36
Total reagents	100	100
Water		20
Ethylene glycol/triton X 100		20

3.10.2 Swelling behaviour

The swelling behaviour of the two sets of hydrogels was studied in deionised water and in PBS pH 7.2 at room temperature. The weight change was monitored at different time intervals till the hydrogels showed constant weight change. The fractional weight change was transformed to percentage using the following empirical relationship:

Dynamic weight change (%) = (Final weight-Initial weight/Initial weight) x 100. The measurements were made in triplicate and average data was used for calculation.

Chapter Four

4.1 Results and Discussion 1

Modeling of the impedimetric responses of aflatoxin B$_1$ immunosensor

prepared on electrosynthetic polyaniline platform

4.2 Introduction

Polyaniline (PANi) is the mostly used conducting polymer in biosensor applications due to its favourable storage stability and ease of preparation (Iwuoha et al., 1997). PANi acts as immobilisation platform for bio components and as the electron mediator (Killard et al., 1999). PANi may be deposited onto electrode surfaces through chemical or electrochemical means. Electrochemical polymerization, through galvanostatic, potentiostatic or potentiodynamic means, offers the potential to incorporate a wider range of dopant ions, since the reaction is carried out in the presence of an appropriate electrolyte rather than a chemical oxidant. Electrochemical polymerization also gives better control over film properties, such as thickness and morphology. This is the most common method for PANi film preparation for sensor applications (Grennan et al., 2001; Morrin et al., 2003). PANi films do not retain their conductive properties in non-acidic media (Naudin et al., 1998). The neutral environment is required for most immunoreactions to take place optimally. As a result, the electropolymerization is preferentially carried out in presence of a dopant. The most common dopant is poly vinylsulphonic acid (PVS ion). The inclusion of the dopant maintains electrical neutrality in the oxidised form of the polymer and also leads to increase in its structural stability and conductivity at a broader range of pH values

(Michaelson et al., 1993). Poly styrene sulphonic acid (PSSA) was the dopant of choice in this study. PSSA has been previously used in our laboratory for the preparation of PANi nanocomposites (Iwuoha et al., 2006).

Electrochemical impedance spectroscopy is an effective method to probe the interfacial properties of modified electrode and often used for understanding chemical transformations and processes associated with the conductive supports (Katz and Wilner, 2003). Frequency dependence of the impedance of the electrode double layer yields useful information about the adsorption kinetics and dynamics of charge transfer at the electrode interface and are strongly influenced by the nature of the electrode surface and structure of the electrical double layer (Vetterl et al., 2000). The adsorption or desorption of insulating materials on conductive supports is anticipated to alter the interfacial electron-transfer features (capacitance and resistance) at the electrode surface.

In immunosensors, a redox couple serves as a probe for the insulating properties and the density of the adsorbed layer. In the presence of the redox probe, electron transfer is observed and Faradaic impedance is measured. The formation of antigen-antibody will change the electrochemical impedance because the electrode is coated with a blocking layer. When antigens bind to the surface-immobilized antibodies, the access of the redox couple is hindered to a higher degree than in the absence of antigens. As the Faradaic reaction of a redox couple becomes increasingly hindered, the charge transfer resistance will increase.

4.3 Material characterisation

Polymerization of PSSA-doped aniline was done in different ratios from 1:0.1 to 1:0.5 (Aniline: PSSA). The optimum ratio was found to be 1:0.2. The peaks became broader with increasing concentration of PSSA accompanied with a shift of oxidation peak potentials to more positive values. This could be attributed to the structure of PANi which changes from a compact to an expanded structure, allowing the generation of free volume which is immediately occupied by solvated counter ions, when polyaniline changes from a reduced state to an oxidized state. Here oxidation of PANi leads to the creation of positively charged PANi forcing H^+ ions to diffuse out of the film, and leaving negatively charged PSSA to counterbalance the charge on PANi. This is accompanied by solvent migration into the film to solvate the created polyions. With the increase in concentration, extra energy is needed to perform this conformational change, ion and solvent transport. Working at constant temperature, the only way to obtain this is by means of an electric overpotential. Thus, the oxidation potentials of polyaniline positively shift with an increase in concentration. Another reason is that the charge transfer resistance increases with increase in concentration which also causes peak shift and broadening (Otero and Boyano, 2003). The PANi-PSSA was seen to be redox active in the potential region studied, exhibiting two distinct sets of redox peaks as shown in Figure 4.1. The redox couple A/B occurring at 276 mV is attributed to the transformation of PANi from the reduced leucoemeraldine (LE) state to the partly oxidized EM state. The redox couple E/F at 700 mV corresponds to the transition of PANi from (LE) to pernigraniline (PE) (Akcelrud et al., 1997).
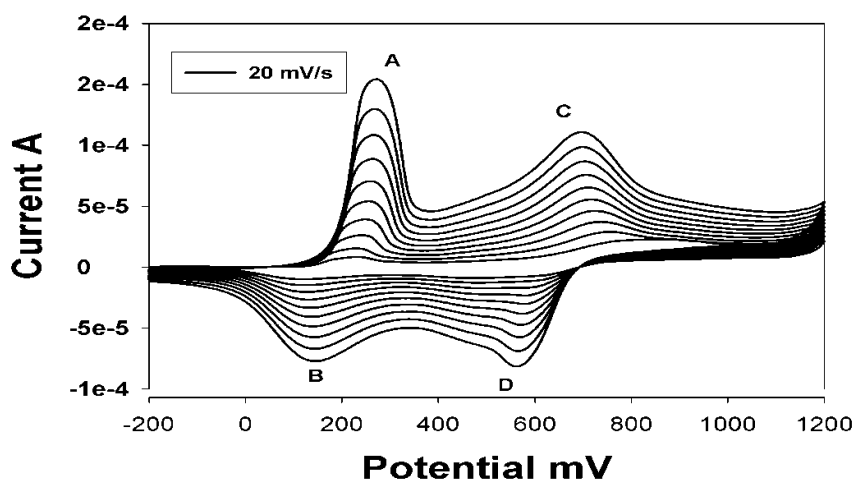
Figure 4.1 Polymerization of Aniline/PSSA in 1 M HCl at a scan rate of 20 mV/s.

Differential pulse voltammetry was chosen as a marker to investigate the changes of the electrode behaviour after each modification step. Figure 4.2 shows differential pulse voltammogram of different modified electrodes in 0.1 M PBS. When electrode surface has been modified by some materials, the electron transfer kinetics of Pt/PANi-PSSA is perturbed. After the Pt/PANi-PSSA was modified with the AFB_1-Ab and incubated in BSA, a decrease in the anodic peaks was observed (Figure 4.2). The reason is that the immobilization of the antibody insulates the electrode and perturbs the interfacial electron transfer considerably.

Figure 4.2 Differential pulse voltammogram (DPV) of Pt/PANi-PSSA (a); Pt/PANi-PSSA/AFB$_1$-Ab (b); Pt/PANi-PSSA/AFB$_1$-Ab/BSA (c). The scan rate was 10mv/s.

Figure 4.3 Nyquist plots for Pt/PANi-PSSA at the different potential

Figure 4.4 Electron transfer resistance and double layer capacitance for Pt/PANi-
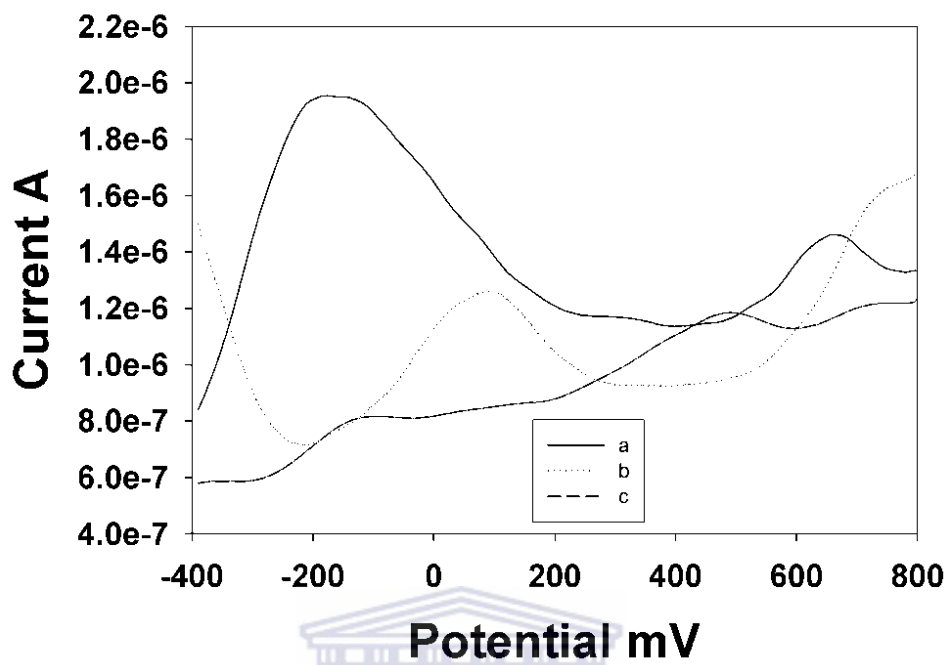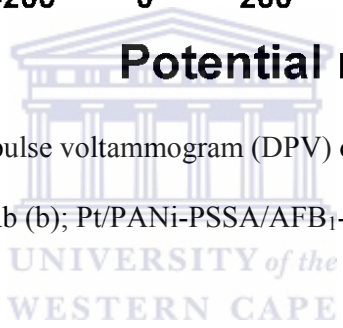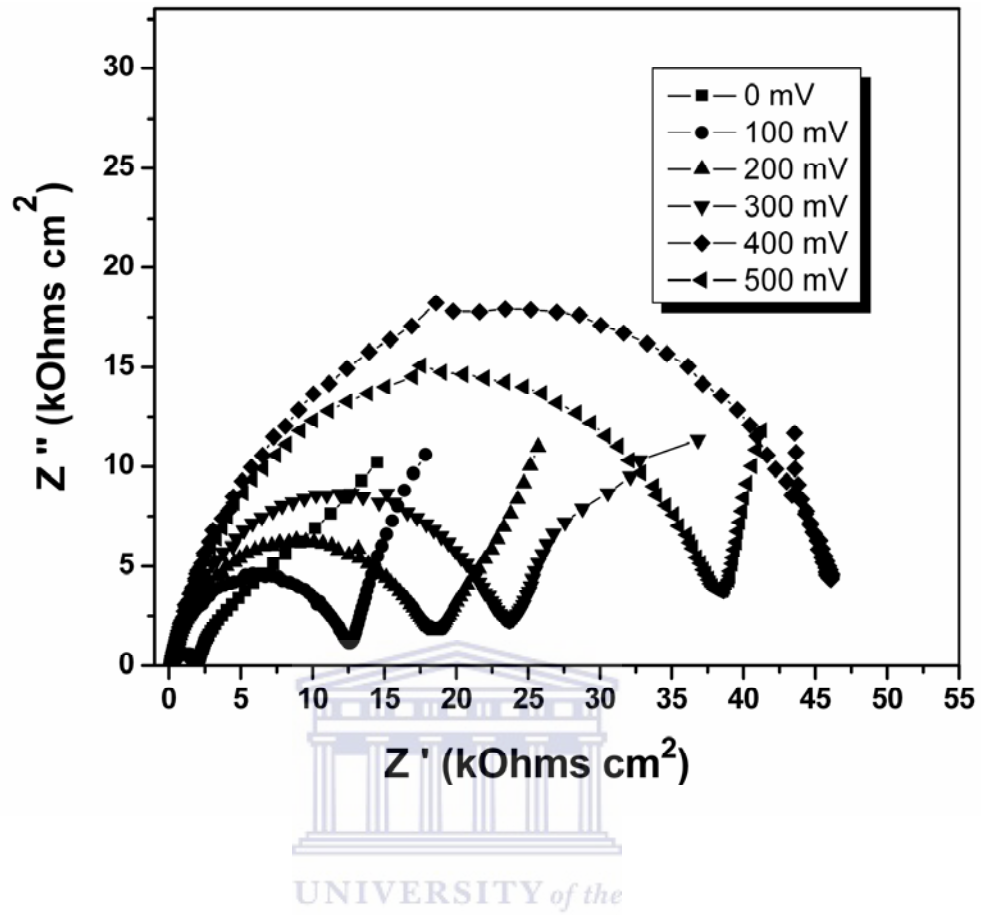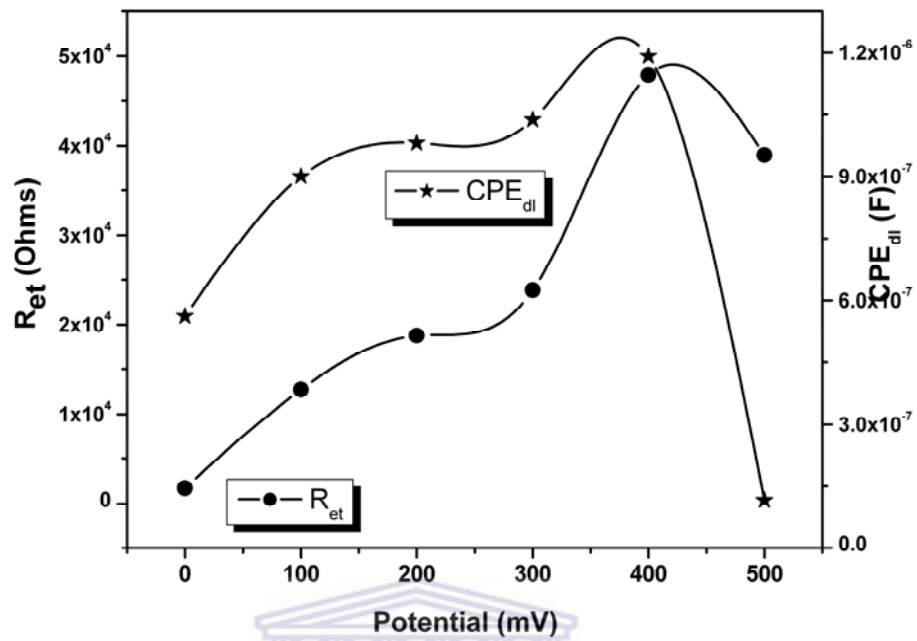
PSSA at different potentials.

Antigens and antibodies are charged protein molecules; formation of the bioaffinity complexes between them could be affected by the charge applied onto the electrode surface. The interfacial electron transfer resistance and double layer capacitance was measured at various potentials (0-500 mV) as shown in Figure 4.3, allowing for the electrical probing of the system when different charges exist on the electrode. The optimal potential was found to be 0 mV as can be seen in Figure 4.4 The decrease of R_{et} and CPE_{dl} at 500 mV could be attributed to conversion of emeraldine radical cation to emeraldine forms of PANi (Iwuoha et al., 2006). A Nyquist diagram of the electrochemical impedance spectrum is an effective way to measure the electron-transfer resistance. Figure 4.5 shows representative Nyquist diagrams of the electrochemical impedance of Pt/PANi-PSSA (curve a), after antibody immobilization (curve b) and after immobilisation and incubation in BSA (curve c).

Based on the general electronic equivalent model of an electrochemical cell and the behaviour of the Pt/PANi-PSSA electrode, equivalent circuits which consists of electrolyte resistance (R_s), constant phase element (CPE_{dl}) describing double layer properties, electron transfer resistance (R_{et}) and Warburg element (Z_w) (Bard and Faulkner, 2001) was proposed for interpretation of the impedance measurement of this system. The two elements of the scheme (R_s) and (Z_w) represent the properties of the bulk solution and the diffusion of the redox probe; thus they are not affected by the reaction occurring at the electrode surface. The other two elements (CPE_{dl}), and (R_{ct}) depend on the dielectric and insulating

features at the electrode/electrolyte interface. The best fit for biolayer was obtained when capacitance of double layer was represented by CPE element in electrical equivalent circuit. The impedance of CPE is given by equation:

$$Z = \frac{1}{A(j\omega)^{\varphi}}$$

Where A is constant, ω is angular frequency, j – imaginary unit and φ is phase angle (varies from 0 to 1) (Bard and Faulkner, 2001). When φ is close to 0, the CPE represents resistance; when φ moves between 0.9 and 1, CPE can be considered as capacitance, as in our case.

As can be seen in Figure 4.5, curve a includes a semicircle and a linear portion, which correspond to the electron transfer and diffusion processes, respectively. However, in the case of curve a it can be observed that slope of the straight line at the lowest frequencies is higher than 45 ºC and it indicates more capacitive properties of the interface.

For curve b and c, the linear portion diminishes indicating a purely kinetic controlled process. For fitting data (curves b and c) simplified electrical equivalent circuit was used as shown on Figure 4.5 (upper graph). The diameter of the semicircle represents the electron-transfer at the electrode surface. This resistance controls the electron transfer kinetics of the redox-probe at electrode interface, which is relative to the concentration of the analyte.

The electron transfer resistances of Pt/PANi-PSSA, after antibody immobilisation and after incubation in BSA were 0.458, 720 and 1066 kΩ, respectively. These

results indicate that electrochemical impedance spectroscopy was capable of monitoring the change in electron-transfer resistance resulting from the immobilization of the antibody. The correlation between electron transfer resistance and immobilisation of antibodies has been reported (Yang et al., 2004; Patolsky et al., 1999).
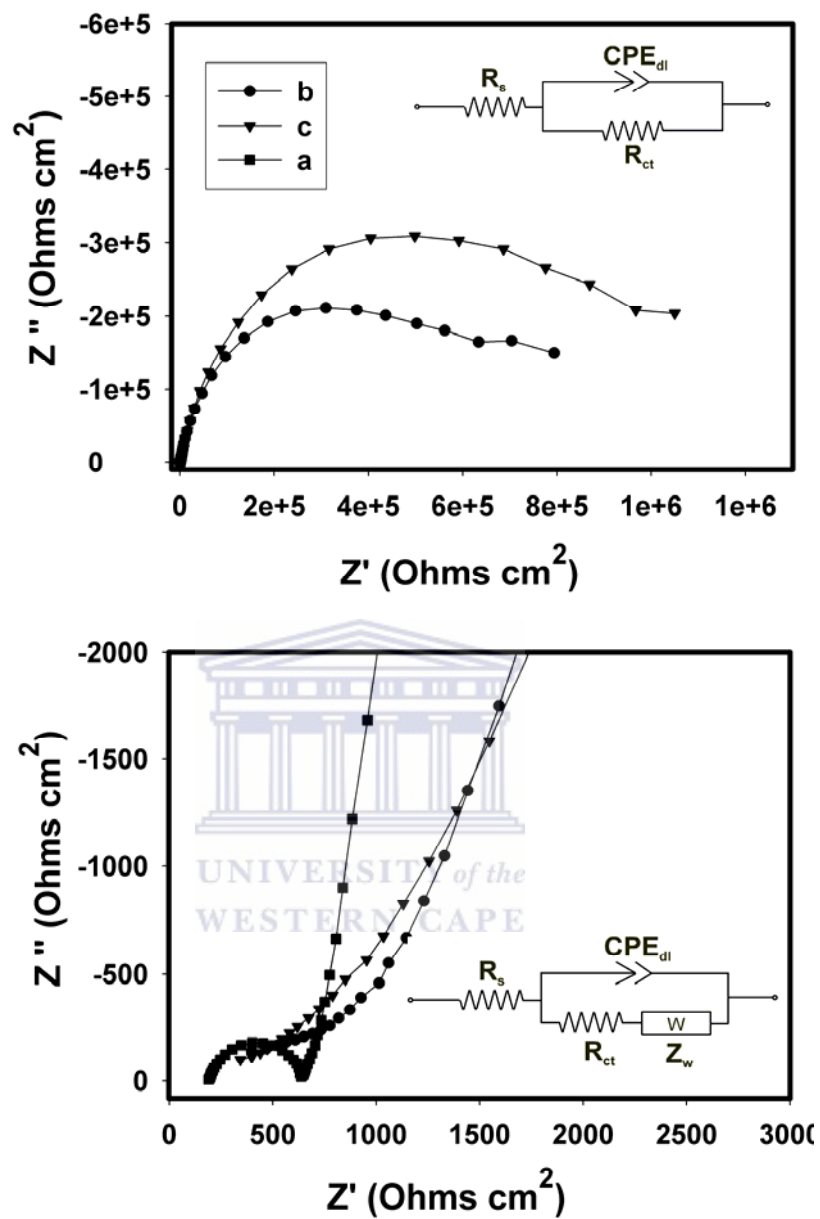
Figure 4.5 Nyquist diagram showing (a) polymer film; (b) polymer film after immobilisation; (c) polymer film after immobilisation and incubation in BSA.

Experiments were carried out to check the effect of AFB_1 on the PANi/PSSA layer in the absence of the antibody. Figure 4.6 shows the Nyquist diagrams of

Pt/PANi/PSSA and Pt/PANi/PSSA/AFB$_1$. Table 4.1 summarizes the values of the important diagnostic parameters. It was found that there was no significant difference between the two diagrams implying that AFB$_1$ had no effect on PANi/PSSA layer. These results suggest that the antibody plays a role in recognition of AFB$_1$.
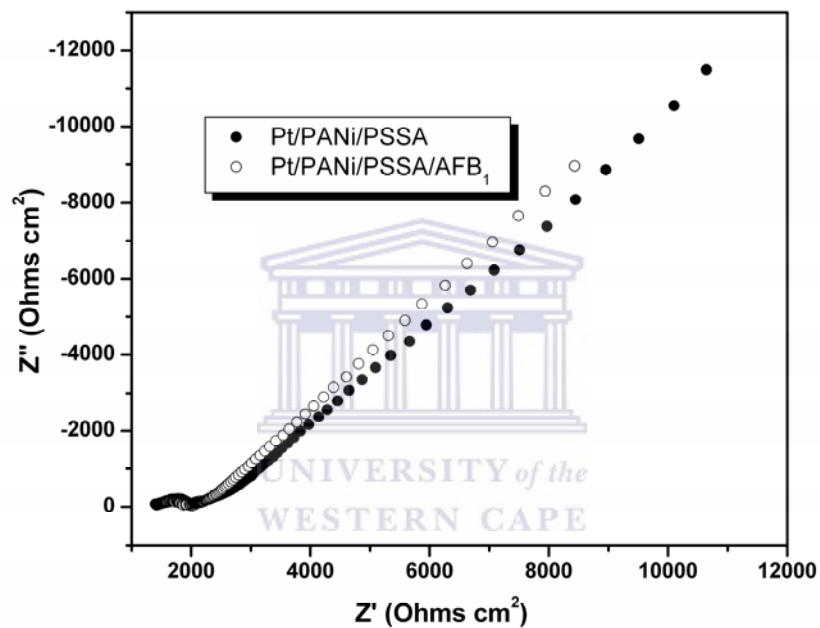
Figure 4.6 Nyquist diagrams for Pt/PANi/PSSA and Pt/PANi/PSSA/AFB$_1$ electrodes

Table 4.1: Diagnostic parameters for Pt/PANi/PSSA and Pt/PANi/PSSA/AFB1 electrodes.

Element	Pt/PANi/PSSA	Pt/PANI/PSSA/AFB$_1$
Solution Resistance (Rs) (Ω)	1470	1514
CPE(F)	2.099E-7	3.010E-7
R$_{et}$ (Ω)	532.7	455

4.4 Application

Increasing the concentration of the AFB$_1$ standards led to increase of the impedance as shown in figure 4.7. As mentioned earlier Nyquist plots are an effective way to monitor the electron transfer resistance. The Nyquist plots were used to model the electrical components of the immunosensor to equivalent electrical circuits consisting of electrolyte resistance (R_s), constant phase element (CPE$_{dl}$) describing double layer properties, electron transfer resistance (R_{et}) and Warburg element (Z_w). R_{et} was extracted and used as the analytical signal. The antibody-antigen interactions cause changes in the (CPE$_{dl}$) and (R_{et}). Increasing concentrations of AFB$_1$ introduces a kinetic barrier at the electrode interface which results in an increase of the (R_{et}).
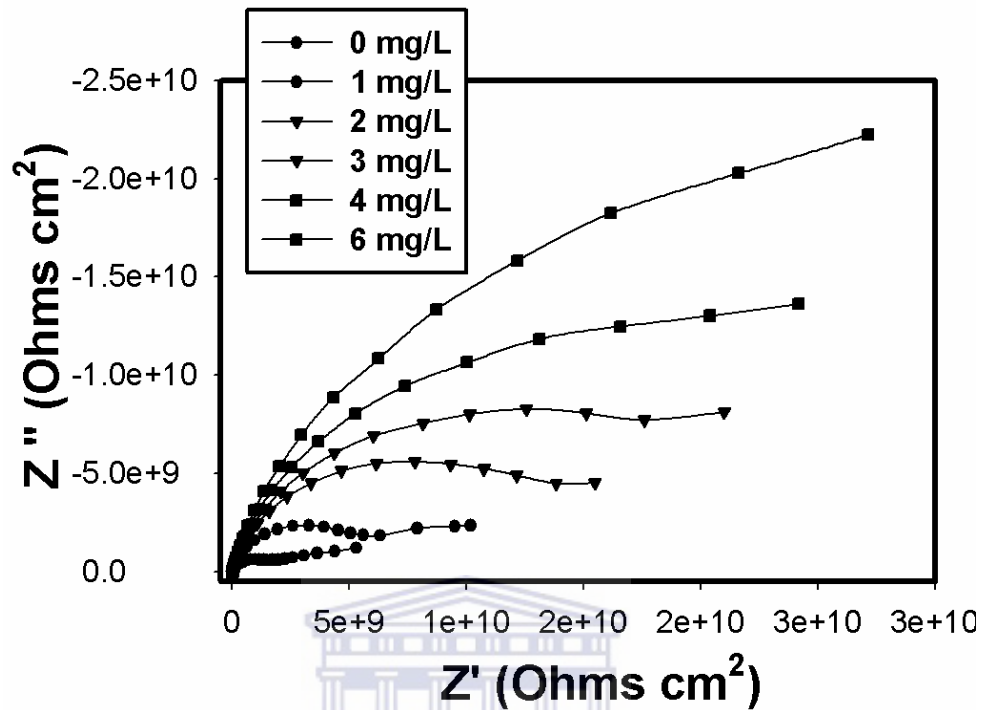
Figure 4.7 Nyquist plots for different concentrations of AFB$_1$

Figure 4.8 shows the derived calibration plot that corresponds to the electron transfer resistance (R$_{et}$) at the Pt/PANi-PSSA/AFB$_1$-Ab/BSA electrode with different concentrations of aflatoxin. The detection limit was found to be 0.1 mg/L and a sensitivity of 869.6 kΩL/mg. The detection limit was calculated from the equation of the calibration of the immunosensor, at R$_{et}$ = 0 Ω while the sensitivity was calculated from the slope of the calibration curve. The linear regression was R$_{ct}$= 842372[AFB$_1$] - 85296, with a correlation coefficient 0.99.
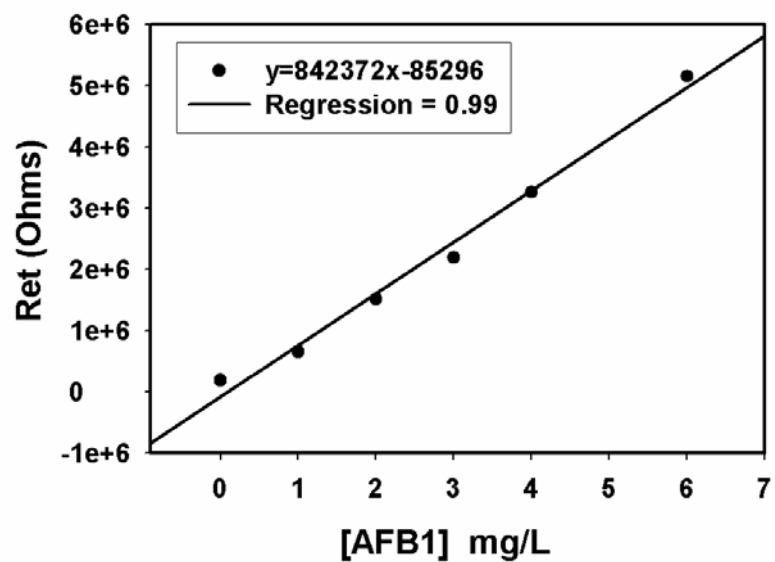
Figure 4.8 Electron transfer resistance of the immunosensor after reaction with the

different concentrations of AFB$_1$.

Chapter Five

5.1 Results and Discussion 2

Electrochemical Immunosensor Based on Polythionine/Gold Nanoparticles

for the Determination of Aflatoxin B$_1$

5.2 Introduction

Among the immunochemical approaches, the enzyme-linked immunosorbent method is the most widely applied. Spectrophotomeric ELISAs specific for AFB$_1$ (Dutta and Das, 2000; Kolosova et al., 2006), total aflatoxins (Ayciek et al., 2005; Zheng et al., 2005) and AFM$_1$ (Yaroglu et al., 2005; Rastogi et al., 2004) have been developed and their simplicity, adaptability and sensitivity have been demonstrated. In order to achieve higher sensitivity and move to the use of disposable probes, electrochemical immunosensors for aflatoxins based on indirect competitive ELISA format have been proposed (Micheli et al., 2005; Pemberton et al., 2006). These immunosensors require the use of labelled secondary antibodies for detection which requires highly qualified personnel and tedious assay time. To achieve label free immunosensors, direct electrochemical immunosensors for AFB$_1$ based on electrochemical impedance spectroscopy (Owino et al., 2007), optical waveguide lightmode spectroscopy (Adanyi et al., 2007) and room temperature ionic liquids (Sun et al., 2008) have been reported.

The search for a simple and label free amperometric immunosensor is of considerable interest. Among the various conducting polymers, thionine (phenothiazine) is a redox dye which has been studied extensively due to its potential utility in sensor applications (Ruan et al., 1998; Xiao et al., 1999). Its electroactivity lies not only in the heterocyclic nitrogen atoms and nitrogen bridges, but also in its free amine groups (Reid et al., 2001). In addition polythionine (PTH) has the susceptibility to chemical modifications due to the abundant amino groups which adsorb metal ions and various organic halogen substances, thus preventing proteins from damage (Dohno et al., 2003).On the other hand, gold nanoparticles have been extensively used as a matrix and cytochemical label for the immobilization and study of macromolecules such as proteins, enzymes and antibodies (Storhoff et al., 1998; Tang et al., 2004; Xu et al., 2004). Modification of electrode surfaces with gold nanoparticles provides a microenvironment similar to that of the proteins in native systems and gives the protein molecules freedom of orientation (Liu et al., 2003).

5.3 Preparation of gold nanoparticles

The approximately 20-nm (diameter) Au nanoparticles (Au NP) was prepared using the procedure reported previously (Yuan et al., 2004). Briefly 2 mL of 1% (w/w) sodium citrate solution was added to boiling solution of 50 mL of 0.01% (w/w) $HAuCl_4$. The maximum absorption of the synthesised colloidal Au in the UV-vis spectra was 520 nm (Figure 5.1) and the solution was stored in a refrigerator in a dark-coloured glass bottle before use. The particle sizes were

determined by transmission electron microscopy (Figure 5.2). Larger-sized Au NP can discontinuously assemble and the smaller sized Au NP may generate continuous arrays of particles on the base of the layer. The packing of smaller-sized Au NP-bound protein is denser than the larger-sized Au NP due to the high surface to-volume ratio of Au NP (Doron et al., 1995).
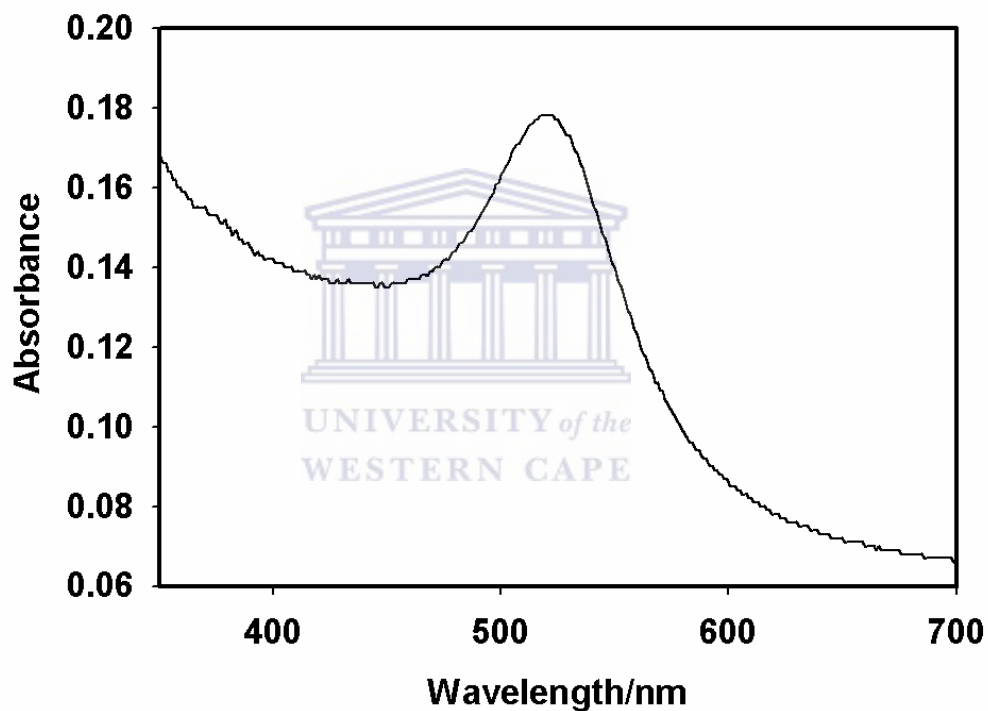

Figure 5.1 UV-Vis spectrum of gold nanoparticles synthesised by adding 2 mL of 1% (w/w) sodium citrate solution to a boiling solution of 50 mL of 0.01% (w/w) HAuCl4

Figure 5.2 TEM images of gold nanoparticles

5.4 Electropolymerization of multiporous thionine film

The GCE was first reduced in pH 6.5 acetate buffer solution containing 1×10^{-4} M thionine at -1500 mV to make it negatively charged, which could interact with the positively charged species of thionine in mildly acidic conditions. Subsequently cyclic voltammetry was performed at a bias voltage of -400 to +1200 mV at a scan rate of 50 mV/s. When the applied potential exceeded +1100 mV, the electropolymerization reaction proceeded and formed cation-radical species onto the GCE (Yang et al., 1999)]. This process resulted in multiporous structure, which facilitated the assembly of AuNP. The oxidation potential in the first step was the most important factor for electropolymerization of thionine and should not be less than 1100 mV. Two reasons suffice for this; in order to achieve the formation of polythionine (PTH) film, the electrode potential must be larger than the potential at which the oxidations of $-NH_2$ groups of thionine molecule occurs and the modified cation must be necessarily associated with the surface activation of GCE. During the process of thionine electropolymerization, a pair of quasi reversible redox peaks with a cathodic peak potential (E_{pc}) of -250 mV and an anodic peak potential E_{pa} of 100 mV, increased gradually and tended to become stable with the increasing scan number (Figure 5.3a). On removal of the electrode from the dye-containing solution, a golden film was seen on the electrode surface. When the film-covered electrode was washed and examined in background acetic acid buffer (pH 6.5), the CV (Figure 5.3b) confirmed the presence of surface attached electroactive material. Figure 5.4a show that in the potential scan range from 5 to 50 mV/s, the anodic peak currents of GCE/PTH electrode are

proportional to the scan rate (υ). The peak current (I_{pa}) linearly varied with the scan rate (Figure 5.4 a inset). The linear regression obtained is 0.99 which indicates the characteristics of thin layer electrochemical behaviour (Murray, 1984). It is thus suggested that nearly all electroactive PTH (red) is converted to PTH (ox) on the forward scan and vice versa.
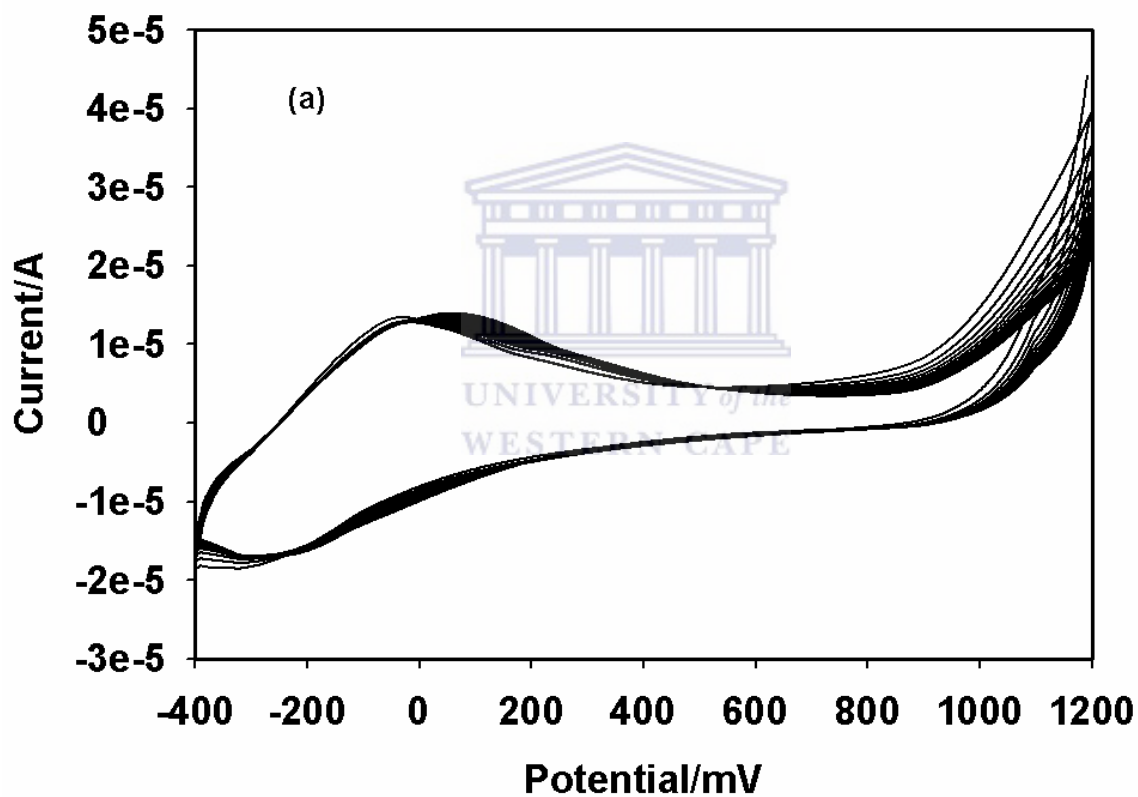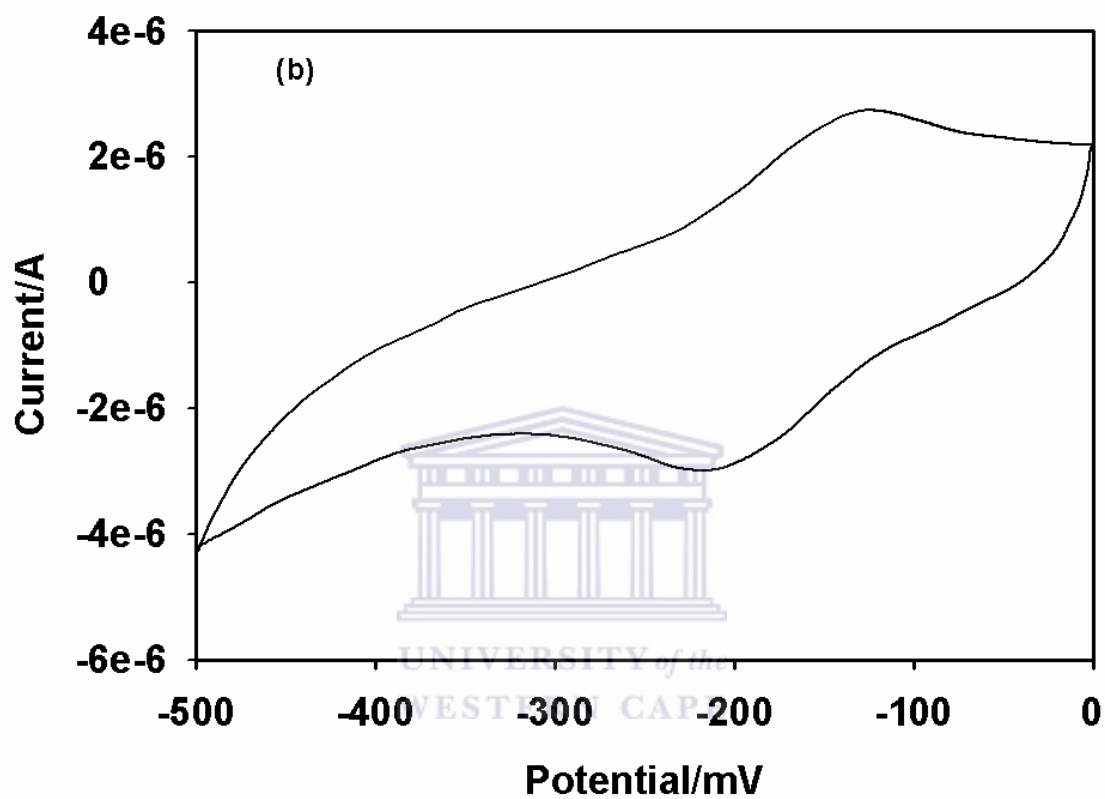
Figure 5.3 (a) Cyclic voltammograms of the growth process of the multiporous

PTH on GCE in acetic buffer (pH 6.5) containing 0.1 mM thionine. Scan rate 50

mV/s and (b) PTH-modified GCE in pH 6.5 acetic acid buffer. Scan rate 50 mV/s
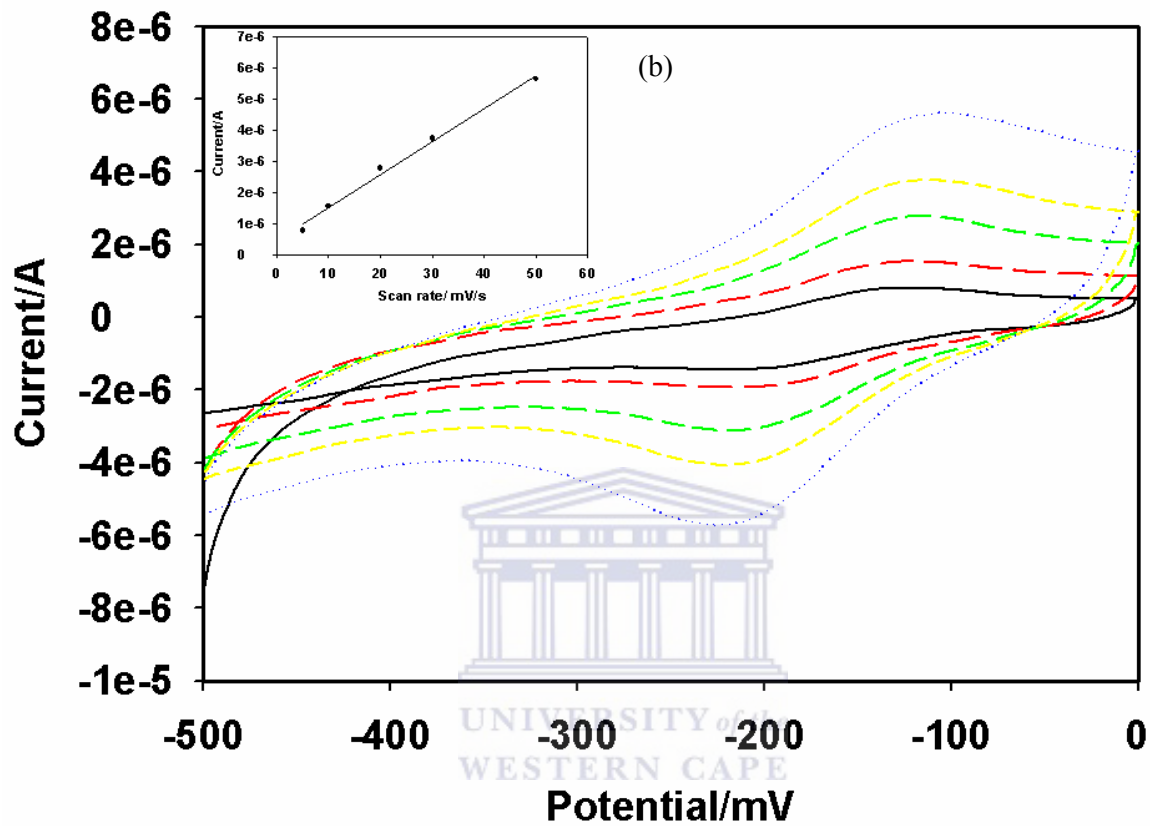
(a)
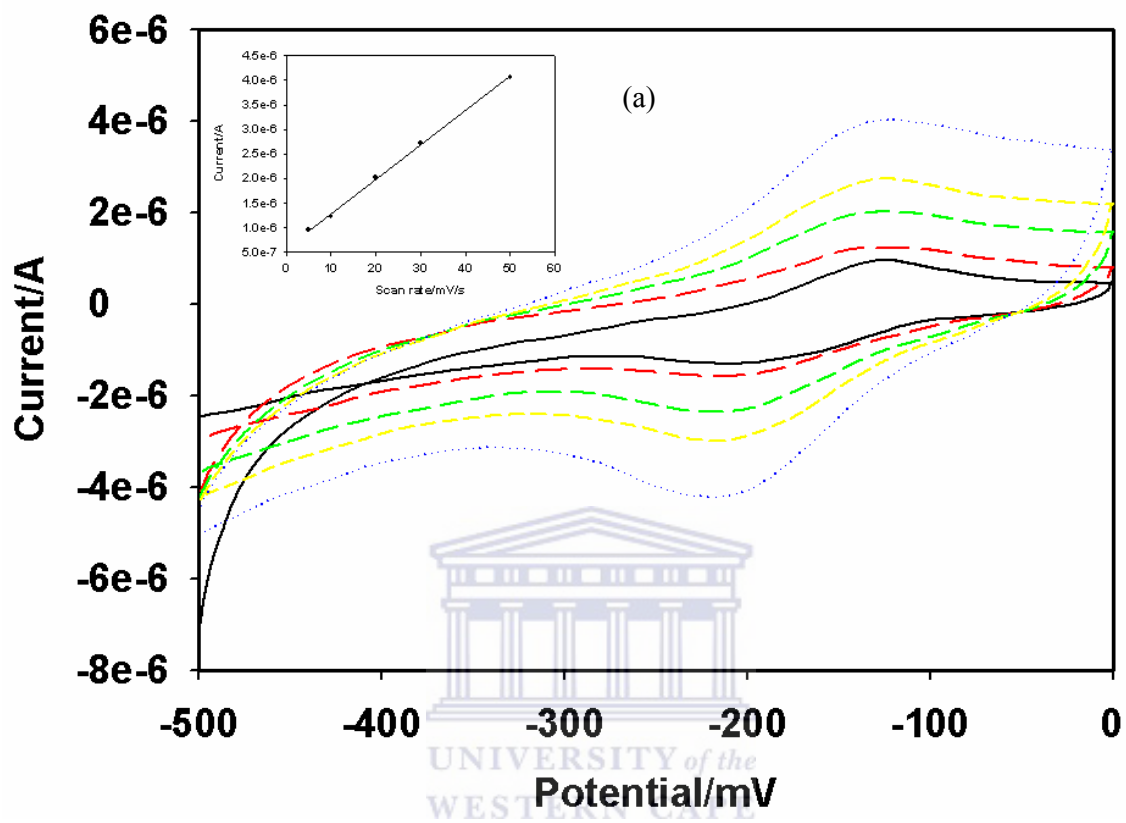
Figure 5.4 Cyclic voltammogram of (a) PTH/GCE and (b) AFB$_1$-BSA/nano-Au/PTH modified GCE in pH 6.5 acetic buffer at 5, 10, 20, 30 and 50 mV/s. insets; dependence on anodic peak current on different scan rates.

5.5 Interaction of Polythionine with gold nanoparticles.

The interactions of polythionine with gold nanoparticles has been carried out by Ding et al, 2006 using UV-vis absorption, fluorescence, Fourier transform infra red spectroscopy and transmission electron microscopy. The results showed that the nitrogen atoms of both the NH_2 moieties of thionine strongly bind to the gold nanoparticles surfaces through the electrostatic interaction of thionine with gold nanoparticles. Thionine molecules not only bind to a particle to form a compact layer via both the NH_2 moieties of thionine, but also bind two particles via their two NH_2 moieties, respectively.

5.6 Binding of the BSA-AFB1 conjugate to Citrate Coated Gold nanoparticles

The interaction between protein molecules and colloidal gold nanoparticles is very strong due to the very high surface-to-volume ratio and their high surface energy (Shipway and Willner, 2001). BSA has a preference for binding to negatively charged surfaces. However, the preferential binding of BSA is somewhat unexpected because the isoelectric point of BSA is 4.6 and therefore BSA is negatively charged at pH 7.0 which is the pH at which the many experiments are carried out. Regardless of the overall charge, BSA has 60 surface lysine groups that can have electrostatic interactions with negatively charged moieties (Tkachenko et al., 2004). Two possible mechanisms of BSA binding to nanoparticles have been suggested: either end on or side-on binding, in which end-on binding results in a higher surface coverage of BSA on the surface.

Proteins can be attached to the surface by chemical cross linking reagents, or they can spontaneously assemble because of the electrostatic forces. In the layer by layer approach, the binding of a protein to the surface of a colloid is achieved by electrostatic interactions (Stein et al., 2003). However, self assembly can also occur by protein denaturation at the electrode surface. During the formation of an adsorbed layer on the surface, each adsorbing molecule undergoes 3 steps (1) transport towards the surface, (2) attachment to the surface, and (3) spreading on the surface (Malmsten, 2003). These steps are consistent with the two possible hypotheses for the interaction between BSA and citrate-coated gold surface or nanoparticles. The first is an electrostatic binding hypothesis and the second is a displacement hypothesis. The electrostatic binding hypothesis states that the attraction between the positive surface residues (at basic pH values) is responsible for the strong binding of BSA to citrate-coated gold nanoparticles. In this hypothesis, the protein attaches itself to the passivating layer on the gold surface, with little direct interaction between BSA and the gold surface. The displacement hypothesis requires citrate to be displaced by BSA upon adsorption, with the amino acids (functional groups) lysine (amine), histidine (imidazole), and cysteine (thiol) among others interact directly with the gold surface. Spreading or structural changes in the adsorbing protein on the surface can lower the free energy of the system. Changes in protein structure are most often the result of denaturation that occurs during the displacement of the citrate stabilizer. Consequently, the displacement hypothesis can be divided into two possible outcomes: (1) displacement by protein in its native structure and (2) denaturation of proteins on the surface. If denaturation occurs during the displacement, then the protein

unfolds near the surface and exposes hydrophobic residues and presents specific functional groups that interact with the gold surface.

5.7 Electrochemical characteristics on the electrode surface

The stepwise assembly was characterised by CV. Cyclic Voltamograms of various modifications of the electrodes are shown in Figure 5.5. Curve a is the CV of a bare GCE. It did not exhibit any wave over this potential range in the blank solution. After electropolymerization, a quasi redox CV wave with peak to peak to peak separation of about 62 mV at 10 mV/s was obtained (Figure 5.5 b). The waves can be ascribed to the redox activity of PTH mediator. In comparison with Figure 5.5 b, the peak currents increased after nano-Au modification (Figure 5.5 e).The reason is that nanometer-sized colloids play an important role similar to a conducting wire or electron conducting tunnel, which makes it easier for the electron transfer to take place. However the peak currents decreased (Figure 5.5 d) after AFB_1-conjugate was adsorbed, which indicated that the AFB_1-conjugate had been immobilized on the electrode surface. Subsequently the modified immunosensor was blocked with HRP, a further decrease of peak currents could be attributed to the adsorption of the protein HRP (Figure 5.5 c). The surface concentration (Γ^*) was 7.06 x 10^{-11} and 9.65 x 10^{-10} mol/cm^2 for PTH/GCE and AFB_1-BSA/nano-Au/PTH modified GCE respectively. This indicated that AFB_1-BSA conjugate was successfully immobilized on the electrode surface supporting the observation in Figure 5.5 d. The same observations were seen with the stepwise assembly and blocking using BSA (Figure 5.6a-5.6e). However there

was a shift to a less negative potential for the redox peak. BSA was employed to act as a control for the evaluation of HRP catalytic activity.

Figure 5.5 Cyclic voltammograms of the different electrodes in working buffer (pH 6.5), (a) bare electrode; (b) PTH modified GCE; (c) AFB_1-BSA/nano-Au/PTH modified GCE blocked with HRP; (d) AFB_1-BSA/nano-Au/PTH modified GCE; (e) nano-Au/PTH modified GCE. Scan rate 10 mV/s
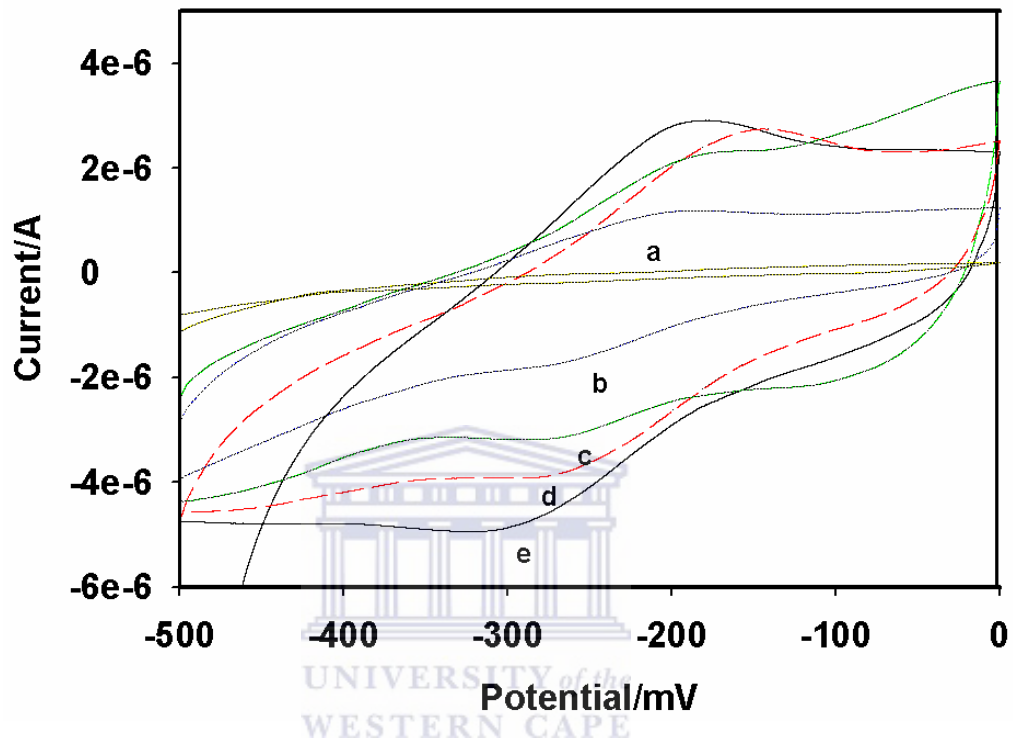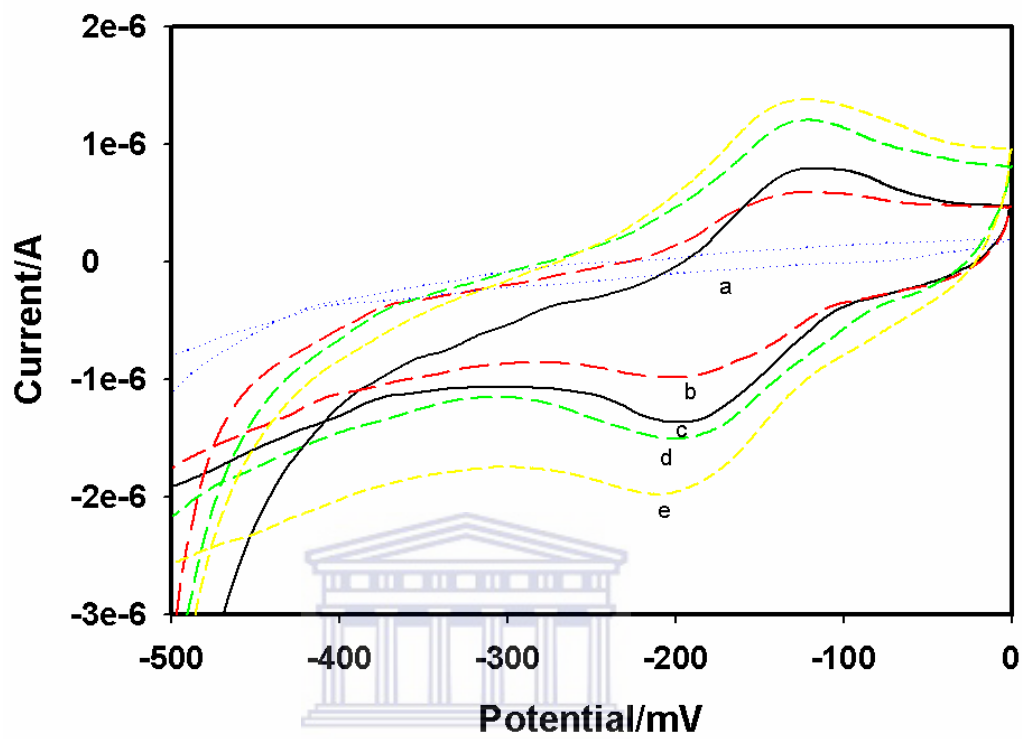
Figure 5.6 Cyclic voltammograms of the different electrodes in working buffer (pH 6.5), (a) bare electrode; (b) PTH modified GCE; (c) AFB_1-BSA/nano-Au/PTH modified GCE blocked with BSA; (d) AFB_1-BSA/nano-Au/PTH modified GCE ; (e) nano-Au/PTH modified GCE. Scan rate 10 mV/s

5.8 Assay of the HRP enzymatic catalytic activity

The employment of the HRP in the fabrication of the immunosensor played two roles. HRP was used to block possible remaining active sites of the nano-Au layer and avoid non specific adsorption. It was also able to amplify the current with the innate amplification properties of enzymes. Figure 5.7 depicts the CVs of the proposed immunosensor in the presence and absence of H_2O_2. One couple of oxidation-reduction peaks, which represents the cyclic voltamogram of PTH, is observed in the absence of H_2O_2 (Figure 5.7a). However, an enhancement of the cathodic peak and a concomitant decrease of the anodic peak current could be seen in the presence of 3.2 µM H_2O_2 (Figure 5.7b). It can thus be concluded that the HRP attached to the immunosensor surface and it retained its enzymatic catalytic activity (Ruan et al., 1998).

The response mechanism is summarized as follows

$$H_2O_2 + HRP_{(red)} \longrightarrow H_2O + HRP_{(ox)}$$
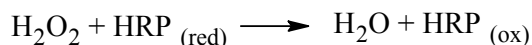
Then, the oxidized HRP oxidized $PTH_{(red)}$ to $PTH_{(ox)}$

$$HRP(ox) + PTH_{(red)} \longrightarrow HRP(red) + PTH_{(ox)}$$
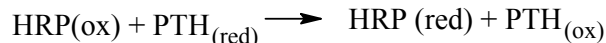
$PTH_{(ox)}$ was then reduced to $PTH_{(red)}$, resulting in the cathodic catalytic current:

$$PTH_{(ox)} + H^+ + 2e^- \longrightarrow PTH_{(red)}$$

Polythionine oxidized form: $PTH_{(ox)}$ Polythionine reduced form: $PTH_{(red)}$
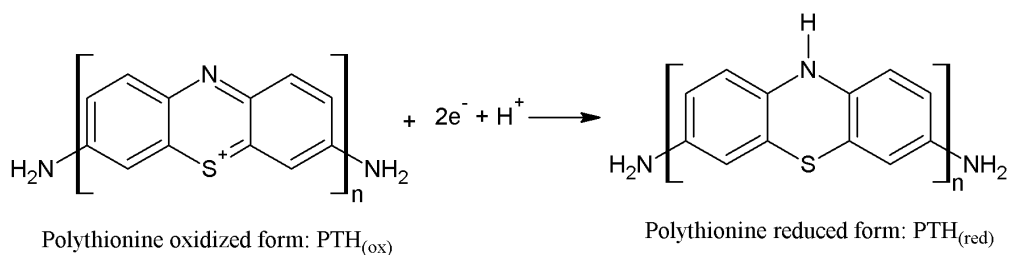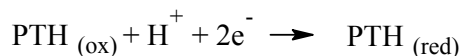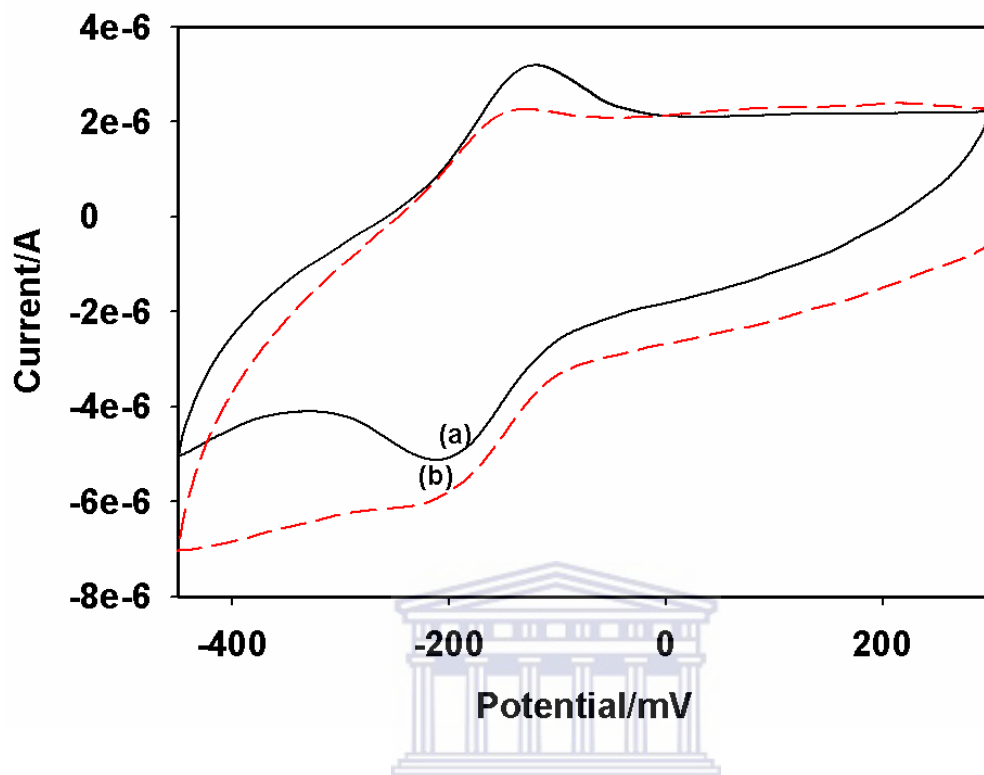
Figure 5.7 Cyclic voltammograms of the immunosensor in working buffer (pH 6.5) in the absence (a) and presence of 3.2 µM H_2O_2 (b). Scan rate 10 mV/s

5.9 Optimization of experimental conditions

An investigation of the influence of the amount of H_2O_2 on the response is of great importance, since the amplifying performance of the immobilized HRP is H_2O_2 dependent. As shown in Figure 5.8, with increasing H_2O_2 concentration for 0.4 µM, the reduction peak current in pH 6.5 working buffer increased and reached a maximum response at the H_2O_2 concentration of 3.2 µM. When H_2O_2 concentration was greater than 3.2 µM, the response decreased slightly owing to the irreversible transition of the immobilized HRP to its higher oxidized and inactive form at higher H_2O_2 concentrations (Ju et al., 1999). As a result, 3.2 µM H_2O_2 was chosen for the test.
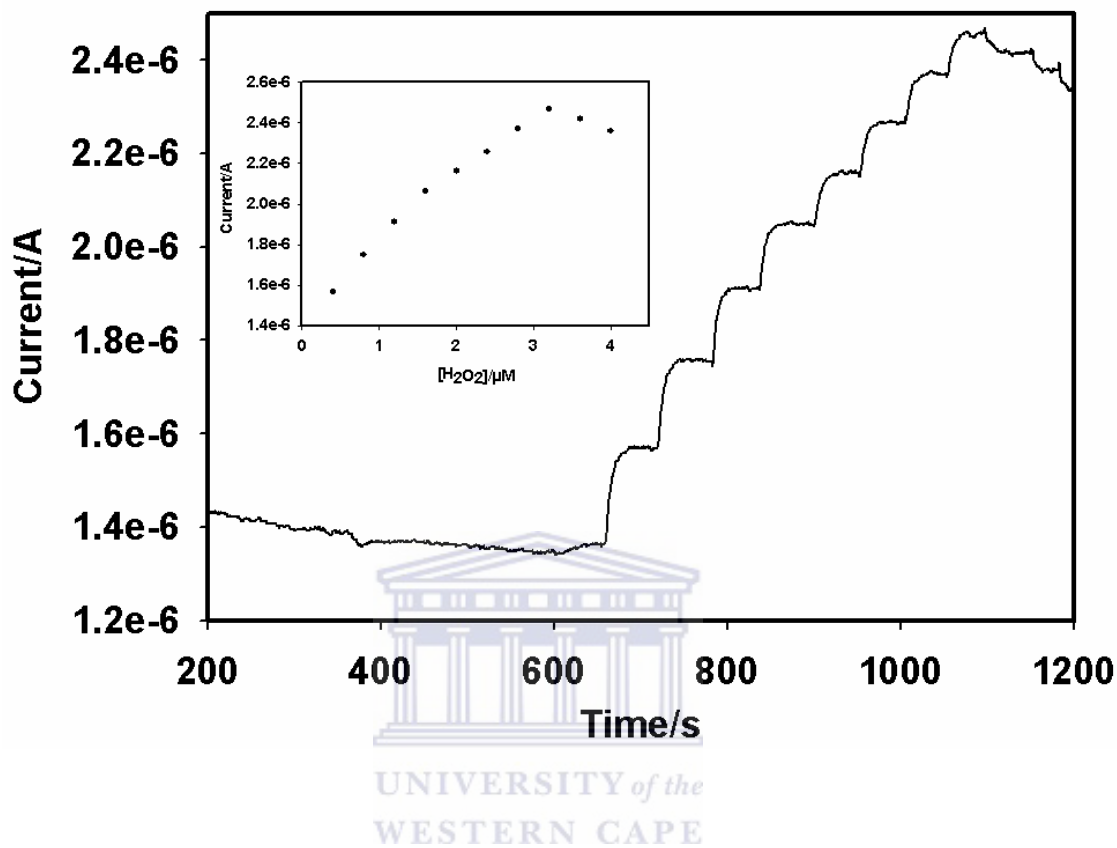
Figure 5.8 Amperometric response of the fabricated immunosensor to successive addition of H_2O_2 in a stirred 0.1M (Acetate buffer) pH 6.5. Inset: calibration curve between current and concentration of H_2O_2.

5.10 pH studies

To give an indication of the optimal pH, polythionine film was characterised in solutions with different pH values from 3.5-7.5. Figure 5.9 shows the stability and high electroactivity in solutions with pH ranges from 3.5 -6.5. The highest current was observed at pH 6.5. Thus pH 6.5 was chosen as the optimal pH for the fabrication of the immunosensor in order to retain the bioactivity of AFB_1-conjugate and HRP. Enzymes tend to denature at low pH values.
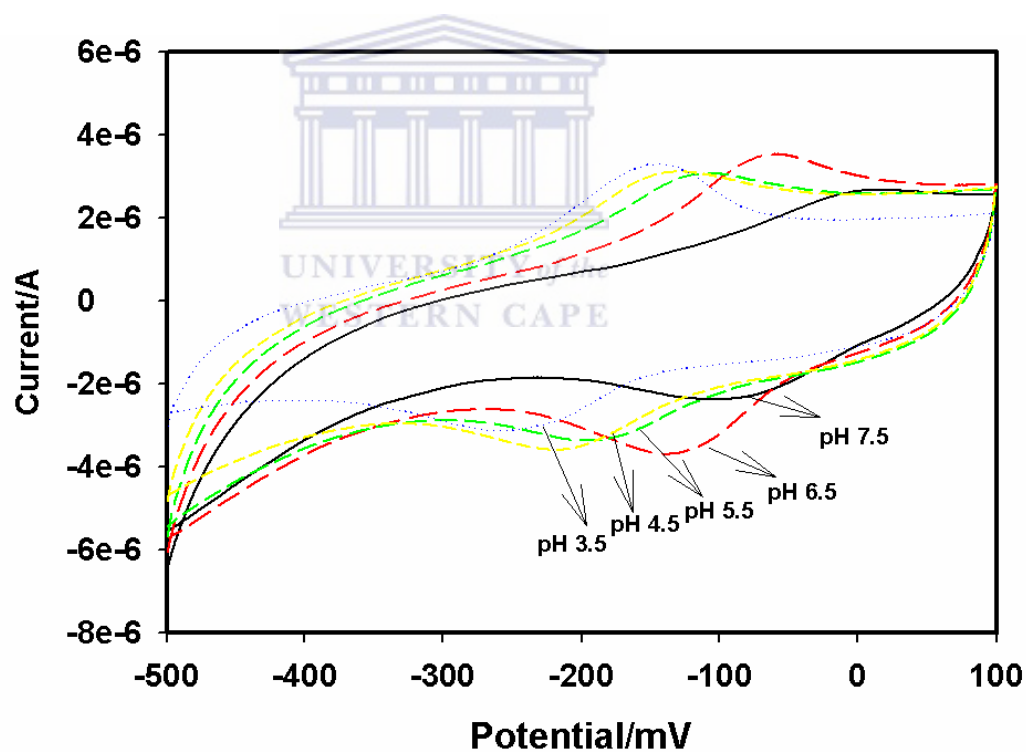
Figure 5.9 Cyclic Voltammograms of the PTH film characterisation in various pH solutions (3.5-6.5). Scan rate 10 mV/s

As the pH was increased, potential was observed to shift to more negative values. A plot of the formal potential vs. pH (Figure 5.10) indicated two processes. Between pH 3.5-5.5, the slope gave a value of 53 mV/pH which was close to the Nernstian values of 59mV for a two-proton/two electron process. Between pH 5.5-7.5, the slope was 27 mV/pH which is close to the Nernstian value of 29.5 for a one proton/two electron process. (Bruckenstein et al., 1990).
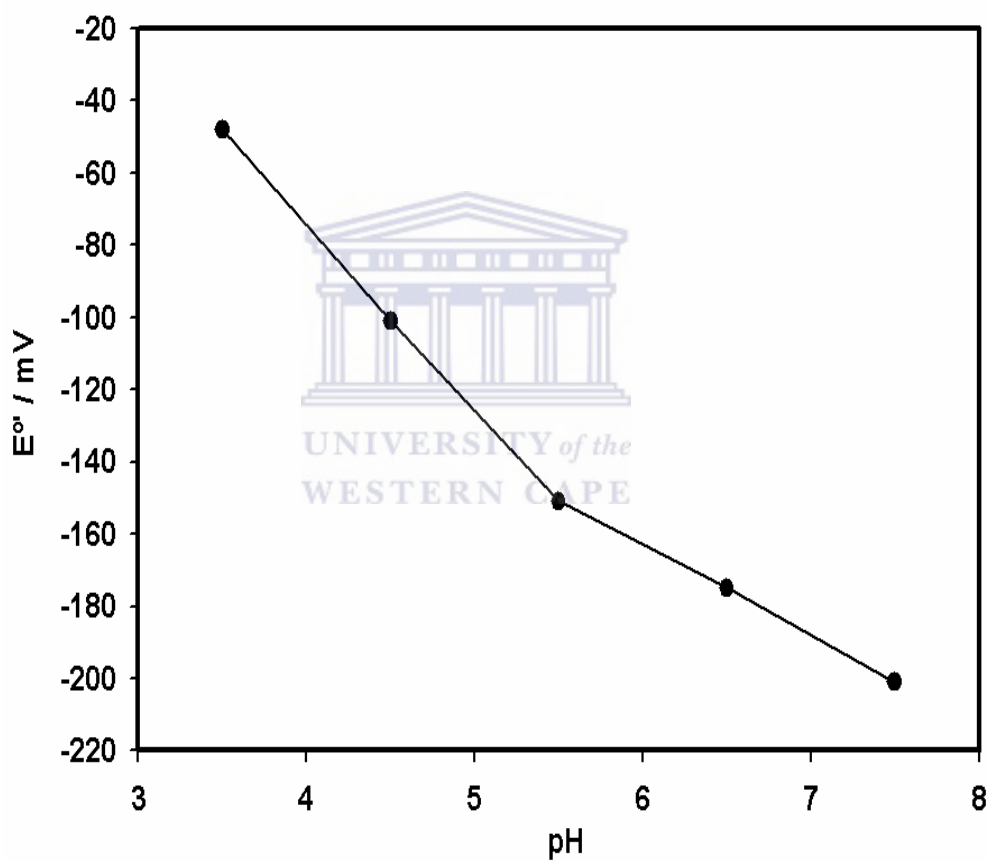
Figure 5.10 Plot of formal potential and pH

5.11 Temperature

Although 37 ^{o}C is the best incubation temperature for antibody-antigen reaction, the immunoproteins and HRP do not maintain their activities for a long time at this temperature. Thus 25 ^{o}C was employed as the optimum temperature for practical applications.

5.12 Perfomance of the immunosensor

As the background current is limiting in analytical determination of electroactive species, the experiments were carried out using differential pulse voltammetry. Figure 5.11 shows the DPV when the concentration of aflatoxin was increased at the modified electrode. As expected, the peak current was inversely proportional to the analyte concentration in the working buffer. The detection principle is based on the inhibition of the active centre of HRP by forming antigen-antibody complex. The current measurement is attributed to the direct electron transfer of the adsorbed HRP, thus the formation of the antigen-antibody complex introduces a local current change of the adsorbed HRP towards reduction of H_2O_2. The current change depends on the concentration of AFB_1. Increasing concentrations of AFB_1 led to electron transfer resistance of the adsorbed HRP which consequently lowered the current response (Lu et al., 2008). Figure 5.12 gives the DPV response of the immunosensor blocked with BSA.
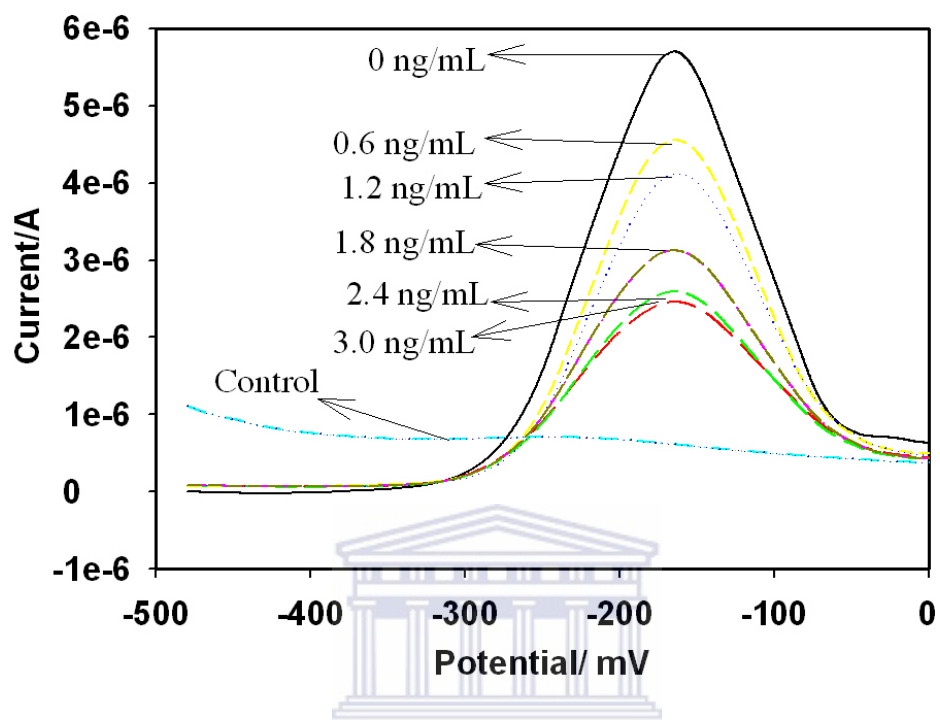
Figure 5.11 Differential pulse voltammograms of various concentrations of AFB_1

from 0, 0.6, 1.2, 1.8, 2.4, and 3 ng/mL under optimal conditions (immunosensor

blocked with HRP.
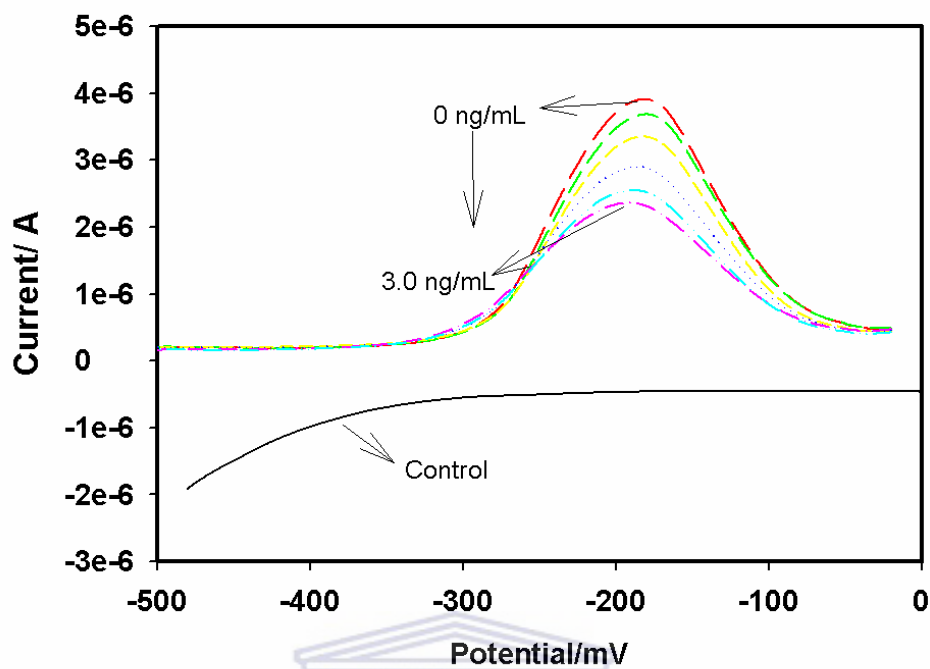
Figure 5.12 Differential pulse voltammograms of various concentrations of AFB_1 from 0, 0.6, 1.2, 1.8, 2.4, and 3 ng/mL under optimal conditions (immunosensor blocked with BSA.

All measurements were carried out in triplicate to confirm the reproducibility of results. The relative standard deviation (RSD) was 3.1%, 2.9%, 2.4% and 2.1% for 0.6, 1.2, 1.8 and 2.4 ng/mL respectively for the HRP blocked immunosensor while for the BSA blocked immunosensor the RSD was 2.8%, 3.0% 5.1% and 4.0% for the same concentration range. Thus the precision of the proposed immunosensor was acceptable. The calibration graphs are given in Figure 5.13.
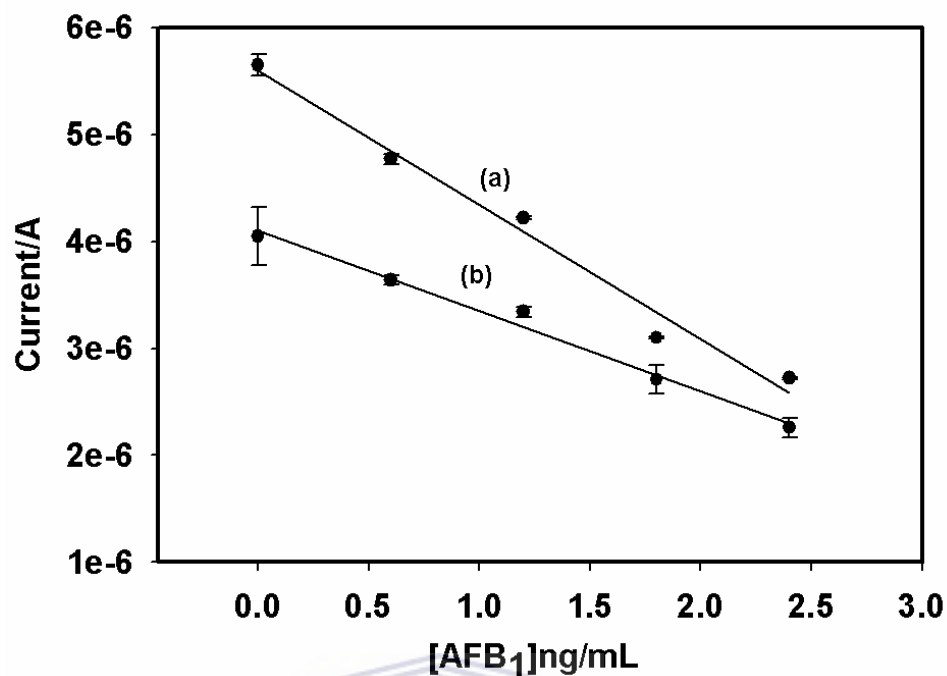
Figure 5.13 Calibration plots of AFB1 with the (a) HRP blocked immunosensor and (b) BSA- Blocked immunosensor.

The calibration curve exhibited good linearity in the range 0.6-2.4 ng/mL. The regression equation for AFB_1 was I_p (μA) = -1.23e-6 [AFB_1] + 5.31e-6 with a correlation coefficient of 0.991. The detection limit was 0.07 ng/mL. For the BSA blocked immunosensor, the regression equation was I_p (μA) = -5.66e-6 [AFB_1] + 3.72e-6. The detection limit was calculated as 3 X standard deviation of the blank/ sensitivity. Sensitivity was calculated from the slopes of the respective curves,

5.13 Comparison with other electrochemical AFB$_1$ immunosensors

The analytical performance was compared with those of other AFB$_1$ electrochemical immunosensors (Piermarini et al., 2007; Owino et al., 2007; Sun et al., 2008). The results are summarised in Table 5.1.

Table 5.1: Comparison of the analytical performance of the proposed immunosensor with other electrochemical immunosensors for detection of AFB1

Immunosensor fabrication	Linear range	Detection limit (ng/mL)	Reference
96-well screen printed microplate	0.05-2	0.03	(Piermarini et al, 2007)
Anti-AFB$_1$/PANi/PSSA/Pt	0.1-0.6	0.1	(Owino et al., 2007)
HRP-anti-AFB1/AuNP/ TiO2/RTIL/Nafion/GCE	0.1-12	0.05	(Sun et al., 2008)
HRP/Anti-AFB$_1$/Au NP/PTH/GCE	0.6-2.4	0.07	This work

As can be seen, the linear range and detection limit of the developed immunosensor are acceptable. This can be attributed to PTH being a good electron mediator which guarantees good reversibility of the electrode reaction process and the nano Au layer which provided a microenvironment similar to that of proteins in native systems, which retained the activity of proteins.
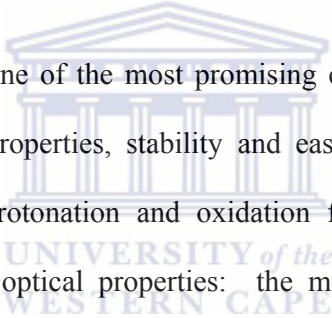
Chapter Six

Synthesis and characterization of poly (2-hydroxyethyl methacrylate)-polyaniline based hydrogel composites

6.1 Introduction

Hydrogels are hydrophilic and cross linking polymeric materials capable of absorbing a large amount of water while maintaining a three-dimensional network structure. The most commonly used monomers for synthesis of hydrogels are mono and multifunctional methacrylates and their derivatives (Gupta et al., 2002). Methacrylate monomers consisting of an alkyl group, an acrylate ester group, and a functional carboxyl group can react with a wide range of monomers and functionalized molecules providing flexible polymer chains. Alkyl methacrylates are clear and volatile liquids that are slightly soluble in water and highly soluble in alcohols, ethers, and organic solvents (Parker et al., 1998). Methacrylate hydrogels are prepared by interconnecting the lineal polymeric chains with cross-linkers establishing a three-dimensional network of strong chemical bonds. The beginning of polymerization requires thermal, photochemical, free radical or ionic activation of the monomers (Bean et al., 2005). The most commonly used type of polymerization procedure in preparation of methacrylate hydrogels is addition polymerization (free radical polymerization) initiated by free radical initiators such as 2-2'-azino-bis [3-ethyl-benzothiazozolininine-6-sulphonic acid] (AIBN) or dimethoxyl-2-phenylacetophenone (DMPA) (Konno et al., 2004). Methacrylate hydrogels are made up of two different monomers giving copolymers whose

properties depend on the nature and concentration of the monomers, polymerization conditions and the reactivity of the functional groups involved (Bayramoglu et al., 2005; Kim, 2005). For example, 2-Hydroxyethyl methacrylate (HEMA) is a water-soluble monomer that polymerizes at low temperature (from -20 to + 10 ^{o}C). The presence of hydroxyethyl groups confers high hydrophilicity to the material (Klomp et al., 1983). Copolymerization of HEMA with other monomers (such as aniline) yields hydrogels of varying physical and chemical properties such as degree of swelling, mechanical strength, optical properties and oxygen permeability (Montheard et al., 1992).

Polyaniline (PANi) is one of the most promising conducting polymers due to a good combination of properties, stability and ease of synthesis. It exists in a variety of reversible protonation and oxidation forms, differing in electrical, electrochemical and/or optical properties: the most reduced form, commonly named leucoemearaldine (LE), consists of phenylene rings joined together by amine-type nitrogen atoms. The fully oxidized polyaniline (pernigraniline) (PE) presents phenylene and quinoid rings in 1:1 ratio, separated by imine nitrogens. The half oxidized form (emeraldine) (EM) has imine and amine atoms of nitrogen in equal numbers, but the ratio of phenylene to quinoid rings is 3:1 (Kang et al., 1998). As a consequence PANi conducting composites have found practical applications in different fields, including conducting glues (Hanhi et al., 1997), conducting membrane materials (Misoska et al., 2001; Davey et al., 2001), paint coatings for anticorrosion protection (Wessling and Posdorfer, 1999) and sensor materials (Gangopadhyay, 2001). One approach for preparation of PANi

composites is physical blending, which can either be solution blending of substituted /doped soluble PANi or dry blending of PANi with another polymer followed by melt processing. Physical blending has been reviewed recently by Pud et al ., 2003, who have highlighted the serious difficulty, related to the great variety of preparative methods of PANi blends or composites, of rationalising differences in the properties of materials prepared under seemingly similar conditions. The response of these materials seems to be governed by the specific physicochemical interactions among the different components (PANi-dopant, PANi-host polymer, dopant-host polymer), which in turn depend on method and conditions of material formation, quantitative ratios between material components and raw material properties. A number of conducting polymer hydrogel composites has been synthesised. These include polypyrrole-hydrogel composites (Han et al., 2001; Brahim et al., 2002a) and a semi-intepenetrating PANi–polyacrylamide networks (Lira et al., 2005). The two hydrogels were prepared by a synthetic method based on aniline polymerisation in the presence of a matrix polymer or inside it. The main advantages of this method are the relative low cost of aniline as starting material and the uniformity of PANi particles distribution in the host polymer.

6.2 Synthesis

In the formulation of the hydrogel, HMMA was used as the co-monomer, TEGDA was the cross linker, and DMPA was the photo initiator which was employed to effect the free radical polymerization, poly HEMA was added to increase the viscosity of the hydrogel while 3-Sulfopropyl methacrylate potassium salt was

144

used as a dopant. Prior to formulation HEMA, HMMA and TEGDA were each passed over inhibitor remover columns to remove the polymerization inhibitor, hydroquinone monomethyl ether. Structures of the compounds are given in Figure 6.1

2,2-dimethoxy -2-phenylacetophenone (DMPA)

2-Hydroxyethyl methacrylate (HEMA)

Tetraethylene glycol diacrylate (TEGDA)

N-[Tris (hydroxyethyl) methyl] acrylamide (HMMA)

(3-sulfopropyl) methacrylate potssium salt
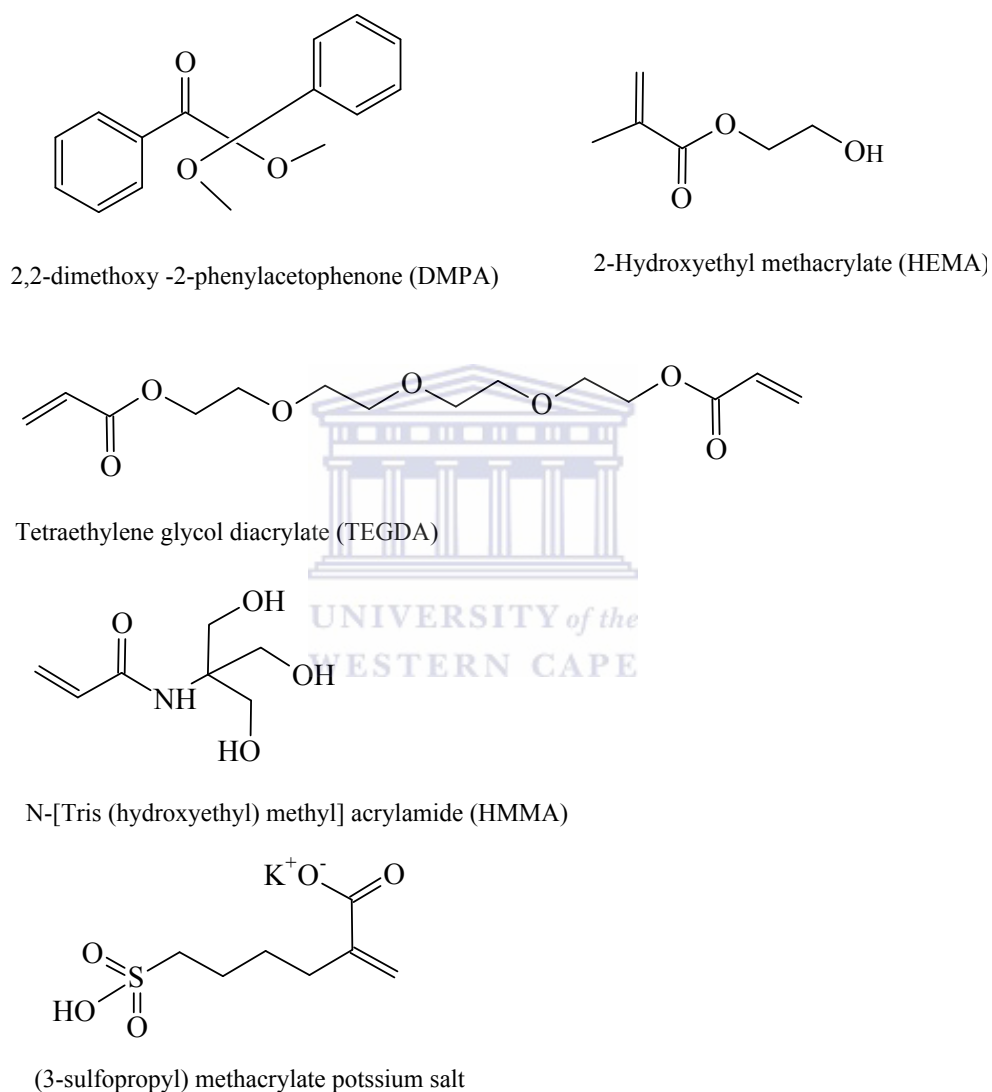
Figure 6.1 Chemical structure of compounds used in the synthesis of hydrogels

The concentration of APS is important for successful synthesis of the conducting gel. At high APS concentration (1.5 M) over oxidation was seen to take place characterized by the gels turning black in colour. At low APS concentration (0.5 M), surface aniline molecules are rapidly polymerized and the pores of the gel are quickly blocked to prevent the diffusion of APS inside the gel, this was evident when the gels were cut, and the green colour was not uniform. 0.1M APS was chosen as the optimal concentration since it gave rise to homogenous green coloured gels, typical of the protonated emeraldine form of PANi.

6.3 FT-IR spectral analysis
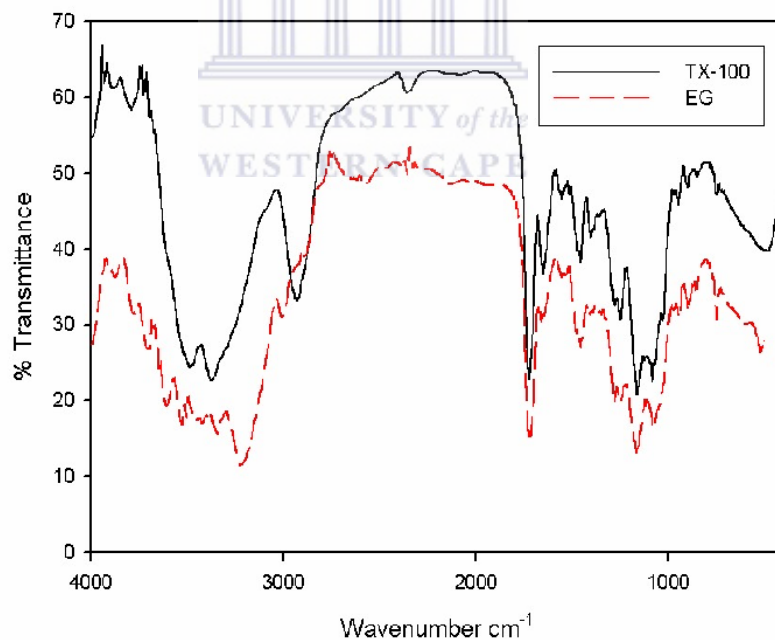
Figure 6.2 FT-IR spectra of the respective hydrogels

There is a close resemblance of peaks between hydrogels synthesised with ethylene glycol (EG) and Triton X-100 (TX-100). The peaks at 3226-3366 cm^{-1} as shown in Figure 6.2 are due to polymeric association of O-H stretching vibration mode. The peak at 2918 cm^{-1} for the hydrogel prepared using TX-100 is due to –C-H group absorption resulting from the vibrational mode. For the hydrogel prepared using ethylene glycol the peak at 2992 cm^{-1} can be attributed to asymmetrical stretching of the CH$_2$ group. The strong absorption band at 1712 cm^{-1} is due to the C=O group which indicates that HEMA has been incorporated in the hydrogel. The peak at 1152 corresponds to C-H in plane bending of phenylene. Bands at 1272 cm^{-1} belong to the stretching vibrations of C-N in the quinoid imine units of PANi (Cataldo and Maltese, 2002). The characteristic absorption peak of PANi due to phenylene ring deformation was observed at 1446 cm^{-1} (Trchova et al., 2001). These observations indicated that aniline was successfully polymerised within the hydrogel network.

6.4 Swelling behaviour

In order to determine the amount of water incorporated in the network structure formed by UV irradiation, the swelling ratios of the hydrogels are summarized in Table 2. There was no significant difference between water uptakes of the hydrogels in water and in PBS. The EG hydrogels showed a higher water uptake than the TX100 hydrogels. This could be attributed to the structure of TX-100; it contains a planar benzene ring which connects both the hydrophilic and hydrophobic group at the meta position. It can be observed that the swelling ratio

depends on the characteristic of their network structure. The EG hydrogels disintegrated after 48 hours while the TX 100 ones remained stable even after 48 hours. The values obtained for the EG hydrogels are comparable to HEMA based hydrogel (Ling and Jee) and a polypyrrole based hydrogel (Kim et al., 2000).

Table 6.1: Swelling ratios of hydrogels in water and PBS (pH 7.2)

Hydrogel	Swelling Ratio (%)	
	Water	Phosphate buffer
EG	82±2	74 ± 1
TX-100	48±1	46±1

6.5 Thermogravimetric analysis

Figure 6.3 depicts the thermo gram obtained for the hydrogels. The first step, starting at practically at room temperature and going up to 130 ^{o}C, corresponds to the expulsion of imbibed water from the polymer matrix. The second step in the range 220 to 270 ^{o}C, is associated with the dopant elimination and degradation reactions. The third step, commencing at 270°C is assigned to degradation of PANi chain, in agreement with the literature (Rannou et al., 1997).
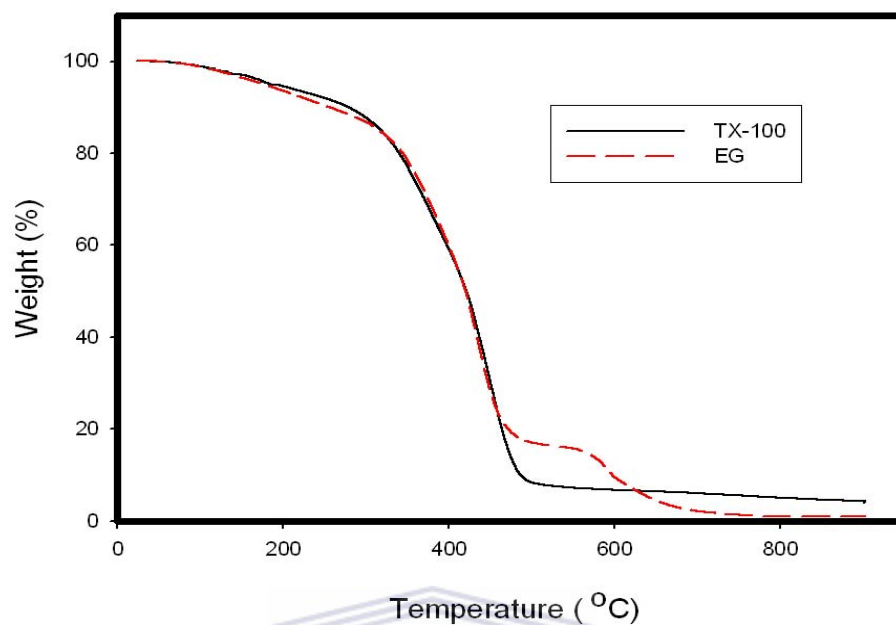
Figure 6.3 Thermogravimetric analyses of the hydrogels

6.6 Morphological studies

The SEM images of hydrogels are shown in Figures 6.4 and 6.5. The EG hydrogel displays non uniform pore sizes leading to a more open and loose network structure, TX100 hydrogels on the other hand displays a more uniform and compact pore size. TX-100, which bears a chain of approximately 10 ether groups, plays a role in organizing the structure of the gel and creating well defined uniform pores. These observations are in good agreement with the swelling studies in which the EG hydrogels were seen to have a higher degree of water uptake as compared to the TX-100 ones. A similar phenomenon has been observed for dextran based diacrylate hydrogels (Sun and Chih-Chang, 2006).
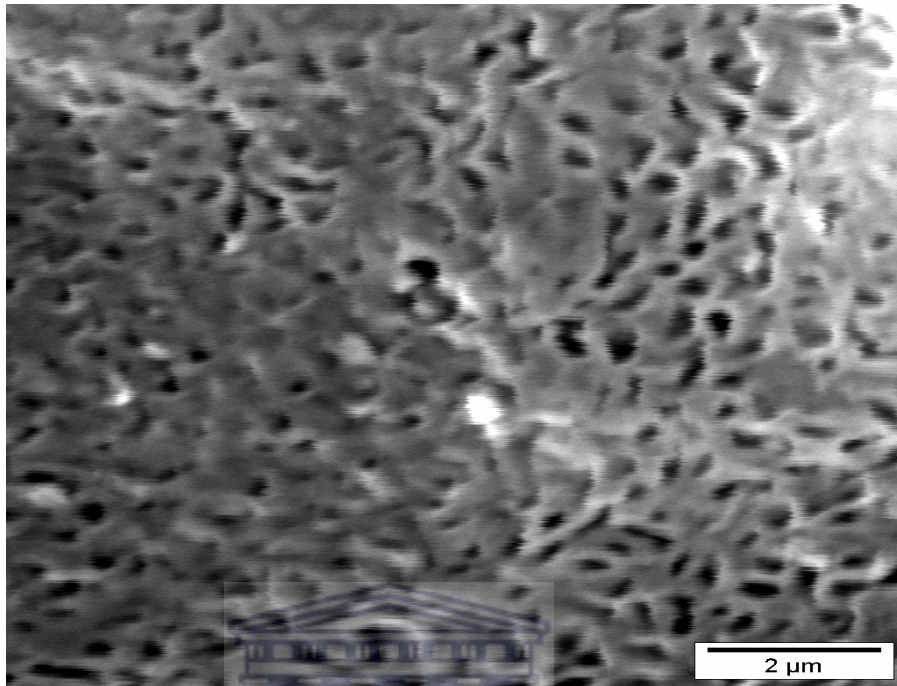
Figure 6.4 Electron microscopy of hydrogel prepared using TX   100
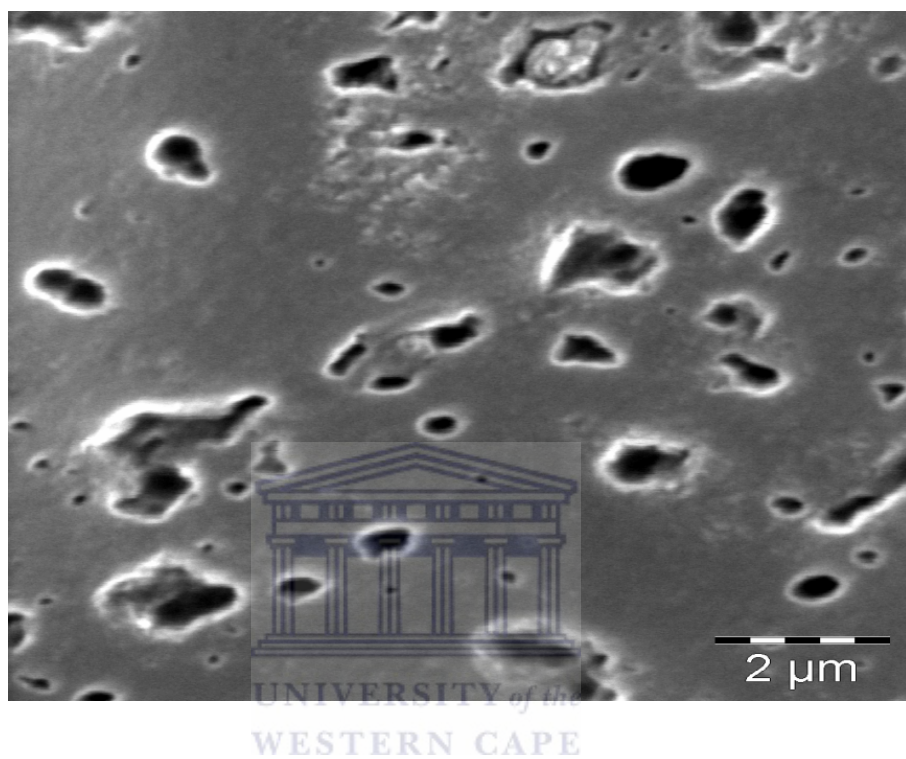
Figure 6.5 Electron microscopy of hydrogel prepared using ethylene glycol

6.7 Cyclic Voltammetry

A pair of redox peaks was observed for the TX-100 hydrogel at different scan rates investigated (20-500 mV /s) as shown in Figure 6.6. When the scan rate was altered from 20 to 500 mV/s, the cyclic voltammograms of the hydrogel film demonstrated that both I_{pa} and I_{pc} shifted in response to the change in the scan rate. As the scan rate was increased E_{pa} shifted to more positive values whilst E_{pc} became more negative. Hence smaller values of ΔE_p at low scan rate were obtained when compared with the fast scan rate. The smallest ΔE_p (41 mV) attained was at scan rate of 20 mV/s, When the scan rate was increased 25 times almost a six fold increase in ΔE_p was observed. The large ΔE_p value indicates that the charge process is quasi-reversible. The changes of the ΔE_p value with scan rates are attributed to the partial control of the charge-transfer step with respect to that of the diffusion step when the scan rates increase. In theory, when the charge-transfer is fast and completely reversible, there should be no change in ΔE_p with scan rates (Plambeck, 1982). If the process of charge transfer in the hydrogel film is almost reversible, the Randles-Sevik equation may provide information regarding the diffusion behaviour in the film. The dependence of the anodic current on the square root of scan rates of for the hydrogel film can be examined by using a plot of the current I_{pa} against $v^{1/2}$ according to Randles Sevik equation. A strong linear relationship, i.e. I_{pa} $(10^{-6}$ A) = 4. 718 x 10^{-7} $v^{1/2}$ $(Vs^{-1})^{1/2}$- 2.93 x 10^{-7} (R^2 = 0.991) was observed for such a plot (Figure 6.7). This linearity indicates a diffusion controlled electrode process. The current ratios of cathodic and anodic peak currents I_{pc}/I_{pa} was found to range from 0.82 to 0.66 for scan rates from 20-

500 mV/s suggesting that the anodic reaction is more facile than the cathodic reaction. This is due to the low mobility of the oxidation product or a faster depletion owing to a homogenous chemical reaction. Of interest was the absence of peaks in PBS for pristine PANi (Figure 6.8) since the ultimate aim is to apply the HEMA hydrogels as a bio recognition membrane for immobilization of antibodies in detection of mycotoxins. The presence of hydroxyethyl groups confers high hydrophilicity and biocompatibility to the material and its use as a matrix in enzyme immobilization has been demonstrated successfully (Arica et al., 2004; Dorreti et al., 1994; Schulz et al., 1999).
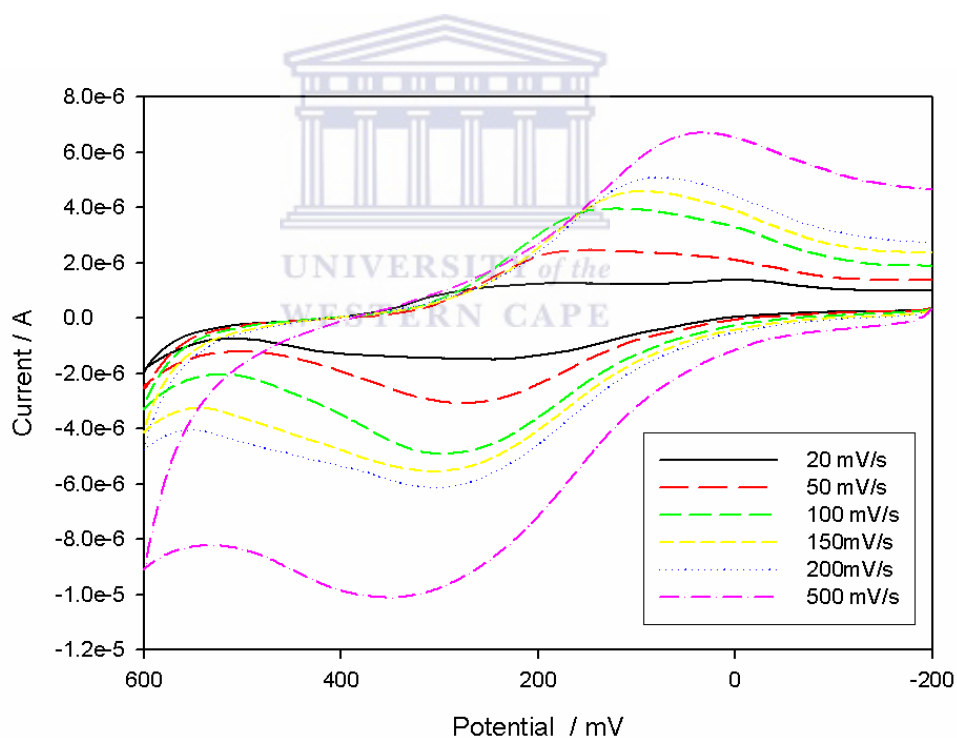
Figure 6.6 Cyclic voltammetry of the hydrogel in PBS (pH 7.2) at different scan rates
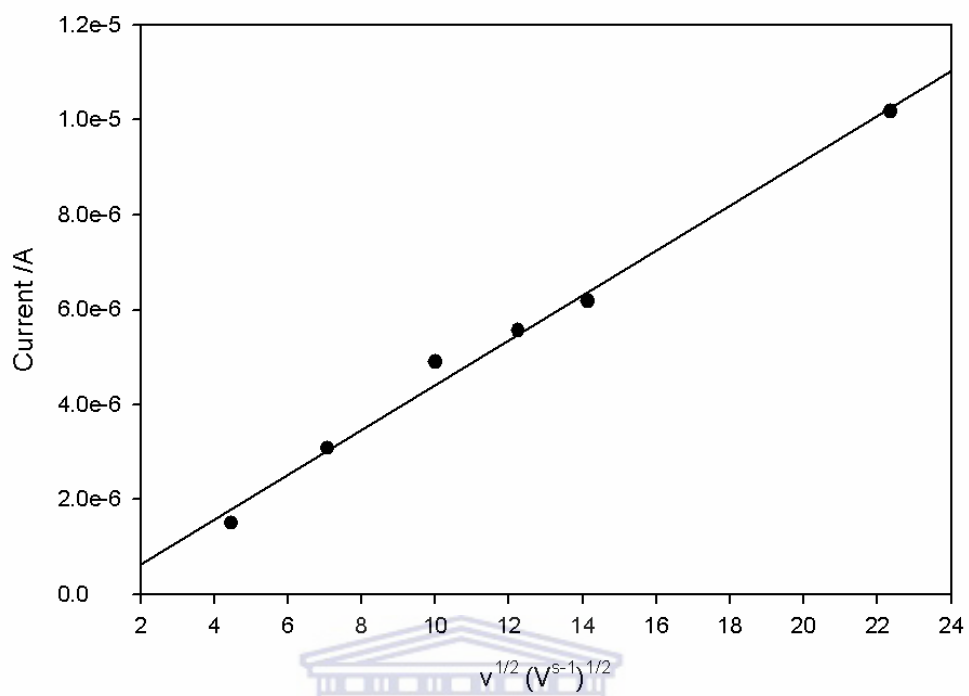
Figure 6.7 A Randles-Sevik plot of the Pt/hydrogel electrode
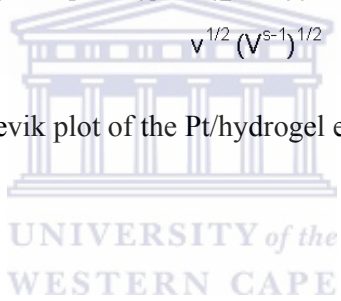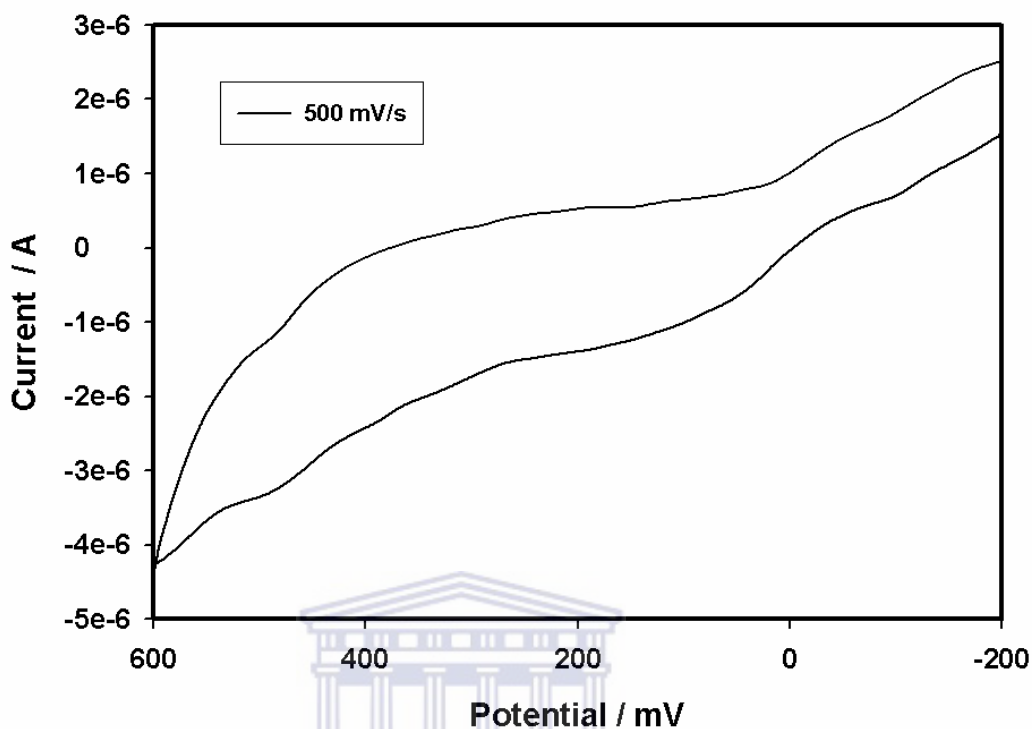
Figure 6.8 Cyclic voltammetry of pristine PANi at 500 mV/s in 0.1 M phosphate buffer solution (pH 7.2)

6.7 Electrochemical Impedance Spectroscopy

A Nyquist diagram of the electrochemical impedance spectrum is an effective way to measure the electron-transfer resistance. Figure 6.10 shows representative Nyquist diagrams of the electrochemical impedance of pristine PANi and the hydrogel. Based on the general electronic equivalent model of an electrochemical cell and the behaviour of the Pt/PANi-and Pt/hydrogel electrode, equivalent circuit which consists of electrolyte resistance (R_s), constant phase element (CPE_{dl}) describing double layer properties, electron transfer resistance (R_{et}) (Bard

155

and Faulkner, 2001) was proposed for interpretation of the impedance measurement of this system. The (R_s) represent the property of the bulk solution; thus it is not affected by the reaction occurring at the electrode surface. The other two elements (CPE_{dl}), and (R_{ct}) depend on the dielectric and insulating features at the electrode/electrolyte interface.

As can be seen in Fig. 6.10, the two curves consist of a semicircle which corresponds to the electron transfer process, typical of a kinetically controlled process. For fitting data simplified electrical equivalent circuit was used as shown on Figure 6.9. The diameter of the semicircle represents the electron-transfer at the electrode surface.
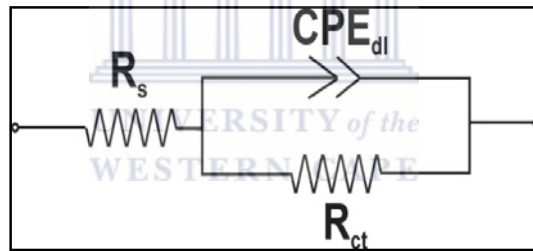
Figure 6.9 Equivalent circuit used to model impedance data.

This resistance controls the electron transfer kinetics at electrode interface. Important diagnostic parameters for Pt/PANi and Pt/hydrogel are given in table 6.2
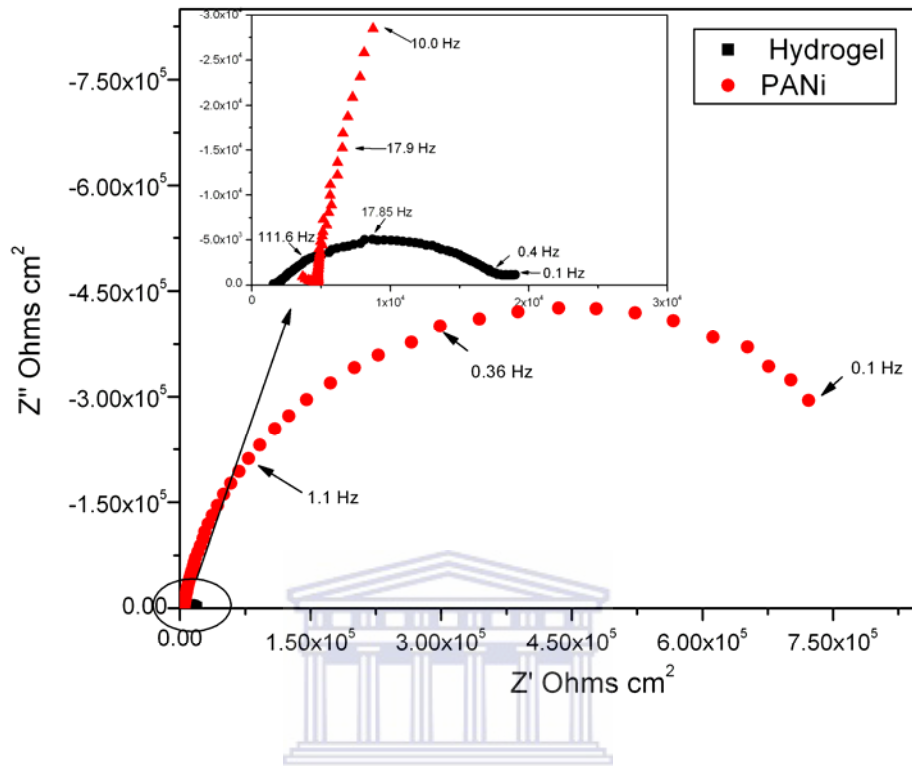
Figure 6.10 Nyquist plots for Pt/PANi and Pt/ hydrogel films in 0.1M phosphate

buffer solution (pH 7.2)

Table 6.2: Diagnostic parameters for Pt/hydrogel and Pt/PANi electrodes

Element	Pt/hydrogel	Pt/PANi
Solution Resistance (Rs) (Ω)	1695	4613
CPE(F)	3.53E-6	7.68E-7
R_{ct} (Ω)	17059	9.49E5

The low R_{ct} of Pt/hydrogel electrode as compared to Pt/PANi electrode can be related to electron hopping along the modified polymer backbone leading to increased conductivity of the doped Pt/hydrogel electrode. This is attributed to the use of 3-Sulfopropyl methacrylate potassium salt as a dopant in the formulation of the hydrogel. The inclusion of the dopant maintains electrical neutrality in the oxidised form of the polymer and also leads to increase in its structural stability and conductivity at a broader range of pH values (Michaelson et al., 1993).These observations correlates to the electroactivity of the hydrogel seen using cyclic voltammetry.

Chapter seven

Conclusions and recommendations

7.1 Conclusions

This study explored the development of an impedimetric Aflatoxin B_1 immunosensor prepared on an electrosynthetic platform. The modification of the electrode surface and the interaction between antibody and aflatoxin could be studied by impedance spectroscopy. Introduction of biomolecules such as AFB1-Ab, and BSA and the aflatoxin standards increases the electron transfer resistance. The electron transfer resistance could be used to measure the amount of AFB_1 bound to the immunosensor. The study is novel as we report for the first time an immunosensor based on PANi and Aflatoxin B_1.

The research also involved the fabrication of an AFB_1 amperometric immunosensor based on polythionine/gold nanoparticles. Immobilization of AFB_1-BSA conjugate on the GCE/PTH/AuNP was achieved. Due to the redox activity of the PTH/GCE membrane, the catalytic activity of AuNP layer and employment of HRP compared with BSA to block possible remaining active sites and amplify the current response, the fabricated immunosensor exhibited a low detection limit, high sensitivity and good reproducibility. The main contribution is that the approach eliminated the use of secondary labelled antibodies in conventional electrochemical immunosensors based on ELISA techniques.

In comparison, the amperometric immunosensor had a lower detection limit as compared to the Impedimetric immunosensor. This could be attributed to the electro catalytic properties of the gold nanoparticles employed in the amperometric immunosensor. Significantly the low detection limit of 0.07 ng/mL is within the limits set by WHO for AFB_1 and its derivatives which is 2 ng/mL.

The other part of the research involved synthesis conductive composite hydrogels made of PANi dispersed in a HEMA network. This was done using water/ EG and water /TX-100 as solvent. FT-IR spectra confirmed the polymerisation of PANi. Thermogravimetric analysis confirmed the stability of the hydrogels up to $270^{o}C$. SEM analysis correlated the pore sizes to the degree of water uptake of the hydrogels. Cyclic voltammetry and impedance analysis confirmed the electroactivity and conductivity of the TX-100 hydrogels in neutral conditions. The main contribution was that the hydrogels synthesised using water/TX-100 was found to be more stable than the one synthesised using water/EG.

7.2 Recommendations

Further research should be directed towards improvement of specificity in order to discriminate more efficiently between closely related forms of aflatoxin. This will involve raising antibodies that are more specific to the different forms of aflatoxins. The advancement of recombinant antibodies should be able this achievement a reality. Sensitivity should also be enhanced, enabling the detection of small amounts of AFB_1 within a high background matrix.

Currently, a lot of research work is geared towards immunosensors for aflatoxins; Ochratoxin seems to be getting some attention of late. There is need to explore the

possibilities of developing immunosensors for other major mycotoxins namely fumonisins and deoxynivalenol. This could be done with the help of Biotechnologists who could play the role of raising antibodies specific to the named mycotoxins.

Attempt to exploit the conductivity of the p (HEMA) -PANi hydrogel composite in neutral conditions for immobilisation of antibodies proved unsuccessful. This was due to the delaminating of the hydrogel film upon prolonged exposure to PBS. The use of N-hydroxy succinamide ester to form a covalent bond with HEMA was also unsuccessful. Further work need to be done using ethylene glycol derivatives such as methoxy-polyethylene glycol (5000)-epoxide. This might help in improving the adhesion of the hydrogel film on the electrode surface. Most hydrogels are prepared using p (HEMA). The use of other methacrylate derivatives such poly (glycidyl methacrylate) p (GMA), polybutyl methacrylate) p (BMA) and polymethylmethacrylate p (MMA) in conjunction with aniline derivatives could give rise to interesting materials that could be exploited in entrapment of biomolecules.

References

Abdel-Hamid, I., Ivnitski, D., Atanasov, P. and Wilkins, E. (1999). *Biosens. Bioelectron.* 14, 309-316.

Aberl, F., Kosslinger, C. and Wolf, H. (1997). Molecular diagnostics of infectious diseases. In: Reischl, U, editor. Methods in molecular medicine, 13, Ottawa, Human Press.

Adanyi, N., Levkovets, I., A. Rodriguez-Gil, S., Ronald, A., Varadi, M. and Szendro, I. (2007). *Biosens. Bioelectron.* 22, 797-802.

Akcelrud, L., Gonclaves, D., Dos Dantos Jr, D. S., Mattoso, L. H. C., Karasz, F. E. and Faria. R. M. (1997). *Synth. Met.* 90, 5-8.

Alarcón, S.H., Palleschi, G., Compagnone, D., Pascale, M., Visconti, A. and Barna- Vetró, I. (2006). *Talanta.* 69, 1031-1037.

Aluoch, A., Sadik, O.A. and Bedi, G. (2005). *Anal. Biochem.* 340, 136-144.

Aizawa, M. in Blum, L.J. and Coulet, P.R. (Ed). (1991). *Biosensor Principles and Application.* Marcel Dekker, New York. 249-266.

Aizawa, M. (1994). *Adv. Clin. Chem.* 31, 247-245.

Angelo, V. and Michelangelo, P. (1998). *J. Chromatogr. A.* 815, 133-140.

Aquino-Binag, C. N., Kumar, N., Lamb, R. N. and Pigram, P. J. (1996). *Chem. Mater.* 8, 2579-2585.

Arica, M.Y., Bayramoglu, G. and Bicak, N. *Process. Biochem.* (2004). 39, 2007-2017.

Atta, N. F., Galal, A., Mark Jr, H. B., Yu, T. and Bishop, P. L. (1998). *Talanta.* 47, 987-999.

Ayciek, H., Aksoy, A. and Saygi, S. (2005). *Food Control*. 16, 263-266.

Badea, M., Amine, A., Palleschi, G., Moscone, D., Volpe, G. and Curulli, A. (2001). *J. Electroanal. Chem*. 509, 66-72.

Barbero, G., Alexe-lonescu, A. L. and Lelidis, I. (2005). *J. Appl. Phys*. 98, 113-119.

Bard, A. J. and Faulkner, L. R. (2001). Electrochemical Methods: Fundamentals and applications Wiley: New York.

Barker, S. A. Immobilization of the biological component of biosensors. in Turner, A. P. F., Karube, I. and Wilson, G. S. (Ed). Biosensors- Fundamentals and Applications. Oxford University Press, Oxford.

Barnett, D., Laing, D. G., Skopec, S., Sadik, O. A. and Wallace, G. G. (1994). *Anal. Lett*, 27, 2417-2429.

Bath, R. V., Shetty, P. H., Amruth, R. P. and Sudershan. R. V. (1997). *Clin Toxicol.* 35, 249-255.

Bäumner, A. J. and Schmid, R. D. (1998). *Biosens. Bioelectron.* 13, 519-529.

Bayramoglu, G., Kacar, Y., Denizli, Y. and Arica, M.Y. (2005). *Process Biochem.* 40, 3505-3513.

Bean, L.S., Heng, L.Y., Yamin, B. M. and Ahmad, M. (2005). *Bioelectrochemistry*. 65, 157-152.

Bender, S. and Sadik, O. A. (1998). *Environ. Sci.Tech*. 32, 788-797

Bendikov, T. A. and Harmon, T. C. (2005) *Anal. Chim. Acta.* 551, 30-36.

Ben Rejeb, I., Arduini, F., Arvinte, A., Amine, A., Gargouri, M., Micheli, L., Bala, C., Moscone, D. and Palleschi, G. (2008). *Biosens.Bioelectron*. *In press.*

Berggren, C., Bjamason, B. and Johansson, G. (1999). *Instrum. Sci. Technol*. 27, 131-137.

Betty, C.A., Lal, R., Sharma, D.K., Yakmi, J.V. and Mittal, J.P. (2004). *Sens. Actuators*, B. 97, 334-343.

Blum, L. J. (1997). Bio-and Chemi-Luminescent Sensors. World Scientific Publishing, Singapore. 5-20.

Brahim, S., Narinesingh, D. and Guiseppi-Elie, A. (2001). *Anal. Chim. Acta*. 448, 27-36.

Brahim, S., Naharaj, D., Narinesingh, D. and Guiseppi-Elie, A. (2002a). *Anal. Lett*. 35, 797-812.

Brahim, S., Narinesingh, D. and Guiseppi-Elie, A. (2002b). *Biosens. Bioelectron.* 17, 973-981.

Brett, M. A. C. and Brett, A. M. O. (1999). Electrochemistry Principles, Methods and Applications,Oxford University Press: New York.

Bruckenstein, C. P., Wilde, C. P. and Hillmann, A. R. (1990). 94, 6458-6464.

Bucci, T., Hansen, D. K. and Laborde, J. B. (1996). *Nat. Toxins* 4, 51-52.

Buerk, D.G. (1993). Biosensors. Theory and applications. Lancaster, PA: Technomic publishing.

Butler, D. and Guilbault, G. G. (2006a). *Sens. Actuators, B*. 113, 692-699.

Butler, D., Pravda, M. and Gulibault, G. G. (2006b). *Anal. Chim. Acta*. 556, 333-339.

Campàs, M. and Marty, J. L. (2007a). *Anal. Chim. Acta*. 605, 87-93

Campàs, M. and Marty, J. L. (2007b). *Biosens. Bioelectron.* 22, 1034-1040.

Carlson, M. A., Bargeron, C .B., Benson, R. C., Fraser, A. B., Phillips, T. E., Velky, J. T., Groopman, J. D., Strickland, P. T. and Ko, H.W. (2000). *Biosens. Bioelectron.* 14, 841-848.

Cataldo, F. and Maltese, P. (2002). *Eur. Poly. J.* 1791-1796.

Cavic, B.A., Hayward, G. L., Thompson, M. (1999). *Analyst*. 124,1405-1420.

Chen, H., Jiang, J. H., Huang, Y., Deng, T., Li, J.S., Li, G. and Yu. R. Q. (2006). *Sens. Actuators, B*. 117-122.

Christina, G. S., Dimitrios, P. N., Anna, M. and Ulrich, J. K. (1998). *Electrochim. Acta.* 43, 3611-3617.

Corry, B., Uilk, J. and Crawley, C. (2003). *Anal. Chim. Acta.* 496, 103-116.

Coulet, P. R. What is a biosensor? (1991). in Blum, L. J. and Coulet, P.R. (Ed). Biosensor Principles and Applications, Marcel Dekker, New York.

Creppy, E.E. (2002). *Toxicol. Lett.* 127, 19-28.

Crosfet, V.V., Erdosy, M., Johnson, T. A., Buck, R. P., Ash, R. B. and Neumann, M. R. (1995). *Anal. Chem.* 67, 1647-1653.

Crowley, E., O'Sullivan, C. and Guilbault, G. G. (1999). *Anal. Chim. Acta*. 389, 171-178.

Crowther, J. R. (1995). ELISA- Theory and Practice, Humana Press, Totowa.

Cui, X., Pei, R., Wang, Z.,Yang, F., Ma, Y., Dong, S. and Yang, X. (2003). *Biosens. Bioelectron.* 18, 59-67.

Dai, Z., Yan, F., Yu, H., Hu, X. and Ju, H. (2004). *J. Immunol. Meth*. 287, 13-20

Dan, D., Xiaoxing, X., Shengfu, W. and Aidong, Z. (2007). *Talanta.* 71, 1257-1262

Darain, F., Park, J. S and Shim, Y. B. (2003). *Biosens. Bioelectron.* 18, 773-780.

Darain, F., Park, D. S., Park, J. S., Chang, S.C. and Shim, Y. B. (2005). *Biosens. Bioelectron.* 20, 1780-1787.

Davey, J. M., Ralph, S. F. Too, C. O. Wallace, G. G. and Partridge, A. C. (2001). *React Funct Polym.* 49, 87-98.

DeLisa, M. P., Zhang, Z. and Shiloach M. (2000). *Anal. Chem.* 72, 2895-2900.

Dijksma, M., Kamp, B., Hoogvliet, J.C. and Bennekom, van W.P. (2001). *Anal. Chem.* 73, 901-907.

Ding, Y., Zhang, X., Liu, X. and Guo, R. (2006). *Physicochem. Eng. Aspects.* 290, 82-88.

Diniz, F. B., Ueta, R. R., Pedrosa, da C. A. M., Areas, da C. M., Pereira, V. R. A., Silva, E. D., da Silva, J. G., Ferreira, A. G. P. and Gomes, Y. M. (2003). *Biosens. Bioelectron.* 19, 79-81.

Dispenza, C., Presti, L.C., Belfiore, C., Spadaro, G. and Piazza, S. (2006). *Polymer* 47, 961-971.

Dohno, C., Stemp, E. D. A. and Barton, J. K. (2003). *J. Am. Chem. Soc.* 125, 9586-9587.

Doko, M. B., Canet, C., Brown, N., Sydenham, N., Mpuchane, S. and Siame, B. A., 1996. *J. Agric. Food. Chem.* 44, 3240-3243.

Domenici, C., Schirone, A., Celebre, M., Ahluwalia, A. and De Rossi, D. (1995). *Biosens. Bioelectron.* 10, 371-378.

Doron, A., Katz, E. and Willner, I. (1995). *Langmuir*, 11, 1313-1317.

Dorreti, L.D. Ferrara, Lora, S. and Palma, G. (1994). *Anal. Lett.* 27, 2455-2470.

Dutta, T. K. and Das, P.(2000). *Mycopathologia*. 151, 29-33.

Dzantiev, B. B., Yazynina, E. V., Zherdev, A. V.,Y. Plekhanova, Y. V,
Reshetilov, A. N., Chang, S. -C. McNeil, C. J. (2004). *Sens. Acuators, B.* 98, 254-261

Eaton, D. L. and Groopman, J. D. (Eds). (1994). The toxicology of Aflatoxins. Academic Press, New York.

Eriksen, G. S. and Alexander, J. (Eds). 1998. Fusarium toxins in cereals-a risk assessment. Nordic Council of ministers; Tema Nord 1998: 502, pp 7-27 Copenhagen.

Evtugyn, G. A., Eremin, S. A., Shaljamova, R. P., Ismagilova, A. R. and Budnikov, H. C. (2006). *Biosens. Bioelectron.* 22, 56-62.

Fabre, B., Burlet, S., Cespuglio, R. and Bidan, G. (1997). *J .Electroanal. Chem.* 426, 75-83.

Fähnrich, K.A., Pravda, M. and Guilbault, G. G. (2003). *Biosens. Bioelectron.* 18, 73-82.

Farace, G., Lillie, G., Hianik, T., Payne, P. and Vadgama, P. (2002). *Bioelectrochemistry.* 55, 1-3.

Feng, C., Xu, Y. and Song, L. (2000). *Sens. Actuators, B.* 66, 190-192.

Ferreira, A. A. P., Colli, W., Costa, P.I. and Yamanaka, H. (2005). *Biosens. Bioelectron.* 21, 175-181.

Ferreira, A.A.P., Colli, W., Alves, M.J.M., Oliveira, D.R., Costa, P.I., Guell, A.G., Sanz, F., Benedetti, A.V. and Yamanaka, H. (2006). *Electrochim. Acta.* 51, 5046-5052.

Gaag, V. D. B., Spath, S., Dietrich, H., Stigter, E., Boonzaaijer, G., Osenbruggen, V. T. and Koopal, K. (2003). *Food Control.* 14, 251-254.

Gangopadhyay, R. and De, A. (2001). *Sens Actuator, B.* 77, 326-329.

Gao, Q., Cui, X., Yang, F., Ma, Y. and Yang X. (2003). *Biosens. Bioelectron*, 19, 277-282.

Garifallou, G.Z., Tsekenis, G., Davis, F., Higson, P. J. Pinacho, D. G., Sanchez-Baeza, F., Marco, M. P., and Gibson, T. D. (2007). *Anal. Lett*, 40, 1412-1422.

Garland, J. E., Pettit C. M. and Roy, D. (2004). *Electrochim. Acta*. 49, 2623-2635.

Ghindilis, A. L., Atanasov, P., Wilkins, M. and Wilkins E. (1998). *Biosens. Bioelectron.* 13, 113-131.

Gizeli, E. and Lowe, C. R. (1996). *Curr. Opin. Biotechnol*. 7, 66-71.

Gonzalez-Bellavista, A. G., Macanas, J., Munoz, M. and Fabregas, E. (2007). *Sens. Actuators. B.* 125, 100-105.

Gonzalez-Penas, E., Leache, C. and Viscarret, M. (2004). *J. Chromatogr. A*. 1025, 163-168.

Gooding, J. J., Wasiowych, C., Barnett, D., Hibbert, D. B.; Barisci, J. N. and Wallace, G.G. (2004). *Biosens. Bioelectron*. 20, 260-268.

Grant, S., Dauris, F., Law, K. A., Berton, A. C., Collyer, S. D. and Higson, S. P. J., Gibson, T. D. (2005). *Anal.Chim. Acta.* 537, 163-168.

Grennan, K., Killard, A. J., and Smyth, M. R. (2001). *Electroanalysis*. 13, 745-748.

Grennan, K., Strachan, G., Porter, A. J., Killard, A. and Smyth, M. R. (2003). *Anal. Chim. Acta*. 500, 287-298.

Gupta, P., Vermani, K. and Garg. S. (2002). *Drug. Discov. Today*. 7, 569-573.

Hammet, A. and Hillman, A. R. (1987). *J. Electroanal.Chem*. 233, 125-146.

Han, J. S., Lee, J. Y. and Lee, D. S. (2001). *Synth Met.*121, 301-306.

Hanhi, K., Lonnberg, V. and Pyorala, K. (1997). WO Patent 9,706, 213.

Harlow, E. and Lane, D. (1988). Antibodies- A Laboratory Manual, Cold Spring Harbor Laboratory. New York.

Harrison, L. R., Colvin, B. M., Green, J. T., Newman, L. E. and Cole, J. R. (1990). *J. Vet. Diagn. Invest.* 2, 217-221.
Hazi, J., Elton, D. M., Czerwinski, W. A., Schiewe, J, Vicente-Beckett, V.A. and Bond, A. M. (1997). *J. Electroanal. Chem*. 437, 1-15.

Hock, B., Dankwardt, A., Kramer, K. and Marx, A. (1995). A review: *Analytica Chimica Acta*. 311, 393-405.

Holzhäuser, D., Delatour, T., Marin-Kuan, S., Guignard, D., Piguet, J., Richoz, C., Bezen, B. S. and Carin, C. 2003. *Toxicol. Lett.* 144: 65-71.

Hussain, F., Birch, D. J. S. and Pickup, J. C. (2005). *Anal. Biochem*. 339, 137-143.

International Agency for Research on Cancer (IARC), (1993). Monographs on the evaluation of carcinogenic to humans; Some naturally occurring substances, food items and constituents, heterocyclic aromatic amines and mycotoxins. IARC, WHO, pp 397.

Ionescu, R. E., Gondran, C., Cosnier, S. and Gheber, L. A. (2005). *Talanta*. 66, 15-20.

Ivaska, A. and Lindfors, T. (2001). *Anal. Chim. Acta*. 437, 171-182.

Ivnitski, D. and Rishpon, J. (1996). *Biosens. Bioelectron.* 11, 409-417.

Ivnitski, D., Wolf, T., Solomon, B., Fleminger, G. and Rishpon, J. (1998). *Bioeletrochem. Bioenerg.* 45, 27-32.

Iwuoha, E. I., Villaverde, D. S., Gracia, P. N., Smyth, R. M. and Pingaron, J. M. (1997). *Biosens. Bioelectron.* 12, 749-761.

Iwuoha, E. I., Mavundla, S. E., Somerset, V. S., Petrik, L. F., Klink, M. J. Sekota, M. and Baker, P. (2006). *Microchim. Acta.* 155, 453-458.

Jarvis, B. B. and Miller, J. D. (2005). *Appl. Microbiol. Biotechnol.* 66, 367-372.

Jia, W., Tchoudakov, R., Segal, E., Joseph, R., Narkis, M. and Siegman, A. (2003). *Synth. Met*. 132, 269-278.

Jie, M., Ming, Y.C., Jing, D., Cheng, L. S, Huai na, L., Jun, F. and Xiang, C. Y. (1999). *Electrochem.Commun*. 1, 425-428.

Jiménez, C., Bartrol, J., de Rooij, N. F. and Koudelka-Hep, M. (1997). *Anal. Chim. Acta.*352, 169-176.

John, R., Spencer, M., Wallace, G. G., and Smyth, M. R. (1991). *Anal.Chim.Acta*, 249, 381-385.

Jorcin, J. B., Orazem, M. E., Pebere, N. and Tribollet, B. (2006). *Electrochim. Acta*. 51, 1473-1479.

Jovanovi, V. M., Markievi, L., Stankovi, S., Stankovi, R. and Jovanovi, M. S. (1995). *Electroanalysis*. 7, 574-578.

Ju, H. X., Yan, G. F. and Chen, H. Y. (1999). *Electroanalysis.*11, 124-129.

Kaden, H., Jahn, H. and Bethold, M. (2004). *Solid State Ionics*. 169, 129-133.

Kaifer, A. E., Kaifer, M. G. (1999). Supramolecular Electrochemistry, Wiley-VCH, Germany

Kahlert, H. (2002). Electroanalytical methods: Guide to Experiments and Applications. (Ed.) Scholz, F. New York: Springer. 261- 278.

Kang, E.T., Neoh, K.G. and Tan, K. L. (1998). *Prog. Polym. Sci*. 23, 277-324.

Karube, I. and Nomura, Y. (2000). *J. Mol. Catal. B: Enzym.* 10, 177-181.

Karyakin, A. A., Karyakina, E. E. and Schmidt, H. L. (1999). *Electroanalysis.* 11,149-155.

Katz, E. and Willner, I. (2003). *Electroanalysis.* 15, 913-918.

Kellerman, T. S., Marasas, W. F. O., Theil, P. G., Gelderblom, W. C. A., Cawood., M. and Coetzer, J. A. W. (1990). *J. Vet. Res.* 57, 269-275.

Kerner, Z. and Pajkossy, T. (2000). *Electrochim. Acta*. 46, 207-211.

Khan, R. and Dhayal, M. (2008). *Electrochem. Commun*. 10, 492-495.

Killard, A. J., Deasy, B., O'Kennedy, R. and Smyth, M. R. (1996). *Trends Anal. Chem*. 14, 257-266.

Killard, A. J., Zhang, S., Zhao, R., John. R., Iwuoha, E. I. and Smyth M. R (1999). *Anal. Chim. Acta,* 400, 109-115.

Kim, B. C., Spinks, G. M. Wallace, G.G. and John, R. (2000). *Polymer.* 41, 1783-1790.

Kim, E. K., Maragos, C. M. and Kendra, D. F. (2004). *J. Agric. Food Chem.* 52, 196-200

Kim, G. H. (2005).   *Eur. Poly. J.* 41, 1729-1737.

Klomp, G. F., Hashiguchi, H., Ursell, P.C., Takeda, Y., Taguchi, T. and Dobelle, W. H. (1983). *J. Biomed. Mater. Res.* 17, 865-871.

Kolosova, A. Y., Shim, W. B., Yang, Z.Y. Eremin, S. A. and Chung, D. H. (2006). *Anal. Bioanal. Chem.*384, 286-294.

Konno, T., Watanabe, J. and Ishihara, K. (2004). *Biomacromolecules,* 5, 342-347.

Konopka, A., Sokalski, T., Michalska, A., Lewenstam, A. and Maj-Zurawska, M. (2004). *Anal. Chem.* 76, 6410-6418.

Koul, S., Chandra, R. and Dhawan, S.K. (2001). *Sens. Actuators*, B. 75, 151-159.

Kreuzer, M. P., Pravda, M., O'Sullivan, C. K. and Guilbault, G. G. (2002). *Toxicon.* 40, 1267-1274.

Kumar, D. and Sharma (1998). *Eur. Polym. J.* 34, 1053-1060.

Lee, C., Kwak, J. Kepley, L. J. and Bard, A. J. (1990). *J. Electroanal. Chem*, 282, 239-252.

Lei, C. X., Gong, F. C., Shen, G. L. and Yu, R. Q. (2003). *Sens Actuators, B*. 96, 582-588.

Li, M. H., Lu, S. H., Ji, C., Wang, Y., Cheng, S., Tian, G., (1980).Experimental studies on the carcinogenityof fungus-contaminated food in Linxian. In: Gelboin, H.V., (Ed), Genetic and environmental factors in experimental and human cancer, vol. 4. Japan science society press, Tokyo pp 139-148.

Li, L. and Walt, D. R. (1995). *Anal. Chem.* 67, 3746-3752.

Li, J., Xiao, L.T., Zeng, G. M., Huang, G.H., Shen, G. L. and Yu, R. Q. (2003). *Anal. Chim. Acta*. 494, 177-185.

Li, H., Wang, D. Q., Liu, B. L. and Gao. L. Z. (2004). *Colloids Surf. B*. 33, 85-88.

Li, X., Yuan, R., Chai, Y., Zhang, L., Zhuo, Y. and Zhang, Y. (2006). *J. Biotechnol.* 123, 356-366.

Li, Y., Wang, P., Wang, L. and Lin, X. (2007). *Biosens. Bioelectron*. 22, 3120-3125.

Liedberg, B., Nylander, C. and Lundstrom, I. (1995). *Biosens. Bioelectron*. 10, 1-9.

Lillie, G., Payne, P. and Vadgama, P. (2001). *Sens. Actuators, B*. 78, 249-256.

Ling, L. and Lee, L. J. (2005). *Polymer*. 46, 11540-11547.

Lira, M. L., Susana, I. and Cordoba de Torresi. (2005). *Electrochem. Commun*. 7, 717-723.

Liu, S. Q., Leech, D. and Ju, H. X. (2003). *Anal. Lett.* 36, 1-17.

Lopez, M.A., Ortega, F., Dominguez, E. and Katakis, I. (1998). *J. Mol. Recognit.* 11, 175-177.

Lu, B., Smyth, M. R., O'Kennedy, R., Moulds, J. and Frame, T. (1997). *Anal.Chim. Acta.* 340, 175-180.

Lu, X., Bai, H., He, P.,Cha, Y., Yang, G., Tan, L. and Yang, Y. (2008) *Anal.Chim. Acta.*615, 158-164.
Macdonald, J. R., Schoonman, J. and Lehnen, A. P. (1982). *J. Electroanal. Chem.* 131, 77-81.

Macdonald, J. R. (1987). Impedance Spectroscopy: Emphasizing Solid Materials and Systems. New York: Wiley.

Macdonald, D. D. (2006). *Electrochim. Acta.* 51, 1376-1388.

Malmsten, M. (2003) Biopolymers at interfaces, 2nd ed., Marcel Dekker: New York, Vol 110.

Mantle, P. G. (2002). *Int. Biodeterior. Biodegrad.* 50,143-146.

Marasas, W. F. O., Welner, F. C., Van Rensburg, S .J. and Van Schalwik, D. J. (1981). *Phytopathology*, 71, 792-796.

Maria, N. V. and Toby, M. (2003). *Biosystems Eng.* 84, 1-12.

McNeil, C. J., Athey, D. and Renneberg, R. (1997). EXS, 81, 17-25.

Medyantseva, E. P., Khaldeeva, E.V. Glushko, N. I. and Budnikov, H. C. (2000). *Anal. Chim. Acta.* 411, 13-18.

Miao, Q. Y. and Guan, G. J. (2004). *Anal. Lett.* 37, 1053-1062.

Michaelson, J. C., McEvoy, A. J. and Gratzel, M. (1993). *Synth. Met.* 57, 1564-1567.

Micheli, L., Grecco, R., Badea, D. and Moscone, G. P. (2005). *Biosens. Bioelectron.* 21, 588-596.

Misoska, V., Ding, J., Davey, J. M., Price, W. E. Ralph, S. F. and Wallace, G. G. (2001). *Polymer.* 42, 8571-8579.

Monk, P. M. S. (2001). Fundamentals of Electroanalytical Chemistry, Wiley, Sussex

Montheard, J. P. Chatzpoulous, M. and Chappard. D. (1992). *Rev. Macromol. Chem. Phys.* 32, 1-34.

Morgan, C. L., Newman, D. J. and Price, C. P. (1996). *Clin.Chem*, 42, 193-209.

Morrin, A., Guzman, A., Killard, A. J., Pingaron, J.M. and Smyth, M. R. (2003). *Biosens. Bioelectron.* 18, 713-716.

Moscou, E. A., Madou, M. J., Bachas, G. L. and Daunert S. (2006). *Sens. Actuators*, B. 115, 379-383.

Mousavi, Z., Bobacka, J., Lewenstam, A. and Ivaska, A. J. (2006). *Electroanal. Chem.* 593, 219-226.

Mullet, W., Edward, P. C. L. and Jupiter, M. T. (1998). *Anal. Biochem.* 258, 161-167.

Murray, R.W. (1984) In: Bard, A. J. (ed) Electroanalytical chemistry. vol 13, Marcel Deker, New York.

Nagwa, H. S., Micheli, L. and Palleschi, G. (2004). *Anal. Chim. Acta.* 520, 159-164.

Naudin, E., Gouerec, P. and Belanger, J. (1998). *Electroanal. Chem*. 459, 1-9.

Nikpour, M., Chaouk, H., Mau, A., Chung, D. J. and Wallace, G. G. (1999). *Synth. Met*. 99,121-125.

Ocypa, M, Michalska, A. and Maksymiuk, K. (2006). *Electrochim. Acta.* 51, 2298-2305.

Ogurtsov, N.A., Pud, A.A., Kamarchik, P. and Shapoval, G.S. (2004). *Synth. Met*. 143, 43-47.

Oliveira, S. C. B., Diculescu, V. C., Palleschi, G., Compagnone, D. and Oliveira-Brett, A. M. (2007). *Anal. Chim. Acta*. 588, 283-291.

Oswald, B., Lehman, F., Simon, L., Terpetschnig, E. and Wolfbeis, O. S. (2000). *Anal. Biochem.* 280, 272-277.

Otero, T.F. and Boyano, I. (2003). *J. Phys. Chem. B.* 107, 4269-4276.

Ouerghi, O., Touhami, A., Renault, J.N., Martelet, C., Ouada, B.H. and Cosnier, S. (2002). *Bioelectrochemistry.* 56, 131-133.

Owino, J. H. O., Ignaszak, A., Al-Ahmed, A., Baker, P.G. L., Alemu, H., Ngila, J.C. and Iwuoha, E. I. (2007). *Anal. Bioanal. Chem*. 388, 1069-1074.

Pajkossy, T. (1994). *J. Electroanal. Chem*. 364, 111-125.

Park, Y. and Park, S. (2002). *Synth. Met.* 128, 229-234.

Parker, S., Martin, D. and Braden, M. (1998). *Biomaterials.* 19, 1695-1701

Parellada, J., Narvaez, A., Lopez, M. A., Dominguez, E., Fernandez, J. J., Pavlov, V. and Katakis, I. (1998). *Anal. Chim. Acta.* 362, 47-57.

Patolsky, F., Zayats, M., Katz. E. and Willner, I. (1999). *Anal. Chem.*, 71, 3171-3180.

Pearson, J. E., Gill, A. and Vadgama, P. (2000). *Ann. Clin. Biochem.* 37, 119-145.

Pemberton, R. M., Hart, J. P. and Mottram, T. T. (2001). *Biosens.Bioelctron.* 16, 715-723.

Pemberton, R. M., Pittson, R., Biddle, N., Drago, G. A. and Hart, J. P. (2006)**.** *Anal. Lett.* 39, 1573-1586.

Piermarini, S., Micheli, L., Ammida, N. H. S., Palleschi, G. and Moscone, D. (2007). *Biosens. Bioelectron.* 22, 1434-1440.

Piermarini, S., Volpe, G., Micheli, L., Moscone, D. and Palleschi, G. (2009). *Food Control.* 20, 371-375.

Pittet, A. (2005). *Mitt.Lebensm.Hyg.* 96, 424-444

Pividori, M. I., Merkoci, A. and Alegret, S. (2000). *Biosens. Bioelectron.* 15, 291-303.

Plambeck, J. A. (1982). Electroanalytical Chemistry: Basic Principles and Applications, John Wiley and Sons, Canada.

Podual, K., Doyle III, F. and Peppas, N. A, (2000a). *Polymer*. 41, 3975-3983.

Podual, K., Doyle III, F. and Peppas, N.A, (2000b). *J. Control Release*. 67, 9-17.

Powner, E.T. and Yalcinkaya, F. (1997). *Sens. Rev*. 17, 107-116.

Prieto, S. B., Campas, M., Marty, J. L. and Noguer, T. (2008). *Biosens. Bioelectron*. 23, 995-1002.

Rannou, P. and Nechtscshein, M. (1997). *Synth. Met*. 84, 755-766.

Rastogi, S., Divedi, P. D., Khanna, S. K. and Das, M. *Food Control*. (2004).15, 287-290.

Pud, A., Ogurtsov, N., Korzhenko, A. and Shapoval, G. (2003). *Prog. Polym. Sci*. 28, 1701-1753.

Purvis, D. Leonardova, O, Farmakovsky, D.and Cherkasov, V (2003). *Biosens.Bioelectron*. 11, 1385-1390.

Qiang, Z, Yuan, R., Chai, Y., Wang, N., Zhuo, Y., Zhang, Y.and Li, X. (2006). *Electrochim. Acta*. 3763-3768.

Rao, V. K., Rai, G. P., Agarwal, G. S. and Suresh, S. (2005). *Anal. Chim. Acta*. 531, 173-177.

Reid, G.D., Whittaker, D. J., Day, M. A., Creely, C. M., Tuite, E. M., Kelly, S. and Beddard, G. S. (2001). *J. Am.Chem. Soc.*123, 6953-6954.

Ruan, C., Yang, F., Lei, C. H. and Deng, J. Q. (1998). *Anal. Chem.* 70, 1721-1725.

Ruan, C., Yang, L. and Li, Y. (2002). *Anal. Chem.* 74, 4814-4820.

Saez, E. I. And Corn, R. M. (1993). *Electrochim. Acta*. 38, 1619-1625.

Sadik, O.A., John, M. J., Wallace, G. G., Barnett, D., Clarke, C., and Laing, D.G. (1994). *Analyst*. 119, 1997-2000.

Sadik, O.A., Xu, H., Gheorghiu, E., Andrescu, D., Balut, C, Gheorghiu, M. and Bratu, D. (2002). *Anal. Chem.* 74, 3142-3150.

Samir, K. S. and Rupali, G. (2005). *Polymer.* 46, 2993-3000.

Santandreu, M., Alegret, S. and Fàbregas, E. (1999). *Anal. Chimica. Acta*. 396, 181-188.

Sapsford, K. E., Ngundi, M. M., Moore, M. H., Lassman, M. E., Shriver-Lake, L. C., Taitt, C. R. and Liegler, F. S. (2006a). *Sens. Actuators*, B. 113, 599-607.

Sapsford, K. E., Taitt, C. R., Fertig, S., Moore, M. H., Lassman, M. E., Maragos, C. M. and Shriver-Lake, L. C. (2006b). *Biosens. Bioelectron.* 21, 2298-2305.

Sargent, A., Loi, T., Gal, S. and Sadik, O. A. (1999). *J. Electroanal. Chem.* 470, 144-156.

Sargent, A. and Sadik, O. A. (1999). *Electrochim. Acta*. 44, 4667-4675.

Sarkar, P., Pal, S. P., Ghosh, D., Setford, S. J. and Tothill, E. I. (2002). *Int. J. Pharm.* 238, 1-9.

Schlereth, D. D. and Karyakin, A. A. (1995). *J. Electroanal. Chem.* 395, 221-232.

Schleretth, D. D., Schumann, W. and Schmidt, H. L. (1995). *J. Electroanal. Chem.* 381, 63-70.

Schreiber, A., Feldbrügge, R., Key, G., Glatz, J. F. C. and Spene, F. (1996). *Biosens. Bioelectron.* 12, 1131-11137.

Schulz, B., Riedel, A. and Abel, P.U. (1999). *J. Mol. Catal.B: Enzym.* 7, 85-91.

Sergeyeva, T.A., Lavrik, N.V., Piletsky, S. A., Rachkov, A. E. and El'skaya A.V. (1996). *Sens. Actuators*, B. 34, 283-288.

Sheppard, F. N. Jr., Lesho, M. J., McNally, P. and Francomacaro, A. S. (1995). *Sens. Actuators*, B. 28, 95-102.

Shipway, A. N. and Willner, I. (2001). *Chem. Commun*. 20, 2035-2045.

Si, P., Chi, O., Li, Z., Ulstrup, J., Muller, P.J. and Mortensen, J. (2007). *J. Am. Chem. Soc*. 129, 3888-3896.

Siontorou, C. G., Nikolelis, D. P., Miernik, A. and Krull, U. J. (1998). *Electrochim. Acta*. 43, 3611-3617.

Skotheim, T., Reynolds, J. and Elsenbamer, R (1998). Handbook of conducting polymers, 2nd ed Marcel Dekker, New York.

Stein, E.W. (2003). *Trans. Nanoscience*. 2, 133-137.

Stenberg, M. and Nygren H. (1982). *Anal. Biochem.*127, 183-192.

Stokes, R. J. and Evans, D. F. (1997). Fundamentals of Interfacial Engineering. New York: Wiley-VCH

Stöllner, D., Stöcklein, W., Scheller, F. and Warsinke, A. (2002). *Anal. Chim. Acta.* 470,111-119.

Storhoff, J. J., Elghanian, R., Music, R. C., Markin, C. A. and Lestinger, R. L. (1998). *J. Am.Chem. Soc*. 120, 1959-1964.

Stroka, J. and Anklam, E. (2002). *Trends. Anal. Chem*. 21, 90-95.

Sun, G. and Chih-Chang, C. (2006).   *Carbohy. Polym.* 65, 273-287.

Sun, A., Qi, Q., Dong, Z. L. and Liang, K. Z. (2008). *Sens.   & Instrumen. Food Qual.* 2, 43-50.

Sutar, D. S., Padma, N., Aswal, D.K., Deshpande, S.K., Gupta, S.K. and Yakhmi, J. V. (2007). *Sens. Actuators, B*. 128, 286-292.

Sydenham, E. W., Shephard, G. S., Thiel, P. G., Marasas, W. F. O. and Stockerstrom, S. (1991). *J. Agric. Food. Chem.* 39, 2014-2018.

Tahir, Z. M., Alcocilza, E. C. and Grooms, D. L. (2005). *Biosens. Bioelectron*. 20, 1690-1695.

Tang, J. X. A., Pravda, M, Guilbault, G. G., Piletsky, S. and Turner, A. P. F. (2002). *Anal. Chim. Acta*. 471, 33-40.

Tang, D., Yuan, R., Chai, Y., Dai, J., Zhong, X. and Liu, Y. (2004). *Bioelectrochemistry*. 65, 15-22.

Tang, D. and Ren, J. J. (2005). *Electroanalyis*. 2208-2213.

Taylor, R. F. (1991). Protein Immobilisation, Fundamentals and Applications, Marcel Dekker. New York.

Tijssen, P. (1985). Practice and theory on Enzyme Immunoassay. Elsevier, Amsterdam.

Tkachenko, A. G., Xie, H., Liu, Y. L., Coleman, D., Ryan, J., Glomm, W. R., Shipton, M. K., Franzen, S. and Feldeheim, D. L. (2004). *Bioconjugate chem*. 15, 482-490.

Tothill, I. E. (2001). *Computers and Electronics in Agriculture*. 30, 205-218.

Traitel, T., Cohen, Y. and Kost, J. (2000). *Biomaterials*. 21, 1679-1687.

Trchova, I. Sapurina, Hlavata, D., Prokes, J. and Stjskal, J. (2001). *Synth. Met.* 121, 1117-1118.

Trucksess, M.W., Page, S.W., Wood, G.E. and Cho, T.H. (1998). *J. AOAC Int.* 81, 880-886.

Tsay, Y. G., Lin, C. I., Gustafson, E. K., Appelqvist, R., Magginneti, P., Norton, R. and Charlton D. (1999). *Clin. Chem.*, 37, 1502-1505.

Turner, A. P. F., Chen, B. and Piletsky, S. A. (1999). *Clin. Chem*, 45, 1596-1601.

Tzoris, A., Hall, E. A. H., Besselink, G. A. J. and Bergveld, P. (2003). *Anal Lett*. 36, 1781-1803.

Van Egmond, H. P. and Jonker, A. R. O (2004) Worldwide regulations for mycotoxins in food and feed in 2003. FAO Food and Nutrition paper 81: Report of the food and Agriculture Organization of the United Nations. Rome. ISBN: 9251051623.

Vangelis, G .A. and Dimitrios, P. N. (1997). *Sens.Actuators, B*. 41, 213-216.

Vetcha, S., Wilkins, E. and Yates, T. (2002). *Biosens. Bioelectron.* 17, 901-909.

Vetterl, V., Papadopoulous, N., Drazan, V., Strasak, L., Hason, S. and Dvorak, J. (2000). *Electrochim. Acta*. 45, 961-2971.

Vig, A., Radoi, A., Munoz-Berbel, X., Gyemant, G. and Marty, J. (2009). *Sens.Actuators, B. In press.*

Voss, K. A., Plattner, R. D., Bacon, C.W. and Norred, W. P. (1990). *Mycopathologia.* 112, 81-92.

Wallace, G. G, Smyth, M and Zhao, H. (1999). *Trends. Anal. Chem*. 18, 245-251.

Wang, M., Wang, L., Wang, G., Ji, X., Bai, Y., Li. T., Gong, S. and Li, J. (2004). *Biosens. Bioelectron*. 19, 575-582.

Wang, Z., Yang, Y., Li, J., Gong, J., Shen, G. and Yu, R. (2006). *Talanta*. 69, 686-690.

Wessling, B. and Posdorfer, J. (1999). *Electrochim. Acta*. 44, 2139-2147.

WHO (World Health Organization). (2002). Deoxynivalenol. In: Evaluation of certain mycotoxins in food. WHO Technical Report Series 906. WHO, Geneva, Section 3.4.1, pp35-42.

Wolfbeis, O. S. (2000). *Anal. Chem.* 72, 81-89.

Wolf-Hall, C. E., Hanna, M. A. and Bullerman, L. B. (1999). *J. Food Prot.* 62,962-964.

Wu, X., Kim, J. and Dordrick, J. S. (2000). *Biotechnol. Prog*. 16, 513-516.

Wu, L., Chen, J., Du, D. and Ju, H. (2006). *Electrochim. Acta*. 51, 1208-1214.

Xiao, Y., Ju, H. and Chen, H. Y. (1999). *Anal.Chim Acta.*391, 299-306.

Xu, S.Y. and Han, X. Z. (2004). *Biosens. Bioelectron*. 19, 1117-1120.

Xu, F. J., Cai, Q. J., Li, Y. L., Kang, E. T. and Neoh, K. G. (2005). *Biomacromolecules*. 6, 1012-1020.

Xu, Y. Y., Bian, C., Chen, S. and Xia S. (2006). *Anal. Chim. Acta*. 561, 48-54.

Xuelian, L., Yuan, R., Chai, Y., Zhang, L., Zhuo, Y. and Zhang, Y. (2006). *J. Biotechnol*. 123, 356-366

Yagiuda, K., Hemmi, A. and Ito, S. (1996). *Biosens. Bioelectron*. 11, 703-707.

Yang, R., Ruan, C., Dai, W., Deng, J. and Kong, J. (1999). *Electrochim. Acta*. 44, 1585-1596.

Yang, L., Li, Y.   and Gisela, F. E. (2004). *Anal.Chem.* 76, 1107-1113.

Yaroglu, T., Oruc, H. H. and Tayar, M. (2005), *Food Control*. 16, 883-885.

Yu, H, Yan, F, Dai, Z. And Ju, H. (2003). *Anal. Biochem*. 331, 98-105.

Yu, J. C. C. and Lai, E. P. C. (2005). *React.Funct. Polym*. 63, 171-176.

Yuan, R., Tang, D., Chai, Y., Zhong, X., Liu, Y. and Dai, W. (2004). *Langmuir*. 20, 7240-7245.

Yuan, R., Zhang, L., Li, Q., Chai, Y. and Cao, S. (2005). *Anal. Chim. Acta*. 531, 1-5.

Zachara, J. E., Owska, R. T., Pokrop, R., Zagorska, M., Dybko, A. and Wroblewski, W. (2004). *Sens. Actuators, B.* 101, 207-212.

Zanganeh, A. R. and Amini, M. K. (2007). *Electrochim. Acta*. 52, 3822-3896.

Zayats, M., Raitman, O. A., Chegel, I.V., Kharitonov, A. B. and Wilner, I. (2002). *Anal. Chem.* 74, 4763-4773

Zejli, H. Sharrock, P. Hidalgo-Hidalgo de Cisneros, J. L.; Naranjo-Rodriguez, I. and Temsamani, K. R. (2006) *Talanta.* 68, 79-85

Zhang, L., Yuan, R., Huang, X., Chai, Y. and Cao, S. (2004). *Electrochem.Commun.*6, 1222-1225.

Zhang, X., Shengfu, W., Mei, H. and Yao, X. (2006). *Biosens. Bioelectron*. 21, 2180-2183.

Zheng, H., Humphney, C. W., King, R. S. and Richard, J. L. (2005). *Mycopathologia.*159, 1-9.

Zhou, Y. M., Hu, S. Q., Shen, G. L. and Yu, R. Q. (2003). *Biosens. Bioelectron.* 18, 473-481.

Zhou, A. and Muthuswamy, J. (2004). *Sens. Actuators*, B.101, 8-19.

Zhuo, Y., Yuan, R., Chai, Y., Tang, D., Zhang, Y., Wang, N., Li, X. and Zhu, Q. (2005). *Electrochem. Commun.* 7, 355-360.

Zhuo, Y., Yuan, R., Chai, Y., Zhang, Y., Li, X., Wang, N and Zhu, Q. (2006). *Sens. Actuators, B.* 114, 631-639.

Zotti, G., Zecchin, S., Schiavon, G., Berlin, A. and Penso, M. (1999). *Chem. Mater.* 11, 3342-3351.